UNIVERSITA' DEGLI STUDI DI PADOVA

DIPARTIMENTO DI SCIENZE ECONOMICHE ED AZIENDALI "M.FANNO"

DIPARTIMENTO DI MATEMATICA "TULLIO LEVI-CIVITA"

CORSO DI LAUREA MAGISTRALE IN

ECONOMICS AND FINANCE

TESI DI LAUREA

"CLIMATE DERIVATIVES: SHARING THE LONG-TERM CLIMATE RELATED RISKS"

RELATORE:

CH.MO PROF. CLAUDIO FONTANA

LAUREANDO/A: DIEGO ANTONELLO

MATRICOLA N. 2004264

ANNO ACCADEMICO 2021 – 2022

Dichiaro di aver preso visione del "Regolamento antiplagio" approvato dal Consiglio del Dipartimento di Scienze Economiche e Aziendali e, consapevole delle conseguenze derivanti da dichiarazioni mendaci, dichiaro che il presente lavoro non è già stato sottoposto, in tutto o in parte, per il conseguimento di un titolo accademico in altre Università italiane o straniere. Dichiaro inoltre che tutte le fonti utilizzate per la realizzazione del presente lavoro, inclusi i materiali digitali, sono state correttamente citate nel corpo del testo e nella sezione 'Riferimenti bibliografici'.

I hereby declare that I have read and understood the "Anti-plagiarism rules and regulations" approved by the Council of the Department of Economics and Management and I am aware of the consequences of making false statements. I declare that this piece of work has not been previously submitted – either fully or partially – for fulfilling the requirements of an academic degree, whether in Italy or abroad. Furthermore, I declare that the references used for this work – including the digital materials – have been appropriately cited and acknowledged in the text and in the section 'References'.

Firma (signature)

Abstract

After having realized that climate change does not affect all economic sectors in the same way and that financial instruments already existing are not able to fulfill the need of hedging climate risks, a possible solution has been found in climate derivatives. A market for these novel financial instruments still does not exist: they have been only theoretically conceived. Once explored the literature of climate derivatives and highlighted strengths and weaknesses of each prototype presented, an alternative pricing method for a type of climate derivative, namely temperature option, is proposed and tested through Matlab simulations.

Contents

List of Figures

List of Tables

Introduction

In the recent years much has been said about the climate change. In this respect, the birth of the Friday for Future or the various COPs (Conference of the Parties) may come to mind. The Paris Agreement is surely a landmark in the recent debate about climate change. Its importance is due to the fact that it is a legally binding international treaty on climate change. For the first time, a binding agreement commits all nations at once to put in effort to counter climate change and adapt to its effects. It was adopted by 196 Parties at COP 21 in Paris, on 12 December 2015 and entered into force on 4 November 2016. The long-term goal consists in keeping the increase in global average temperature below 2°C above pre-industrial levels and to pursue efforts to limit it to 1.5°C.

Debates and discussions on the matter have become more numerous: many of them are aimed at finding solutions for climate adaption and climate change mitigation. Adaption consists in anticipating the climate change adverse effects and in taking measures in order to prevent/minimize the possible damages, while mitigation consists in lessening climate change impact by preventing/reducing GHG emissions.

The present thesis fits into this context with the purpose of illustrating a new type of derivatives which is intended to facilitate the sharing of climate risks, the climate derivatives. Since climate change effects are visible over the long term, these financial instruments ought to be characterised by a long maturity (measurable in decades) and pay-off indexed to climate-related variables. The use of climate derivatives can in fact be helpful in the raising of funds for financing adaption projects for instance.

In Chapter 1, the climate change problem is presented. Impacts on economy are examined through a sector-based approach. Insurance sector and all other sectors are separately discussed because of the different financial instruments that can be used to bring short-term relief: CAT bonds and weather derivatives, respectively. These instruments are not suitable for hedging climate risks given their short maturities (from months to 5 years at most). Indeed, climate change effects are barely visible in these limited time spans. The validity of these instruments in the context of the changing climate is also discussed.

In Chapter 2, the climate derivatives are introduced with the purpose of making up for the lack of instruments able to cover the long-term. Indeed, climate change effects are clearly visible right about that time. The analysis of the literature is done: the climate derivatives considered are those ones presented in Bloch, Annan, and Bowles (2010) (and Bloch, Annan, and Bowles (2011)), Chikhani and Renne (2021) and Little et al. (2015).

These three models are discussed highlighting the potentialities and the criticalities of these novel financial instruments. Anyway, there is still no proofs of their performance on the market because they are just theoretical instruments. Many assumptions of these models are debatable: there is no question of finding the perfect instrument, but it is about finding a credible instrument.

Climate linkers, as presented in Chikhani and Renne (2021), are the climate derivatives which have inspired the present thesis: they are credited with the attempt of enhancing the sharing of the risks related to climate change which notably affect some economic sectors and some areas of the world. Even though closed-form solutions are provided for their pricing, the model for pricing requires not only financial and mathematical knowledge, but also physical and climatological understanding.

In Chapter 3, among the range of products presented in the previous chapter, the possibility of pricing temperature options (which is one of the climate linkers proposed in Chikhani and Renne (2021)) in a manner similar to standard options is explored. As we will discuss, the pricing method proposed by the authors is not devoid of criticalities because of the high number of assumptions concerning the climate and economic blocks of the model, the chosen calibration parameters and the use of IAMs outside the scope of first best policy estimation.

Two stochastic models, namely the Vasicek model and the Hull-White one, are used to generate the underlying temperature processes. Monte Carlo simulations are performed in Matlab to simulate the global average temperature paths, compute temperature options prices and test their response to changing inputs. After having discussed the results, the preference is given to one of the two stochastic models by reason of greater capacity to represent climate dynamics.

Although the assumption of an ad hoc climate risk premium is a relevant limitation of the pricing method proposed, it is necessary since the climate derivatives market still does not exist in reality. Assuming a null risk premium would weaken the validity of the pricing model since the reference probability would remain the real-world one.

CHAPTER 1 Climate change for everyone?
1.1 The climate change numbers

By the expression "climate change" is meant the long-term shifts in temperatures and weather patterns. Although these shifts may be natural (due to variations in the solar cycle) as seen many times during the Earth history, human activities have been the main driver of the acceleration of climate change since 19th century, mainly due to burning fossil fuels.[1]

To understand the seriousness of the climatic problem, we just need a quick look at some relevant indexes such as the global land-ocean temperature and sea level ones.

Figure 1: Global land-ocean temperature
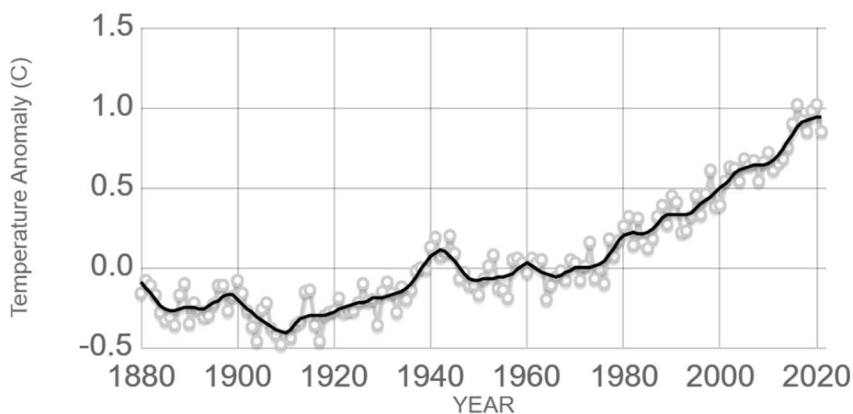
Source: climate.nasa.gov

Looking at ***Figure 1***, it is possible to understand the magnitude of climate change: the graph shows the change in global surface temperature relative to 1951-1980 average temperature. Using this reference temperature, the global temperature change is computed taking the difference between 0.85 (2021) and -0.16 (1880): the global temperature in 2021 proves to be 1.01°C higher than in 1880.

---

[1] 'What Is Climate Change?', United Nations, accessed 3 May 2022, https://www.un.org/en/climatechange/what-is-climate-change.

Figure 2: Sea heating
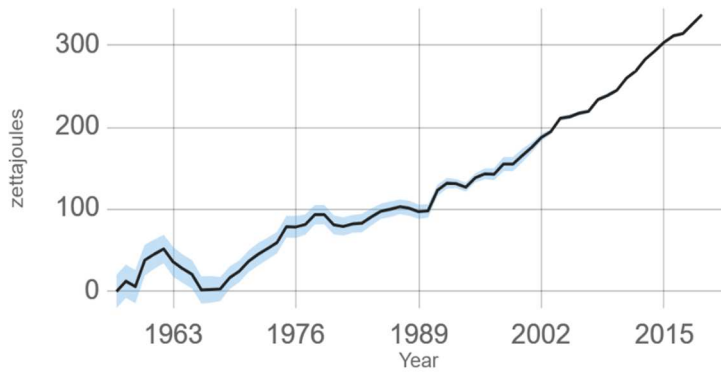
Source: climate.nasa.gov

Although the global warming is evident even on land, 90% of it is occurring in the ocean. Since modern record-keeping began in 1955, water internal heat has been increasing, as shown in **Figure 2**[2]. One-third to one-half of global sea level rise is due to the expansion of water caused by the heat stored in the ocean. Each data point in the chart represents a five-year average (e.g., the 2019 value represents the average change in ocean heat content in the period 2017 – 2021). The last ten years have been the ocean's warmest decade since at least the 19th century with the peak of 2021, the ocean's warmest recorded year.[3] The vast majority of this added energy is stored at the surface (in the range of depth from zero to 700 meters).

This phenomenon is evident in **Figure 3** which shows the annual ocean heat content for the period 1993-2019 compared to the 1993 average.

Figure 3: Ocean heat content compared to 1993 average
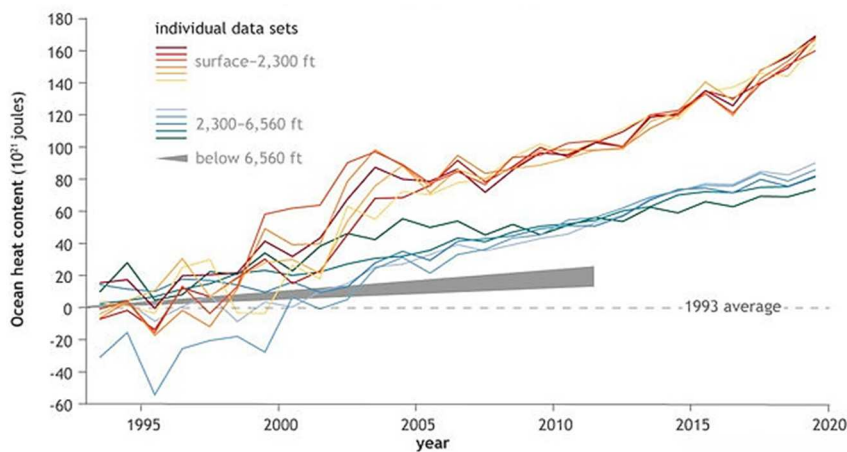
Source: NOAA climate.gov, adapted from SOTC 2019

---

[2] The shaded blue area indicates the 95% margin of uncertainty.

[3] NASA, 'Ocean Heat Content | NASA Global Climate Change', Climate Change: Vital Signs of the Planet, accessed 26 April 2022, https://climate.nasa.gov/vital-signs/ocean-heat.

It is based on multiple data sets: surface to depths of 2,300 feet (700 meters) in warm colours; from 2300 to 6560 feet (700-2000 meters) in cold colours and below 6,650 feet (2,000 meters) as a grey area.[4]

The most evident effect of global warming on land is the melting of ice sheets and glaciers. According to ice mass measurement by NASA's GRACE satellites, Antarctica mass variation since 2002 is proved to consist in a decrease of 152 billion metric tons per year (***Figure 4***), while Greenland one consists in a decrease of 275.0 billion metric tons per year (***Figure 5***).[5] NSIDC/NASA satellite observations show that September Arctic Sea ice extent[6] is declining at a rate of 13% per decade, relative to the 1981 to 2010 average.[7]

Figure 4: Antarctica mass variation since 2002
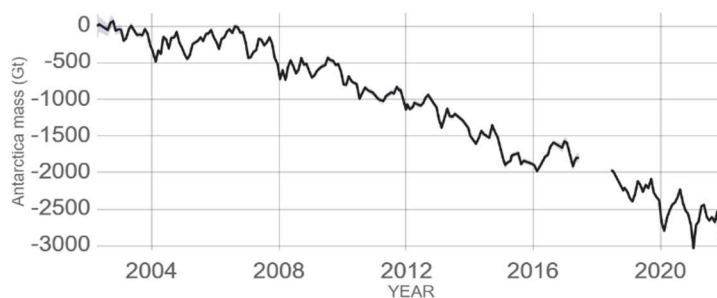
Source: climate.nasa.gov

Figure 5: Greenland mass variation since 2002
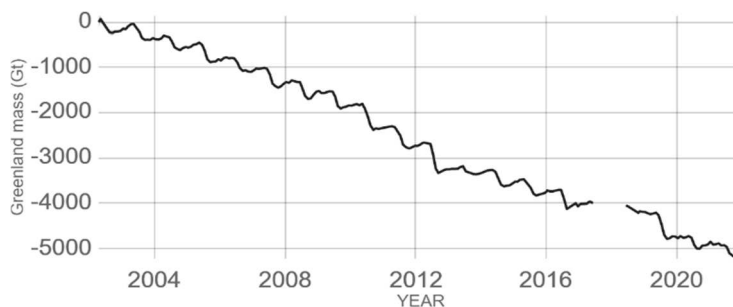
Source: climate.nasa.gov

---

[4] 'Climate Change: Ocean Heat Content', Climate.gov, accessed 2 May 2022, https://www.climate.gov/news-features/understanding-climate/climate-change-ocean-heat-content.

[5] NASA, 'Ice Sheets| NASA Global Climate Change', Climate Change: Vital Signs of the Planet, accessed 26 April 2022, https://climate.nasa.gov/vital-signs/ice-sheets.

[6] Arctic sea ice reaches its minimum each September.

[7] NASA, 'Arctic Sea Ice Minimum | NASA Global Climate Change', Climate Change: Vital Signs of the Planet, accessed 26 April 2022, https://climate.nasa.gov/vital-signs/arctic-sea-ice.

The additional water deriving from melting ice sheets and glaciers and the expansion of seawater due to its warming are the two factors mainly causing the sea level rise.[8]

Figure 6: Sea level rise and causes
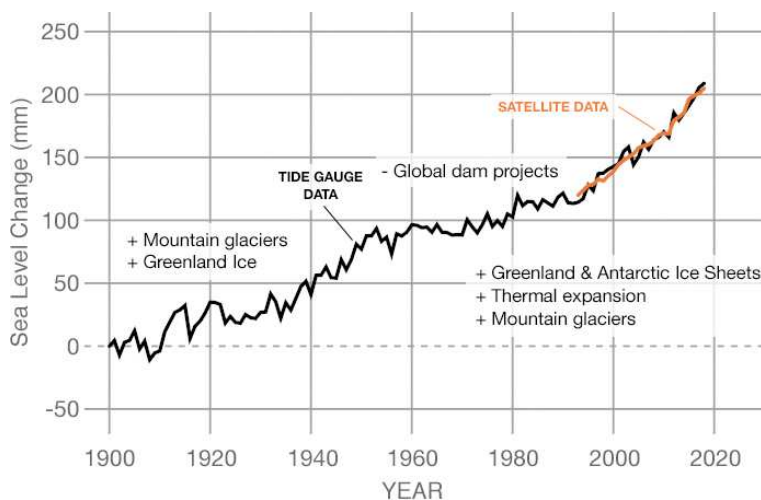
Source: climate.nasa.gov

Figure 6 tracks the change in sea level and reports the main causes. The signs + and − are used to distinguish factors that cause global mean sea level to increase and those that cause sea level to decrease. The orange line, starting from 1993, represents the data collected by satellites which are characterised by greater accuracy. In the period 1993-2017 sea level is risen of about 101 millimetres.

It is easy to understand that these phenomena cannot be considered in isolation because they are strongly interconnected . In addition to their strong interconnection, another serious problem is related to the speed at which they are occurring.
Quoting the words of D. Fagre[9]:
"Things that normally happen in geologic time are happening during the span of a human lifetime".
Indeed, as stated in IPCC (2012), the frequency and the intensity of most types of extreme events are thus expected to significantly change. Climate change will in fact lead to changes in the spatial extent, duration and timing of extreme weather and climate events. Unprecedented extremes are expected. Changes in extremes can be related to changes in their mean, variance, shape of the probability distribution, or all of these. Moreover, weather or climate events which

---

[8] NASA, 'Sea Level| NASA Global Climate Change', Climate Change: Vital Signs of the Planet, accessed 26 April 2022, https://climate.nasa.gov/vital-signs/sea-level.

[9] research scientist from the U.S. Geological Survey Global Change Research Program

are not extreme (when considered individually) may result in climate extremes as a consequence of their accumulation.

Anyway, it should be reminded that natural variability is still the cause of many extreme weather and climate events: these extremes would still occur even if there were no anthropogenic changes in climate. Thus, it can be said that anthropogenic changes are additional to natural multi-decadal variations in climate.

Figure 7: Billion-dollar disasters by year (CPI adjusted)
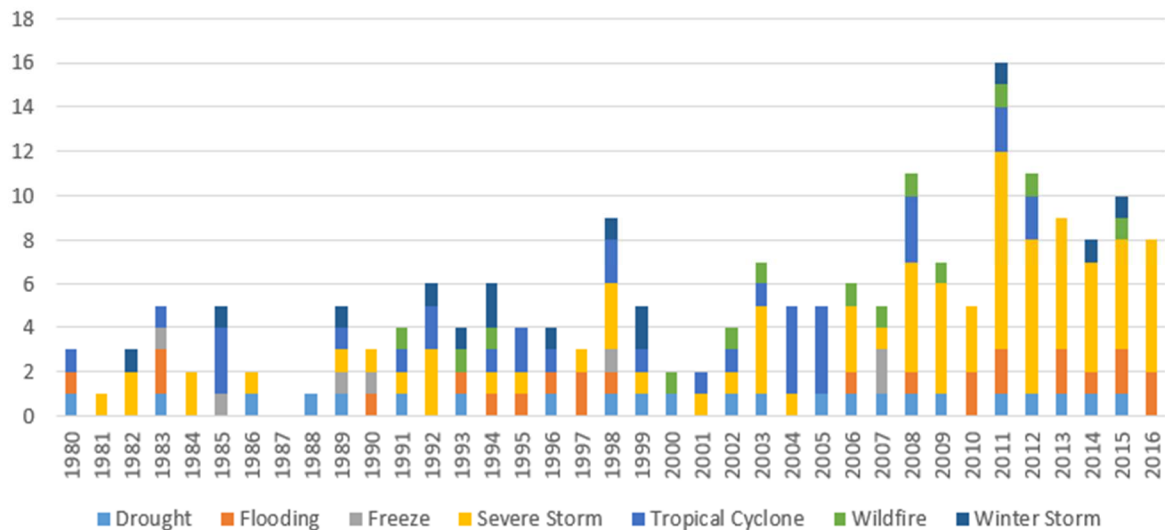
Source: NOAA/NCEI National Centre for Environmental Information (2016)

Looking at the period 1980-2016 shown by **Figure 7**, it is noticeable that in the last decade there has already been an increase in the frequency/intensity of extreme events as the spike in the amount of disaster-related losses with respect to the previous decades witnesses. The item which has registered the most relevant rise and so has the biggest impact on the increase in the amount of billion-dollar losses is that one related to severe storms. Indeed, the other items have remained almost constant.

1.2 Insurance difficulties

In 1992 Dr Gerhard Berz, at that time Head of Munich Re's Geoscience Research Group, in Berz (1992) already recognised that "*the increased intensity of all convective processes in the atmosphere will force up the frequency and severity of tropical cyclones, tornados, hailstorms, floods and storm surges in many parts of the world*" as a result of climate change and warned about the consequences for all types of property insurance. Anyway, quoting Ceres (2013), in 2012 few insurers had "*explicit policies to identify or manage the trends of global climate change*" and many did not "*seem to understand the difference between climate variability and climate change*".

The results of the "Insurance Regulator State of Climate Risks Survey", conducted by the Deloitte Centre for Financial Services and reported in Deloitte United States (2019), reveal that still in 2019 many regulators either were not aware of how prepared insurers were to deal with this threat or were not fully confident that they were indeed prepared. One-third of the regulators surveyed in fact was unaware of insurers' preparedness to deal with the potential impacts of climate change on their financial stability and less than 15% of the regulators believed that insurers were largely or fully prepared. Moreover, one-third of them did not know whether insurers' risk models were up to the challenge of capturing and testing climate related risks.

It is important to note that, regardless of their awareness, the insurers 'exposure to risks associated with climate change is massive. According to rating agencies, whose attention has been increasingly drawn by those risks to the insurance industry, the volatility for these firms will be magnified by the effects of the climate change and thus risk management challenges will proliferate. Existing lines of insurance are already being affected by a dramatic surge of pay-outs. According to Swiss Re Institute 2018 Sigma study, as reported in Collier, Elliott, and Lehtonen (2021) and shown by *Figure 8*, disasters produced the record-high amounts of $144 billion in insured losses and of $337 billion in economic losses that were mainly concentrated in the southeast United States and the Caribbean. The 10-year averages were of the much smaller amounts of $58 billion and $190 billion, respectively.

Figure 8: Insured losses in US$ billion at 2020 prices
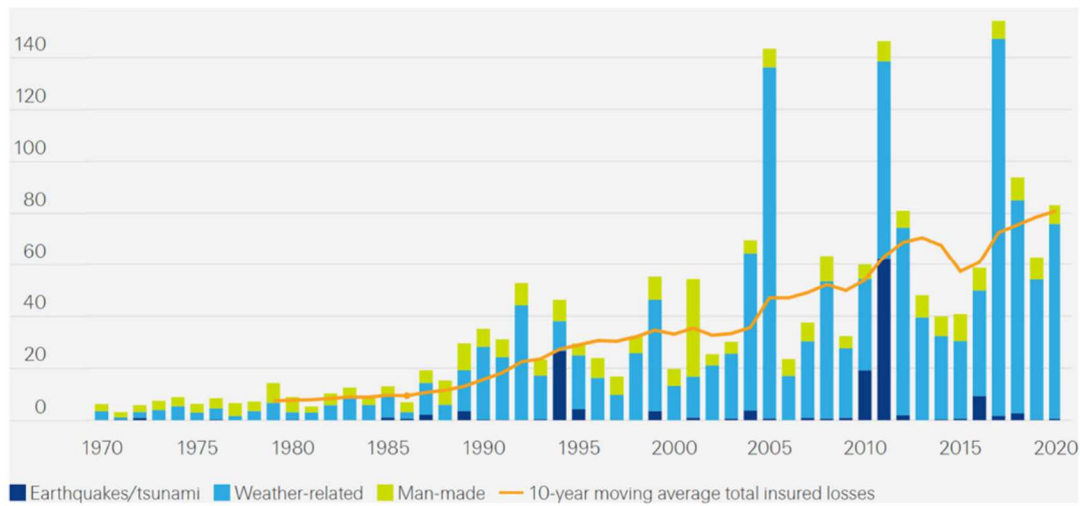
Source: Swiss Re Institute (2020). News release

Although not all the losses suffered by insurers are weather-related, the authors link the largest part of the drastic increase of losses to climate change. They believe that losses will keep increasing dramatically in the future due to the impact of climate change on the frequency and the severity of natural catastrophes which will likely cause the sharp increase in the number and the size of claims.

Potential un-insurability associated with increasing frequency and magnitude of extreme weather events was already recognised before 2009. The United Nations Environment Programme´s Finance Initiative (UNEPFI) reported that by 2025, insurers may have withdrawn from markets where the risks would have become too high for the pool of premium available. Warner et al. (2009) reports that CERES[10], a sustainability non-profit organization based in the US, had identified a growing move by insurers to reduce coverage in coastal areas in its country. Regulators are becoming concerned about insurer solvency due to these increasingly severe weather-related losses and systemic risks to the insurance industry. They are also sensitive to the possibility that spiking insurance premiums and partial or even total withdrawal of coverage in certain areas (certain risks will be de facto uninsurable) could limit the insurance availability and affordability for consumers.[11]

To be more precise, in the short term, theoretically, insurance premiums would rise gradually as long as the underlying trend would be properly considered and the insurance market would absorb such changes without disruption. However, it cannot be excluded that risk knowledge may advance in 'steps' leading to jumps in the price over a short period.

In the long term, insurance premiums could become unaffordable for a part of the population in particular for sectors and areas at greater climatic risk. We could say that the changing climate would indirectly increase social disparities.[12] Not only soaring insurance premiums can lead to the impossibility of insuring for the population: as stated by the UN Global Commission on Adaption, not all localized effects of climate change are insurable. Quoting Jarzabkowski et al. (2019), there may not simply be enough (re)insurance capital to let (re)insurance companies remain solvent ensuring the reliability of insurance pay-outs. If this is indeed the case, they would not be able to provide in full for the global effects of climate change, even though the population could afford the premiums. Anyway, insurance companies still can have an important role signalling, through prices, the increasing unsustainability of some areas under climate change and bridging the gap between the local adaptation to climate change and the policies and development agendas to make it more effective.

---

[10] Coalition for Environmentally Responsible Economies

[11] C. Flavelle, "As Wildfires Get Worse, Insurers Pull Back from Riskiest Areas", New York Times, 20 August 2019, accessed 14 May 2022, https://www.nytimes. com/2019/08/20/climate/fire-insurance-renewal.html

[12] European Commission, 'Sectors affected', accessed 27 April 2022, https://ec.europa.eu/clima/eu-action/adaptation-climate-change/how-will-we-be-affected/sectors-affected_en

Why will certain risks be "uninsurable"? The main problem is that the climate change undermines the "mutualization of risks" by the insurer. This problem has already been discussed many times in the literature concerning the standard natural catastrophe risk.

A type of risk is not insurable when it does not meet certain criteria which are called insurability criteria.

In Biener and Eling (2012), the insurance criteria, which are presented in **Table 1**, are categorized into three classes:

- Actuarial
- Market
- Societal

Table 1: Insurability criteria and their requirements

Insurability Criteria			Requirements
Actuarial	(1)	Randomness (of loss occurrence)	Measurable and independent
	(2)	Maximum possible loss	Manageable
	(3)	Average loss amount and loss frequency	Moderate average loss amount and low loss frequency
	(4)	Loss exposure	Loss exposure must be large
	(5)	Information asymmetry	Moral hazard and adverse selection not excessive
Market	(6)	Insurance premium	Cost recovery and affordable
	(7)	Cover limits	Acceptable
Societal	(8)	Public policy	Consistent with societal values and availability of services
	(9)	Legal restrictions	Allow the coverage

Source: Tavanaie Marvi, Linders (2021)

Natural catastrophe (from here, Nat Cat) risk easily violates the insurability criteria. Indeed, the losses caused by a Nat Cat are not independent in both time and magnitude. Although the large size of the total loss might seem the main uninsurability cause, it per se does not make the risk uninsurable. Indeed, Charpentier and Le Maux (2014) reports that the factor which makes these losses too large to be manageable by most insurers is their simultaneity. For this reason,

catastrophe coverage is offered by only large insurance companies which have easier access to capital and the possibility to pool the risks with independent ones from other regions.

The positive correlation among losses is thus the primary reason that makes Nat Cat risks uninsurable. As a result of this positive correlation, insurers cannot rely on the law of large numbers and so reduce losses variability around their expected value by selling more policies. Moreover, the positive correlation increases the likelihood of observing extremely large losses in an event which creates a heavy-tail loss distribution for a Nat Cat risk. Given the industry regulations requirements about the maintenance of a reserve commensurate with the risk borne, a Nat Cat risk with a heavy-tail distribution is not conducive for insurers. Indeed, it can easily make the required reserve increase by a significant amount. Referring to *Table 1*, it is possible to say that only criteria 5 and 8, concerning the information asymmetry and the public policy respectively, are properly met. In fact, insurers are deemed to have superior understanding about the risk and there is no conflict with societal values in their activity. Clearly, there is no room for an improvement in a situation of climate change and in the future even criterion 5 might be not met due to the worsening of the insurers' understanding about the risk.

Insurance companies' way to deal with natural catastrophes was found almost 30 years ago. They were aware of their need to distribute the catastrophe risk going over to small and geographically limited populations of policyholders. The financial instruments so far used to distribute catastrophe risks into large pools of financial capital are the CAT bonds.

In section 1.4, these financial instruments are illustrated and the reason why their effectiveness is challenged by climate change is discussed.

1.3 Other sectors difficulties

Clearly, not only insurance sector will be affected by climate change: the global economy as a whole will suffer its impact. Just to get an idea, it is useful to consider the concept of climate damage function as exposed by Wade and Jennings (2016) and Neumann et al. (2020). Climate damage functions express the economic damages as function of climate inputs: they quantify the economic risks resulting from climate change and plot the output level lost over a range of warming estimates. They are based on regression analyses using only the damage output of more detailed and complex sectoral models, the so-called process based models, which aim at reflecting the complex structural, biological, physical and economic relationships explaining the way climate change affects economy. Thus, climate damage functions can be a simpler alternative (while not a perfect substitute) to process-based models. An economic climate damage is measured as the fractional loss in annual economic output at a given level of warming with respect to the output in the same economy with no warming. Although all climate damage

functions predict a greater loss in annual economic output as the warming level rises, among the different estimated climate damage functions there is no consensus for what concerns the way in which damages evolve as warming gradually increases. The differences are really noticeable in *Figure 9* which shows the climate damage forecasts at a given level of warming based on estimates by Dietz and Stern (2014), Weitzman (2012) and Nordhaus (2013).

Figure 9: Climate damage functions
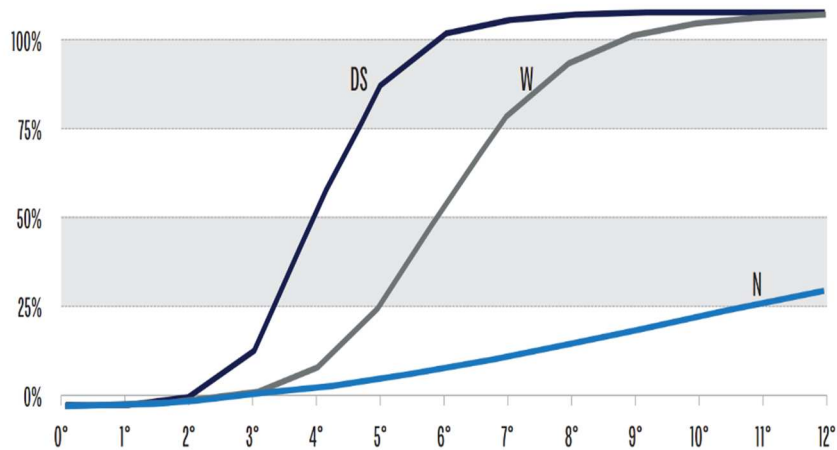
Source: Covington and Thamotheram (2015)

Additional benchmark studies aiming to address the economic impacts of climate change from the literature are reported and summarized in *Table 2*.

Table 2: Estimates of economic losses from climate change

Study	Warming	Impact as % on GDP	Comment
Mendelsohn, Schlesinger, Morrison and Andronova (2000)	2.0°C by 2060	A cumulative effect of a loss of 0.3% of GDP in 2060	Most damages will involve agricultural sector. Only OECD[13] economies may gain from warming. Individual countries' damages can be different with respect to continental averages.
Mendelsohn, Schlesinger and Williams (2000)	2.5°C by 2100	Cumulative market impact costs do not exceed 0.1% of GDP in 2100	The market impact costs will vary from country to country. High latitude countries are expected to gain, while low latitude ones are expected to lose.

---

[13] Organization for Economic Co-operation and Development

Stern (2005)	Baseline scenario of between 2.4°C and 5.8°C by 2100	An average loss of 5% of global GDP per annum over the next two centuries	Estimates are based on a no action scenario. Costs of extreme weather alone could reach 0.5 – 1% of world GDP per annum by 2050.
IPCC, Fifth Assessment (2014)	Approximately 2.0°C	A loss of 0.2% - 2.0% of GDP per annum	There are large differences of impact among countries. Delaying mitigation efforts to 2030 is estimated to increase the difficulty of transitioning to low long-term emission levels.

Source: Wade and Jennings (2016)

However, as also reported in some of the papers shortly summarized in ***Table 2***, the effects are tougher in certain sectors.

In particular, the sectors hard hit are:

- Agricultural
- Energy
- Tourism

Agricultural sector

Agriculture is highly dependent on the climate: climate change and climate variability impacts on agricultural production would surely concern the crop yields and the location where crops can be grown. The crop season has lengthened and will keep lengthening resulting in earlier onset of growth in spring and longer growing season in autumn. For any particular crop, the increased temperature will have a different effect depending on the crop's optimal temperature for growth. In some areas, warming may benefit the types of crops that are typically planted there or, if temperature exceeds those crops' optimum temperature, may force farmers to shift to crops not previously suitable because growing in warmer areas.[14]

Some areas (e.g., southern Europe) will suffer a negative impact altogether because of high temperatures, water shortage and extreme weather events: they may trigger lower yields, higher yield variability and, over the long haul, the reduction in areas suitable for cultivation. Extreme temperatures and precipitation patterns can harm crops and reduce yields especially when

---

[14] OA US EPA, 'Climate Impacts on Energy', Overviews and Factsheets, accessed 5 May 2022, https://19january2017snapshot.epa.gov/climate-impacts/climate-impacts-energy.

causing extreme events such as floods and droughts. Other areas (e.g., northern Europe) may experience the growth of the agricultural sector due to new crop varieties, higher yields and expansion of suitable areas for crop cultivation.[15] It would be possible thanks to longer crop seasons, more frost-free periods and fewer cold spells.

Tourism sector

Climate change will also affect tourism and recreational activities causing important damages to regions where tourism plays an important role in the economy. Extreme temperatures will considerably make southern Europe less suitable for tourism during the key summer months. Conversely, its suitability will improve in other seasons. Moreover, sea level rise and storm surge would worsen beach erosion phenomenon.[16] Areas living off winter tourism will be negatively affected due to the reduction in snow cover and the shortening of the cold season. The number of days ideal for recreational snow activities in fact will likely decrease due to the warming climate and changes in precipitation patterns.

Hiking and recreation in parks (e.g., in the Southwest and Mountain West in the U.S.) could be affected by the increasing number of wildfires.[17] Fires' impact will also be strong on degraded ecosystems in southern Europe: longer and more severe fire seasons are expected in the future.

Energy sector

The energy system has to deal with climate threats which not only already exist, but also are projected to increase. Indeed, climate change is expected to reduce demand for heating in some areas (e.g., northern and north-western Europe and northern U.S.) and to strongly increase energy demand for cooling in other areas (e.g., southern Europe and southern U.S.), which may further exacerbate peaks in electricity supply in the summer.

The increase in intensity and frequency of heat waves will make energy supply and demand patterns shift, often in opposite directions.

Taking the U.S. energy sector as an example, Wilbanks et al. (2007) reports that an increase of about 5-20% of the demand for energy used for cooling is expected with a 1.8°F (1°C) temperature rise, while a decrease of about 3-15% of natural gas, oil and wood for heating is expected with the same temperature rise. Dell et al. (2014) revised slightly downwards the estimates: a 4.5°F (2.5°C) warming by the end of the century may entail an increase of 10% of

---

[15] European Commission, 'Sectors affected', accessed 27 April 2022, https://ec.europa.eu/clima/eu-action/adaptation-climate-change/how-will-we-be-affected/sectors-affected_en

[16] European Commission, 'Sectors affected', accessed 27 April 2022, https://ec.europa.eu/clima/eu-action/adaptation-climate-change/how-will-we-be-affected/sectors-affected_en

[17] OA US EPA, 'Climate Impacts on Energy', Overviews and Factsheets, accessed 5 May 2022, https://19january2017snapshot.epa.gov/climate-impacts/climate-impacts-energy.

expenditure in annual heating and cooling, while a warming of 9.0°F (5°C) may entail an increase of 22% of that expenditure.

The balance in energy delivery is likely to change: a shift from natural gas and fuel oil to electricity is expected because of the greater air conditioning need than heating one.

Increases in temperature and droughts may reduce the efficiency of power production for fossil fuel, thermal and nuclear power plants due to the limited availability of necessary cooling water in summer.[18] The increased uncertainty in weather patterns deriving from climate change will have a direct negative impact on the production of renewable energy in the long term. Solar and wind power plants will indeed suffer the resulting sunlight and wind reduction. Heat and droughts will harm the production of biomass energy since the crops intended for this purpose will be directly affected.[19]

Climate change will surely also generate cross-cutting issues for businesses, which will be affected in many ways. In particular, climate change is expected to hit disproportionately hard small and medium enterprises causing business operations disruptions, property damages, supply chains and infrastructures disruptions (which will result in increased costs of maintenance and materials) and price rises.[20]

However, it is no coincidence that the sectors considered in this section since impacted by the long run climate risk are primarily affected by weather risks. Indeed, climate change is clearly reflected in weather conditions either in the form of increase in frequency and severity of related catastrophic events or their gradual change.

Anyway, it is certainly easier to hedge the weather risk than the climate one. Nevertheless, it should be remembered that hedging weather risk does not respond to the same need that hedging climate risk would respond to. The financial instruments so far used by many economic activities to hedge the short-term risk deriving from weather phenomena are the weather derivatives. They are not new: these instruments have been on the market for almost 25 years. In section 1.5, these financial instruments are illustrated and the reasons why they are not suitable to hedge the climate risk are discussed.

---

[18] OA US EPA, 'Climate Impacts on Energy', Overviews and Factsheets, accessed 5 May 2022, https://19january2017snapshot.epa.gov/climate-impacts/climate-impacts-energy.

[19] European Commission, 'Sectors affected', accessed 27 April 2022, https://ec.europa.eu/clima/eu-action/adaptation-climate-change/how-will-we-be-affected/sectors-affected_en

[20] European Commission, 'Sectors affected', accessed 27 April 2022, https://ec.europa.eu/clima/eu-action/adaptation-climate-change/how-will-we-be-affected/sectors-affected_en

1.4 Transferring the risk: CAT bonds

Given that the economic viability of traditional insurance companies' activity is challenged by catastrophe risks, transferring large risks exceeding a predefined limit seemed to be a solution. Through reinsurance and 'alternative risk transfer' instruments such as catastrophe bonds and other insurance-linked securities, catastrophe risks are in fact distributed into vastly larger pools of financial capital rather than over relatively small and geographically limited populations of policyholders.

In order to illustrate the factors which make reinsurance possible and the ones which cast doubts on its effectiveness in the future due to climate change, this section mainly relies on Tavanaie Marvi and Linders (2021) and Kurniawan et al. (2021).

Tavanaie Marvi and Linders (2021) considers the direct impacts of natural catastrophes on buildings pertaining to property and casualty type insurance (P&C) to present the possibility of transferring the systematic risk to the capital markets.

For an individual building, the size of the loss depends on the physical features of the building (construction material, floor plan, etc.) and the hazard intensity at the property specific geographical location in the region. Categorizing buildings into classes according to their response to the hazard let the physical characteristics be captured. The loss estimation function, which presents the relationship between the loss size of a building and the specific natural hazard intensity at the property location, is composed of two parts:

1. the deterministic non-decreasing trend $g(\cdot)$ which is function of X, the intensity of a natural hazard. Given that the intensity of the hazard varies in the region, X is the local evaluation of the intensity at the building location.

2. the stochastic term $\sigma_X \varepsilon$, whose variance may change by the hazard intensity.

For simplicity, the following assumptions are made by the authors:

* ε is a random variable with standard normal distribution
* σ_X is the loss standard deviation given the intensity of X around its average value or $g(X)$.

For a specific natural hazard, the building i in a region will suffer the random loss L_i as

$$L_i = g_i(X_i) + \sigma_{X_i} \varepsilon$$

Although the intensity of a natural hazard is varying across a region, its local realizations are related to each other. The intensity variability can be featured by the physical model that underlies the natural phenomenon (also called hazard model), while the event parameters reflecting the characteristics of the specific natural hazard considered can be featured by initial

values and/or boundary conditions of the model. The hazard model is clearly different for each hazard type (e.g., flood, hurricane, earthquake) and requires the calibration for the specific region in which the hazard takes place. The events parameters required for estimating the intensity in a region are indicated by the specific hazard physical model. Given the random magnitude of natural phenomena, the events parameters will be a set of random variables in order to represent such characteristic. The calibrated hazard model determining the intensity of the hazard in any part of the region considered is assumed to be known and denoted by the deterministic function $\mathcal{D}$. Thus, each hazard intensity local evaluation, X_i, can be defined as $X_i = \mathcal{D}(z_i; \Theta)$, where the vector Θ denotes the event parameters required by the model, while the vector z_i encompasses the buildings' location in the region. So, the X_is are all dependent, through the deterministic physical model $\mathcal{D}$, on the event parameters Θ and on the buildings' fixed geographical location z_i.

Since $\mathcal{D}$, for any z_is, is non-decreasing as Θ changes to the event parameters representing an event with lower exceedance probability (so, a less frequent event), X_is and subsequently $g_i(X_i)$s are correlated. Functions $g_i(\cdot)$s are non-decreasing. Even the X_is are non-decreasing with increasing hazard intensity.

There is a positive correlation among building losses which can be attributed to the event intensity (captured by parameters in Θ). Given a specific hazard intensity X_i, the part $g_i(X_i)$ is the deterministic term of the building loss called systematic loss. Aggregating the correlated systematic part of the loss for the individual buildings, the systematic loss of the region can be expressed as

$$L^s = \sum_{i=1}^{N} g_i(X_i) = \sum_{i=1}^{N} g_i\big(\mathcal{D}(z_i; \Theta)\big) = G(\Theta)$$

L^s, which represents the systematic loss of the region (assuming the presence of N buildings in the region), is a deterministic function of Θ given that the location of the buildings z_i, their structural characteristics (captured by $g_i(\cdot)$) and the hazard model of the region (captured by $\mathcal{D}(\cdot)$) do not change. So, it can be simplified to $G(\Theta)$.

Summing the residual losses of the buildings in the region, the residual loss of the region (L^r) is obtained as shown in

$$L^r = \sum_{i=1}^{N} \sigma_{X_i} \varepsilon \sim \mathcal{N}\left(0, \sqrt{\sum_{i=1}^{N} \sigma^2_{X_i}}\right) \text{ or } \mathcal{N}(0, \sigma_\Theta)$$

L^r, which is the sum of N normally distributed random variables, is a normal random variable with $E(L^r) = 0$ and $Var(L^r) = \sum_{i=1}^{N} \sigma^2_{X_i}$. For simplicity, its standard deviation is written as

σΘ. The part $\sigma_{X_i}\varepsilon$, which is uncorrelated among the buildings of the region, is the stochastic term of the building loss called residual loss.

So, in the end, the total loss of the region (L) is equal to the sum of the systematic and the idiosyncratic residual loss of the region as it is possible to see in

$$L = \sum_{i=1}^{N} L_i = \sum_{i=1}^{N} g_i(X_i) + \sum_{i=1}^{N} \sigma_{X_i}\varepsilon = L^s + L^r$$

The part of the natural catastrophe risk which can be transferred to the capital markets by issuing parametric CAT bonds is the systematic one. By transferring the systematic risk to the capital markets, given that the residual loss is uncorrelated among the buildings of a region, the remaining part of the risk, namely the residual risk, becomes idiosyncratic and hence insurable.

After hurricane Andrew hit the Bahamas, Florida and Louisiana in 1992, CAT bonds were created. The effects of the hurricane were disastrous. The hurricane in fact sent eleven insurance companies into bankruptcy. The insurance industry understood that the tail risk linked with natural disasters could have been so severe to jeopardize insurance companies' solvency due to the lack of sufficient reserves to cover it. Entering into a reinsurance treaty with a special purpose vehicle (SPV) let the insurance company diversify natural disaster risk through financial markets and investors. Through a SPV, an insurance securitization is performed: insurance risk is converted into financial or investment risk. The SPV, which would cover losses if an event were to happen, issues securities to finance this coverage, the catastrophe bonds. In exchange for possible loss payments, the cedent insurer pays a premium to the SPV. Catastrophe options are very similar to excess reinsurance as far as the functioning is concerned: the right to a cash payment is given to the purchaser in the event that a specified index of catastrophe losses reaches the strike price previously specified.

CAT bonds potential is undoubtedly huge in a normal situation and the market data prove that it has already been seen.

Swiss Re (2021) reports that the overall market keeps growing and it is well on its way toward its third consecutive year of growth (*Figure 10*). Since 2011, the catastrophe bond market has achieved a Compound Annual Growth Rate (CAGR) of 9.9%. This pace of growth may make a USD 50 billion market possible by the end of 2025.

Figure 10: Catastrophe bond market issued vs outstanding notional
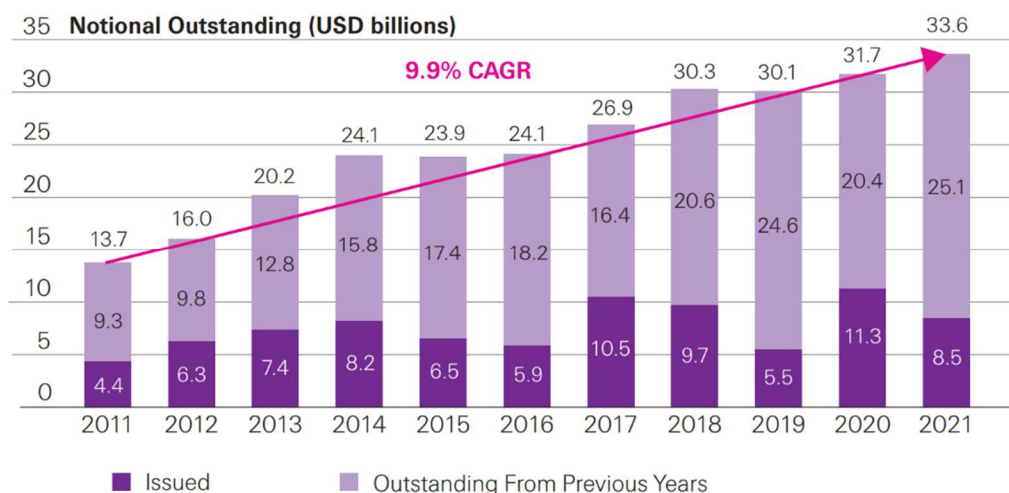
Source: Swiss Re Capital Markets Deal Database, as of June 30, 2021

Anyway, it's not all roses because we still have not considered climate change and CAT bonds are surely not invulnerable to it and its consequences. At the moment, according to Morana and Sbrana (2019), climate change risk may not yet have been properly incorporated in CAT bond multiples (or return per unit of risk), that is to say the coupon to expected loss ratio. This ratio yields a measure of CAT bonds riskiness. Falling CAT bond multiples observed were mainly related to the Fed's expansionary monetary stance and to portfolio shift effects: natural disaster risk is evidently and significantly undervalued. This is consistent with the inconclusive available empirical evidence on the pricing of climatic change in financial markets reported in Monasterolo and De Angelis (2018). To be clearer, the problem would not concern the single issued CAT bond: it would not directly suffer the effects of the climate change because of its short maturity (from one to five years, but usually not higher than 3 years). The real problem would concern the validity of the instrument in itself in the future.

Recovering the model presented for flood losses and the CAT bond price sensitivity analysis performed in Kurniawan et al. (2021), some climate change implications for these instruments are shortly discussed.

According to its regular functioning if a natural disaster occurs during the CAT bond contract and it causes a loss to the sponsor exceeding the threshold H specified in the contract, the loss will be paid by the issuer to the sponsor. Conversely, if no disaster triggers the CAT bond, all money deposited by the issuer as part of the CAT bond will be returned to the investor. Looking for expectations of the formed cash flow structure it is possible to obtain the CAT bond price formula as follows

$$P(t,T) = \mathbb{E}^{\mathbb{Q}}[D(t,T) \cdot \Psi | \mathcal{F}_t]$$

where:

- $P(t,T)$ is the price of CAT bond at time t with the end time of the contract T
- $D(t,T)$ is the discount factor
- Ψ represents the cash flow
- $\mathcal{F}_t$ is a filtration, which is an increasing family of sigma-algebras on the set of states of the world, so that $\mathcal{F}_t \subseteq \mathcal{F}_T$, for all $0 \leq t \leq T$
- the conditional expectation $\mathbb{E}^{\mathbb{Q}}[\,\cdot\,|\mathcal{F}_t]$ represents the expectation under the risk-neutral probability measure $\mathbb{Q}$ given the information available at time t.

The cash flow can be also written as $\Psi = V - \omega V 1_{\eta<T} = V \cdot (1 - \omega 1_{\eta<T})$, where:

- V is the face value of the CAT bond
- η is the trigger time for CAT bond, whose value is the minimum t where the cumulative loss value reaches the threshold H
- ω is the proportion of the invested money V deducted by the issuer as part of the compensation to the sponsor
- 1 is the indicator function of the event $\eta < T$ which means that $\begin{cases} 1 & if\ \eta < T \\ 0 & otherwise \end{cases}$

If a natural disaster occurs after the contract ends ($\eta > T$), at the end of the contract the investor will get all his money back and thus the cash flow will be $\Psi = V$. If a natural disaster occurs before the contract expires ($\eta < T$), the investor will get his money back after deducting the proportion ω, whose value is between 0 and 1 depending on the amount of loss incurred. Thus, the cash flow will be $\Psi = V(1 - \omega)$.

Substituting the cash flow formula in the CAT bond price formula and assuming that the discount factor is independent of the random variable, the following formula for CAT bond pricing at time $t = 0$ is obtained:

$$P(0,T) = D(0,T) \cdot V \cdot \mathbb{E}^{\mathbb{Q}}\big[(1 - \omega 1_{\eta<T})|\mathcal{F}_t\big]$$

Given that the CAT bond presented in Kurniawan et al. (2021) is designed for floods, a model for describing flood losses is needed. Flood losses are modelled by following Merton's Jump Diffusion Process model[21], which can be written as

$$dL_t = \mu dt + \sigma dW_t + (Y - 1)dN_t$$

where:

- μ is the drift or trend, whose value can be found from the average loss

---

[21] Jump processes are used to address the problem of fat tails in losses distribution.

- σ is the volatility, whose value can be found from the standard deviation of losses
- W_t represents the Brownian motion
- Y represents the jump factor which is normally distributed with a μ_J average and a σ_J standard deviation
- N_t declare a standard Poisson process with the parameter λ

Given that the cumulative loss curve must be an increasing monotonous curve, an adjustment procedure is needed to avoid curve downwards movements which may be possible due to model randomness. So, if the loss recorded at time t is lower than the loss recorded at time $t - 1$, then the loss at time t will be reported as equal to the loss recorded at time $t - 1$.

A jump detection is performed by the Sequential Average (SEQAVG) algorithm in order to obtain the jump frequency λ, the average jump μ_J and the jump standard deviation σ_J. In Riley (2008), SEQAVG algorithm is explained in detail. At first, the length of the data group (or group size) is specified. Denote it as $lgth$. The default $lght$, that is the number of data divided by 10, can be used. The jump threshold limit can be set manually. Denote it as lim. Anyway, in Kurniawan et al. (2021), it is the default one, that is $lim = 3 \cdot \sigma_y$ at Averaging Factor (AF), with AF equal to the number of data divided by $lght$. Then, the average of the first group is computed. Thus, the jump limits, which will be considered to detect a jump, are defined as $jump\ limits = average \pm lim$. Looping through all data starting from $i = lgth + 1$, the exceedance of jump limits is verified. If they are exceeded and so there is suspicion of a possible jump at $i = j$, the local average, which is the average over from 1 to $lgth$ points starting at the suspected jump, is computed in order to precisely verify the jump limits exceedance. If the limits are not exceeded and so the jump is disproved, the loop restarts from $i = j + 1$. On the contrary, if the limits are exceeded, the local average computation is performed from $i = j$ to $i = j + lgth - 1$. In the event that the jump is confirmed, the new average, which will become the new base in determining the $jump\ limits$, is computed. The loop restarts from $i = j + 1$. After all data are tested, it is possible to compute the actual frequency averages between jumps and the other parameters.

After having defined the stochastic model for flood losses, the authors have performed a Monte Carlo simulation in order to obtain cash flow expectations and so to compute CAT bond prices. Then, other simulations have been performed to analyse the relationship between CAT Bond

prices and the input parameters N, r, H and ω. The simulations have been performed using the set of parameters presented in **Table 3**.

Table 3: Kurniawan et al. (2021) simulations' parameters

Parameter	Value
T	1
V	10×10^9
μ	8.5802×10^6
μ_J	1.8201×10^7
λ	0.0055
σ	4.8758×10^6
σ_J	3.3335×10^6

Given that the contract for the bond is assumed to be one year, the value of T is 1. The face value V must be determined by the bond issuer: the authors has chosen 10×10^9 rupiahs as a plausible value for the simulation since the loss deriving from floods in 2019 is in billions of rupiahs. The other five parameters are based on the computations performed in the Jump Detection process. The model relies upon maximum rainfall data of the 10-year period 2009-2019 from six urban villages (Keputih, Kedung Cowek, Gubeng, Wonorejo, Wonokromo, and Gunung Sari) in Surabaya, the second-largest city in Indonesia.

Checking the results, it is possible to state that the number of iterations N does not really affect the price of CAT bond and that price changes are not too significant for different values of r. As shown in **Figure 11** and **Figure 12**, the parameters greatly influencing the CAT bond price are the threshold H (even if over 2×10^9 the price remains almost constant) and the proportion ω.

In **Figure 11**, the simulation has been performed setting the value of ω at 0.8, with N = 1000 and r = 0.05.

Figure 11: Price curve by threshold H
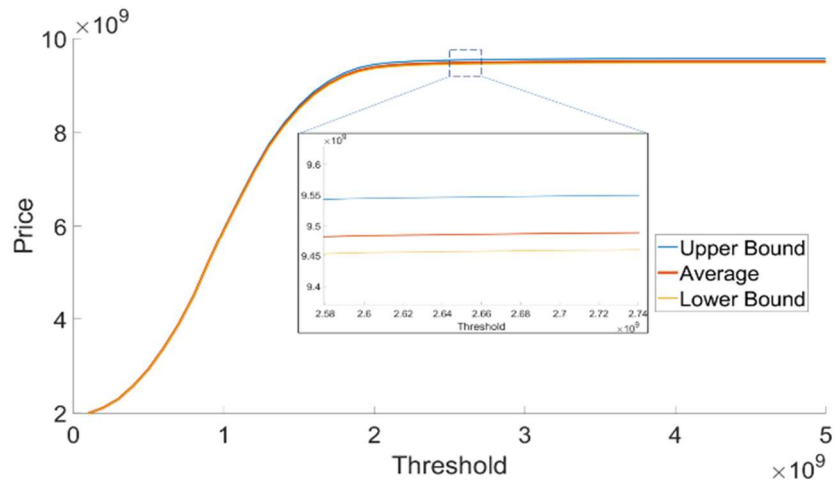
Source: Kurniawan et al. (2021)

In ***Figure 12***, the simulation has been performed setting the value of H at 6×10^8, with $N = 1000$ and $r = 0.05$.

Figure 12: Price curve by proportion ω
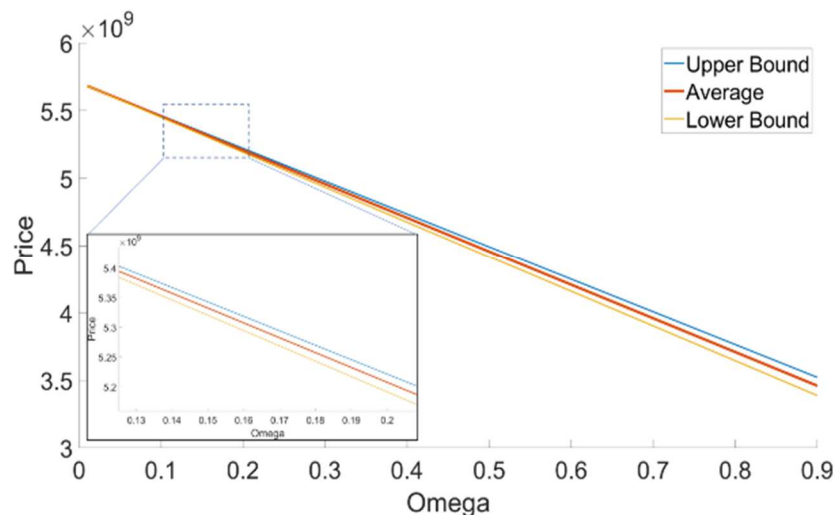
Source: Kurniawan et al. (2021)

Decreasing the threshold and increasing the proportion could be a reasonable move for reinsurance companies because of the increasing frequency and intensity of natural disasters, even if it would have negative effects on prices. Given that CAT bonds' prices are paid by investors to reinsurance companies, very low prices would consist in lower income for reinsurance companies. As the size of catastrophes increases, the limitation of reinsurance markets could emerge: if the risk is too large to aggregate and diversify, the reinsurance industry in its entirety may not be able to provide sufficient capital to cover a loss.

1.5 Weather derivatives, not climate ones

Weather can be either catastrophic or non-catastrophic according to its severity of impact. Catastrophic weather includes the above-mentioned low probability extreme events. These events (e.g., hurricanes) cause massive financial damages threatening lives and properties. Catastrophic weather risk is covered by insurance contracts, offered by insurance companies thanks to the possibility of resorting to insurance securitization.

Non-catastrophic weather concerns seasonal deviations in average, minor deviations from usual or normal weather (e.g. warmer than usual winters). It affects companies' performance resulting in uncertainty in future cash flows. As regards weather derivatives, non-catastrophic weather is concerned. Businesses interested in weather derivatives are mainly belonging to the weather (and climate) sensitive sectors which have been presented in section 1.3.

What does "weather sensitivity" refer to? It refers to the sensitivity of sales, production or costs to meteorological elements such as temperature, rainfall, snowfall, wind, etc. If the volatility of the output of a sector is due to changes in weather, the sector is said to be weather sensitive. The underlying of these derivatives consists of weather data (e.g., daily temperature). Weather derivatives are not created to hedge the price of the underlying: they are suitable for hedging other risks on which the weather has a major influence (e.g. decline in sales in the energy and power sector as a result of a cooler summer than average). Indeed, weather mostly affects the quantity of production and/or demand for a given good, not its sale price: weather derivatives primary objective is thus to hedge volume risk rather than price risk.

Going into detail, they are usually based on HDD and CDD: these acronyms stand for "heating degree day" and "cooling degree day", respectively. In Hull (2015), a single HDD is defined as $HDD = \max(0, 65 - A)$, while a single CDD is defined as $CDD = \max(0, A - 65)$.[22] In these short formulas, A denotes, respectively, the average of the highest and lowest temperature recorded during the day in a specific weather station. In this case the temperatures are measured in degrees Fahrenheit. To summarize, a degree day is a measure of how much a day's average temperature deviates from 65 degrees Fahrenheit/18 degrees Celsius and thus of the volume of energy required for heating or cooling during the day. Monthly HDD and CDD index values consist of the sum of each daily HDD or CDD value. Each daily HDD or CDD value is simply calculated according to how many degrees an average daily temperature deviates above or below respectively from the baseline of 65° Fahrenheit (in the US) and 18° Celsius (in Europe). In Europe, the summer cooling month contracts are not based on CDD, rather they are based

---

[22] The number in the formula is clearly linked to the unit of measurement to which we refer. If the degrees Celsius are used, 65 is replaced by 18.

on a cumulative average temperature (CAT). Each monthly CAT index includes the daily average temperatures' accumulation over a calendar month: the accumulation period starts from the first calendar day of the contract month and ends on the last day of the contract calendar month. A seasonal strip contract is built on the cumulative HDD or CDD values recorded during a five-month period within the season. The traditional heating season for HDD Seasonal Strips runs from November through March. Another heating season encompasses the period December - February. The traditional cooling season for CDD Seasonal Strips runs from May through September. Another cooling season encompasses the period July - August. Likewise, a CAT seasonal strip is built on the cumulative average recorded during the five-month period within the season. CAT seasonal strip's seasons are typically the same of HDD and CDD seasonal strips.[23] Seasonal strips' traditional seasons are summarized in **Table 4**.

Table 4: Seasonal strips' seasons

Strip	Seasons	
HDD Seasonal Strip – Winter	November - March	December - February
CAT Seasonal Strip – Winter	November - March	December - February
CDD Seasonal Strip – Summer	May – September	July - August
CAT Seasonal Strip – Summer	May - September	July - August

Source: CME group website

The derivatives shortly described above are just the most common ones because standardized and traded in the market. As shown in **Table 5**, the weather derivatives traded are slightly different depending on the area of the world for which they are created and on the customization required.

Table 5: Weather derivatives range for different areas

City Locations	Index Used Winter	Index Used Summer	Time Frames for Contracts
United States	HDD	CDD	Weekly, Monthly, Seasonal Strip: A customized season of two to seven consecutive months within the same general season – October through April for Winter, April through October for Summer

---

[23] 'Managing Climate Risk with CME Group Weather Futures and Options – CME group', CME group, accessed 07 May 2022, https://www.cmegroup.com/content/cmegroup/en/education/articles-and-reports/managing-climate-risk-with-cme-group-weather-futures-and-options.html

Canada	HDD	CAT, CDD	Monthly, Seasonal Strip: Same as U.S. contracts
Europe	HDD	CAT	Monthly, Seasonal Strip: Same as U.S. contracts
Asia Pacific	CAT[24]	CAT[24]	Monthly, Seasonal Strip: A customized season of two to seven consecutive months within the same general season – October through April for Winter, April through October for Summer
Australia	HDD	CDD	Monthly, Seasonal Strip: Same as U.S. contracts

Source: CME group website

Other examples of weather derivatives offered by CME group are:

- Hurricane futures and options
- Hurricane seasonal futures and options
- Hurricane seasonal maximum futures and options
- Frost and snowfall indexes

Outside CME group product range, it is possible to arrange derivatives based on other weather phenomena such as rainfall and wind.

One of the main drivers behind the weather derivatives' market growth is the convergence of capital markets with insurance markets as already shown by the spread of catastrophe bonds. Starting from their introduction in 1997, as shown in *Figure 13*, weather derivatives experienced periods of great popularity as the widening of the range of contracts offered by CME group through the years shows. Their popularity ultimately faded leading to only 10 US and 2 European cities traded nowadays.

---

[24] CAT index is formed slightly different: the daily average temperature is defined as the arithmetic average of the hourly temperatures accumulated over a 24-hour period as reported by EarthSat using data received from the Japan Meteorological Agency for the meteorological stations of Tokyo, Osaka and Hiroshima.

Figure 13: Number of listed contracts at the Chicago Mercantile Exchange, by continent, from 1999 to 2018
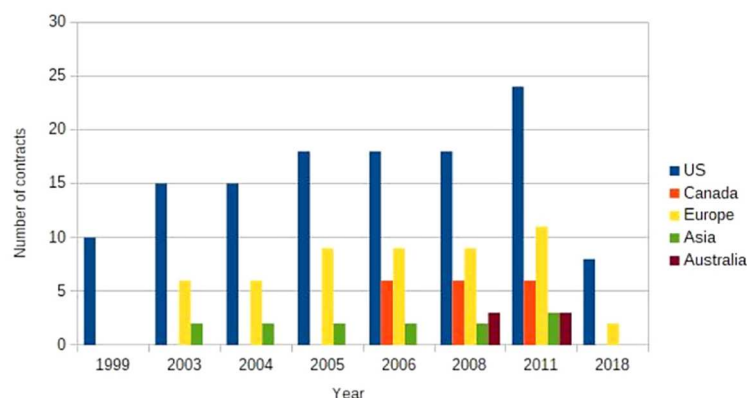
Source: CME group website

Anyway, most of the volumes of weather derivatives business are being traded in OTC market. One main reason behind this shift is the basis risk which is the risk resulting from the differences in weather patterns between the traded location and the hedged location. Weather risk is in fact highly geographically localised: weather varies significantly even considering small distances between locations.

From this simple description it is easy to understand that weather derivatives are very short-term hedging instruments. Their maturities are often expressed in months. In such short maturities it is not possible to clearly see the effects of climate change. Therein lies the problem because climate change has been proving that weather does not necessarily need to be extreme to have serious financial consequences on companies' performance. Indeed, even small but continual adverse weather deviations can cause negative impacts on companies' cash flows and value in the long term. In the future it might be necessary to move the thresholds of these contracts forward because of the progressive extreme climate new ordinariness. Anyway, moving the threshold just means adapting the reference point to changing climatic conditions: the long-term climate risk would be still uncovered and the economic activities would be jeopardized in any case in the long run.

Considering for example the energy sector, weather derivatives can be an efficient way to hedge a problem of one season every now and then. As mentioned in Dell et al. (2014), energy companies sell HDD or CDD contracts in order to manage the risk of diminished revenues under mild weather conditions given that the quantity of energy sold is strongly dependent on consumer demand which is, in turn, driven by temperatures. HDD or CDD contracts can be utilized to guard against the volumetric risks which are based upon the quantity of energy that might be expected to be marketed throughout the course of a heating or cooling season. Anyway, given that warming will likely increase summer peak electricity demand, meeting

increases in demand sooner or later may require investments in new energy generation and distribution infrastructure. Moreover, the system reliability and peak demand management, through new mechanisms to be put in place, will be necessary. This activity can be more expensive than average demand levels.

Although their recently limited popularity and their unsuitability to hedge long term climate risks, there is still room for weather derivatives, especially for what concerns the hedging of the short-term climate change effects. Clearly, they are a transitional solution to face the climatic problem satisfying the short term needs of protection.

The best way to tackle the climatic change would undoubtedly be to speed up the transition to a low carbon economy. In order to limit global warming, GHG emissions, which mainly consist of carbon dioxide (CO_2) and methane (CH_4), must be significantly reduced. Carbon dioxide enters the atmosphere mainly through the burning of fossil fuels and natural materials for transportation, energy production and industrial processes, while the production of natural gas and oil entails the largest part of methane emissions. To realize the low-carbon economy and achieve the zero GHG emissions objective by 2050, according to IEA (International Energy Agency) estimates, total CO2 emissions need to fall by approximately 45% from 2010 levels by 2030 and, to do so, the demand for coal will need to fall by 60% by 2030 with developed markets shifting away from reliance on it as a fuel source to renewables.[25]

It is clear that until the achievement of these challenging goals climate risks will not be spread equally among sectors and areas of the world. The need of instruments which can spread long term climate-related risks is evident. Anyway, these instruments still are not available in the market although some instruments have been theorized. In the following chapter, these hypothetical climate derivatives will be illustrated.

---

[25] 'Climate Risk and the Transition to a Low-Carbon Economy', The Harvard Law School Forum on Corporate Governance, accessed 13 May 2022, https://corpgov.law.harvard.edu/2021/03/02/climate-risk-and-the-transition-to-a-low-carbon-economy/

CHAPTER 2: Climate Derivatives

2.1 Are they really different?

The problems we faced in shortly examining the financial instruments already on the market which might seem suitable to hedge and protect from climate change are mainly their short maturity and so the inability by the indexes they are built on to properly encompass the climate change dynamics.

As shown by ***Figure 14***, there are no financial instruments able to cover the long-term. Without climate derivatives, climate change issue would not be covered: only its short-term effects would be.

Figure 14: Comparison between weather and climate impacts' timescales and economic and risk management
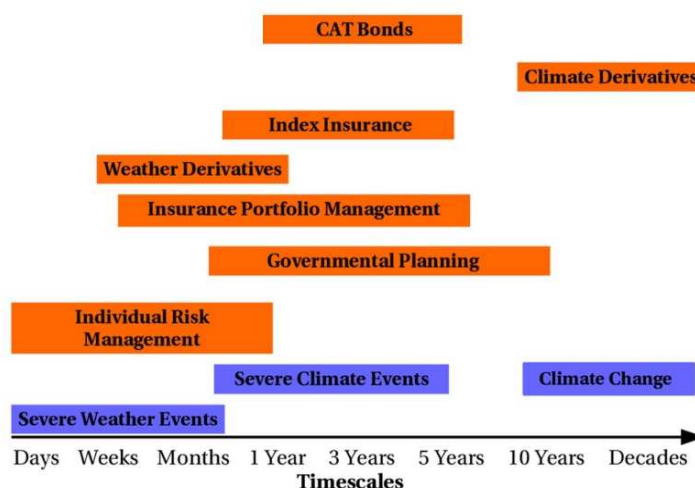
Source: Franzke (2017), modified

For a long time, the expression "climate derivatives" was used with a similar meaning or even as a synonym of "weather derivatives". This misconception is still widespread as a September 2021 "Investment Executive" article by "The Canadian Derivatives Institute" testifies. This article, titled "Hedging against climate risks using weather derivatives"[26], reports that

"Weather derivatives — also known as climate derivatives — were launched in 1999 as a way to hedge against financial losses related to climate risks. Weather derivatives work similarly to insurance."

---

[26] "Hedging against climate risks using weather derivatives", Investment Executive, The Canadian Derivatives Institute, 10 September 2021, https://www.investmentexecutive.com/inside-track_/the-canadian-derivatives-institute/hedging-against-climate-risks-using-weather-derivatives/

The misunderstanding is evident. In addition to the usage of the two expressions as synonyms, in the article it is also implied that even "climate risk" is a synonym of "weather risk". Another example easily found on the Internet is:

"Climate derivatives are financial instruments used to hedge against financial losses related to adverse weather conditions, such as droughts, hurricanes, and monsoons. Climate derivatives, also known as weather derivatives, work in a similar fashion to insurance. The buyer of a climate derivative will receive a monetary payment (as stipulated by the derivative contract) by the seller of the derivative in the event a certain climate-related event occurs or if the buyer suffers any financial loss due to a climate event." [27]

In this case, in addition to the above-mentioned misunderstanding related to "weather" and "climate", climate derivatives seem to have more in common with CAT bonds than with weather derivatives: the payment is subordinated to the occurrence of a predetermined climate event.

Even in academic publications there is no clarity on what climate derivatives are. In Bressan and Romagnoli (2021), published in the "Journal of Financial Stability", without going into much detail, the only distinction between a weather derivative and a climate derivative concerns the higher riskiness of the latter financial instrument. No distinction is made for what concerns the features and the pricing methodology.

Maybe the lack of clarity is due to the fact that at the present time there is no financial instrument on the market with characteristics suitable to hedge climate risk in the long term. Anyway, this is only partially true because it is possible to find that the concept of "climate derivative", even if in a very early phase, was envisioned right a few years after the birth of the weather derivatives' market. In Thornes (2003) climate derivatives, although envisioned as an advisable evolution of weather derivatives, were described as financial instruments having the potential to cope with climate fluctuations since multi-year contracts. In particular, they were expected to hedge against changes in the climate mean and/or standard deviation. The potential great interest by companies having long-term exposure to the climate (e.g., power companies) was already recognised given their sizeable amount of capital related to infrastructures. These instruments were deemed to be of possible interest to companies in need of forecasting the long-term future demand level for their products to plan investments (e.g., water companies). Anyway, there was no model behind the concept of "climate derivative" and for many years this idea remained in the shadows. There are still not so many examples of climate derivatives

[27] "Weather Derivative", Investopedia, J. Chen, 20 May 2022, accessed 14 June 2022, https://www.investopedia.com/terms/w/weatherderivative.asp

in the literature and there is no record of climate derivatives on the market. It is reminded that climate derivatives that will be discussed in the following sections have only been theoretically projected.

Anyway, this lack cannot be an excuse. In the examples provided above the misconception is not just a matter of naming: the proper insight of the key characteristics of climate change is missing. It is evident that there is no consideration of the fact that the long run matters and that climate change effects are strongly correlated and cannot be considered in isolation as a single visible event.

Bloch, Annan, and Bowles (2010) and Bloch, Annan, and Bowles (2011) provide one of the earliest models of proper climate derivatives. After having designed a climate model and the financial instruments in the former paper, an example of application is provided by the authors in the latter paper. They are presented in section 2.2.

The model of climate derivative ("climate linker") which has inspired the present thesis is presented in Chikhani and Renne (2021). As we will see in section 2.3, climate linkers are credited with the attempt of enhancing the sharing of the risks related to climate change which notably affect some economic sectors and some areas of the world. Closed-form solutions are provided for their pricing.

An alternative model of climate derivative is presented in Little et al. (2015). As we will see in section 2.4, this financial instrument maintains the location specificity which characterises weather derivatives, while a wider time span is covered. Its maturity can in fact reach one or two decades.

2.2 Climate derivatives from Bloch, Annan, and Bowles (2010; 2011)

Sea-level rise is the climate change effect addressed in papers by Daniel Bloch and other authors (see Bloch, Annan, and Bowles (2010) and Bloch, Annan, and Bowles (2011)). Each project manager involved in coastal developments in designing such developments decides the degree of sea level rise they must defend against over their useful life. Anyway, the only application of cost-benefit analysis and economic optimization techniques in the decision-making process is suboptimal from an economic welfare perspective because projects are treated in isolation. The cost of such defence, which have multi-decade life-span, is a non-linear function of the degree of sea level rise. The authors believes that, thanks to the introduction of climate derivatives, it would be possible to redistribute risks between projects (both already built projects and newly planned ones). In this way, governments and sea-front developers could hedge the financial disruption due to climate events. In fact, given the immediate disbursement

of funds conditional on meeting certain conditions characterising derivatives (e.g., a predetermined level of sea rise), no assessment of the actual loss incurred is required setting climate derivatives apart from traditional insurances.

Pricing climate derivatives is not like pricing weather derivatives. For weather derivatives pricing, the standard method of combining classical market approaches with a weather forecast model is used. Given their non-tradable underlying, pricing weather products must be based on the actuarial pricing approach of marked-to-model. Anyway, weather data are generally non-stationary and, hence, forecasting weather in the long term is really difficult.

Instead, as regards climate data, the authors believe that they are closer to stationary given the fact that short-term and seasonal variations are filtered out. Thus, climate data can be approximated with a Markov process. To some extent, global mean temperature and, in general, climate predictions are more reliable than few days weather forecasts. In the following sub-sections, the financial instruments and the model upon which they rely are described.

2.2.1 The model

The probability space $(\Omega, \mathcal{F}, \mathbb{P})$, where $\mathcal{F}_t$ is a right-continuous filtration including all $\mathbb{P}$ negligible sets in $\mathcal{F}$ is considered. Given the market price of risk λ (recalled from Alaton, Djehiche, and Stillberger (2002) and assumed to be 0 in Bloch, Annan, and Bowles (2011) for simplicity of exposition), the existence of an equivalent martingale measure $\mathbb{Q}$ is assumed. As a result of the absence of arbitrage opportunities, contingent claims can be valued by taking expectation of their discounted payoffs under the risk-neutral measure.

The global mean temperature can be modelled continuously with a diffusion process. In some cases, the Atmosphere Ocean General Circulation Models (AOGCMs) can be approximated successfully with some linear Markov dynamics.

Bloch, Annan, and Bowles (2010) considers an Ornstein–Uhlenbeck process for the dynamics of the global mean temperature and proposes a realistic semi-empirical model[28] for estimating the global sea-level response.

Chaiyapo and Phewchean (2017) is referred for the mathematical definition of an Ornstein-Uhlenbeck (OU) process. The OU process is the stationary and continuous in probability

---

[28] According to the semi-empirical method, the change in global sea level is related to the change in temperature. It assumes the existence of a statistical relationship between the two which can be extrapolated into the future using the temperature rise simulated by global climate models.

stochastic process which describes the characteristic of a mean-reverting process (it drifts toward the mean). The stochastic differential equation of the OU process is

$$dS_t = \lambda(\mu - S_t)dt + \sigma dW_t$$

where:

- λ is the rate of mean reversion
- μ is the long-run mean
- σ is the process volatility
- W_t is the Wiener process

Returning to the original notation and denoting as $(Y_t)_{t\geq0}$ the global mean temperature (valued in the open subset D under the historical measure $\mathbb{P}$), as $(X_t)_{t\geq0}$ the sea-level process and as $(V_t)_{t\geq0}$ the baseline temperature, the following SDEs are obtained relying on the definition of the OU process.

$$dY_t = \theta(\bar{Y} - Y_t)dt + \sigma_Y(t)d\widehat{W}_Y(t)$$

$$dX_t = \theta(Y_t - V_t)dt + \sigma_X(t)d\widehat{W}_X(t)$$

$$dV_t = \kappa(\bar{Y} - V_t)dt, V_0 = \bar{Y}_0, \kappa < \theta$$

The Brownian motions are uncorrelated, that is $\langle d\widehat{W}_X, d\widehat{W}_Y\rangle_t = 0$.

For the sake of clarity:

- $\bar{Y}$ is the equilibrium or mean value supported by fundamentals (the long-run mean)
- σ_Y and σ_X are the volatilities caused by the shocks
- $\theta > 0$ is the rate of mean reversion, which means the rate by which the shocks dissipate and the variable reverts toward the mean
- $\bar{Y}_0$ is the deviation of spot price from its long-term value. It is a base temperature at which sea level is in equilibrium with climate, so that the rate of change of sea level is proportional to the warming above that level. The baseline temperature at which there is no sea-level rise is assumed to be 0.5°C below the mean temperature of the period 1951–1980.
- $\kappa > 0$ is the rate of mean reversion of the base temperature.

For the model viability, it is necessary that $\kappa < \theta$, so the speed of mean reversion of the baseline temperature must be smaller than that of the global temperature.

Integrating the SDEs, the following solutions are obtained

$$Y_t = \alpha_Y(0, t) + Z_Y^*(0, t)$$

33

$$X_t = \alpha_X(0,t) + Z_{XY}(0,t)$$

where:

- $\alpha_Y(0,t) = Y_0 e^{-\theta t} + \theta \int_0^t \bar{Y} e^{-\theta(t-s)} ds,$

- $\alpha_X(0,t) = X_0 + aY_0 \frac{(1-e^{-\theta t})}{\theta} + a \int_0^t \bar{Y} \left(1 - e^{-\theta(t-s)}\right) ds - a \int_0^t V_s ds,$

- $Z_Y^*(0,t)$ is normally distributed with mean equal to zero and variance equal to $V_{Z_Y^*}(t) = \int_0^t \sigma_Y^2(s) e^{-2\theta(t-s)} ds$

- $Z_{XY}(0,t)$ is normally distributed with mean equal to zero and variance equal to

  $V_{XY}(t) = V_{Z_X}(t) + (\frac{a}{\theta})^2 V_{Z_Y}(t)$ with $V_{Z_Y}(t) = \int_0^t \sigma_Y^2(s)(e^{-\theta(t-s)} - 1)^2 ds$ and

  $V_{Z_X}(t) = \int_0^t \sigma_X^2(s) ds.$

- The weight a is a function of time tending to zero.

2.2.2 The products

After having illustrated the model, the types of financial instruments proposed in Bloch, Annan, and Bowles (2011); Bloch, Annan, and Bowles (2010) are presented: they are the digital coupon swap, the climate default swap and the climate bond.

Digital coupon swap

The maturity is discretized into n time-steps representing the fixing period such that $T = n\Delta t$, that is $T_0 < T_1 < \cdots < T_n$.

For every path of the simulation, the digital coupon swap present value is

$$PV = \sum_{i=1}^n e^{-\int_0^{T_i} r_s ds} \left(SCpn(T_i) I_{\{X_{T_i} < K(T_i)\}} - BCpn(T_i) I_{\{X_{T_i} \geq K(T_i)\}} \right)$$

The coupon $SCpn$ is paid by the buyer of protection in the event that the underlying index X_{T_i} does not reach the strike value $K(T_i)$, while the coupon $BCpn$ is paid by the seller of protection in the event that the underlying index X_{T_i} reaches and passes the strike value $K(T_i)$. For $t \in [0,T]$, the strike $K(t)$ is piecewise constant given by $K(t) = \sum_{i=1}^n k_i I_{[T_{i-1}, T_i]}(t)$ where k_i is a positive constant. Either the coupon $SCpn$ and the coupon $BCpn$ are paid at the considered fixing date T_i. Moreover, they can either be a cash value or a function of time.

Given the linearity of this product, its present value at time $t_0 = 0$ can be rewritten as a sum of digital options

$$PV = \sum_{i=1}^n B(t_0, T_i) \left(SCpn(T_i) E_{t_0}[I_{\{X_{T_i} < K(T_i)\}}] - BCpn(T_i) E_{t_0}[I_{\{X_{T_i} \geq K(T_i)\}}] \right)$$

It is the sum of the difference between the present value of two floating legs where each leg is expressed as a coupon weighted by a probability of exercise.

Letting the coupon $BCpn(T_i)$ be given by

$$BCpn(T_i) = SCpn(T_i) + Sp_T(t_0)$$

where the spread Sp is determined at t_0 and maintains the same value regardless of the reference date i (thus, it is a positive constant), then the par value is

$$Sp_{T,par}(t_0) = \frac{\sum_{i=1}^{n} B(t_0, T_i) SCpn(T_i) \left(2E_{t_0}[I_{\{X_{T_i} < K(T_i)\}}] - 1 \right)}{\sum_{i=1}^{n} B(t_0, T_i) E_{t_0}[I_{\{X_{T_i} \geq K(T_i)\}}]}$$

Given the choice of underlying process' Gaussianity, the pricing framework is similar to that one of the Bachelier model. The swap pricing is explained under the risk-neutral measure.

As results from the reformulation of swap in terms of digital options, the swap price depends on the price of a digital option. Given the maturity T_i and the strike $K(T_i)$, the digital option at time $t_0 = 0$ is

$$D_C(t_0, K(T_i), T_i) = B(t_0, T_i) E_{t_0}[I_{\{X_{T_i} \geq K(T_i)\}}] = B(t_0, T_i) P(X_{T_i} \geq K(T_i))$$

where from $X_t = \alpha_X(0, t) + Z_{XY}(0, t)$, the set of exercise becomes

$$\{\alpha(t_0, T_i) + \sqrt{V_{XY}(T_i)} z \geq K(T_i)\}$$

where $z \sim N(0, 1)$ is a standard Normal random variable.

Therefore, the price of the digital option becomes

$$D_C(t_0, K(T_i), T_i) = B(t_0, T_i) \left(1 - N(\Lambda(T_i)) \right)$$

where $\Lambda(T_i) = \frac{K(T_i) - \alpha(t_0, T_i)}{\sqrt{V_{XY}(T_i)}}$ and $N(\cdot)$ is the cumulative distribution function of the standard normal distribution.

Putting terms together, the digital coupon swap becomes

$$PV(t_0) = \sum_{i=1}^{n} B(t_0, T_i) \left(SCpn(T_i) N(\Lambda(T_i)) - BCpn(T_i) \left(1 - N(\Lambda(T_i)) \right) \right)$$

In the special case where $BCpn(T_i) = SCpn(T_i) + Sp_T(t_0)$ the par value simplifies to

$$Sp_T(t_0) = \frac{\sum_{i=1}^{n} B(t_0, T_i) SCpn(T_i) \left(2N(\Lambda(T_i)) - 1 \right)}{\sum_{i=1}^{n} B(t_0, T_i) \left(1 - N(\Lambda(T_i)) \right)}$$

Climate default swap

The climate default swap allows one to transfer the climate risk of a reference entity named C between two counterparties A and B. Based on climate data, the swap transparently lists the trigger events to recover part of the value of the risky asset.

Assume that:

- A buys protection until swap maturity against the risk of a loss in the event that reference C defaults.

- As a result, A pays a coupon, called the fixed leg of the swap, to the seller B on fixed event dates until the reference C defaults or swap maturity is reached.

- In the event that C defaults before maturity of the swap, the seller of the protection B pays the buyer protection to A.

  Payment can be made in two ways, physical settlement or cash settlement, and it is equivalent to the difference between the nominal of the debt covered by the swap and the recovery rate observed at default time.

    1. In the first case, the buyer of protection A delivers the seller of protection B a number of bonds issued by C corresponding to the nominal of the swap and receives in return the nominal of the swap paid in cash.

    2. In the second case, the seller of protection B provides cash payment corresponding to par value minus the recovery rate $(1 - R)$ to the buyer of protection A. The recovery rate is calculated from quotations obtained after the default event. The spread or margin that cancels the climate default swap (CDS) is called the fair spread or fair margin.

        Assuming coupons are paid until default, ignoring the running coupon and recovery payment at default time, the fair spread, computed equating the fixed leg and the floating leg, would be

        $$s^* = (1 - R) \frac{\int_{T_0}^{T} e^{-\int_{T_0}^{u} r_s ds} P[\tau \in du] du}{s \sum_{i=0}^{N-1} (T_{i+1} - T_i) B(T_0, T_{i+1}) P(\tau > T_{i+1})}$$

        where the probability that the underlying reaches the barrier level during the time increment dt is $P[\tau = dt]$, which is the density of the random variable τ that can be obtained once known the distribution function $dP[\tau \leq t]$.

The similarities between climate and credit default swap are evident. Maintaining the same notation, the credit default swap can be defined, quoting e.g., Amadei et al. (2011), as a contract aimed at transferring a credit exposure on a bond issuer, which is the "reference entity" C, in relation to a given nominal value. The swap buyer A, in exchange for the recurrent payments

of the premium to the seller B until the credit maturity date, will receive a positive payoff from the seller B in the event that a credit event occurs in relation to the reference entity C.

When a credit event occurs, the contract is terminated and the seller B must pay the buyer A the nominal contract value. Again, payment can be made in two ways:

- physical settlement, according to which the swap buyer A delivers the reference entity bonds in exchange for their nominal contract value

- cash settlement, according to which there is no exchange of the underlying securities and the seller B pays the buyer A the difference between the nominal value and the underlying bond market value.

Thus, CDS pricing methodology has been developed similarly to credit default swap one. It would be possible to apply the logic of pricing credit derivative products to climate derivatives replacing the survival probabilities and default time densities with the first-passage complementary distributions and first-passage time density.

The distribution of the first passage time is of critical importance in the valuation of the contract. With the sea-level issue, company A is long the protection against the underlying reaching an up-barrier level b with $b = \lambda X_0$, where λ is a positive constant and $(X_t)_{t>0}$ is the underlying process defined on $(\Omega, \mathcal{F}, P)$ and the default is the first passage time of the barrier $\tau = \inf\{t; X_t > b\}$, which is, for instance, the first time the sea level rises above the barrier level at a given fixing date. On one hand, company A would pay company B the fixed payment Cpn at time at $T_i, i = 1, \dots, N$ where N is the number of payments up to time T. Thus, the fixed payment would be $CpnI_{\{T_i < \tau\}}$ at T_i. On the other hand, company B would pay the recovery value R to company A conditional on the underlying passing of the barrier.

The fixed leg of the climate default swap, assuming continuous payment for simplicity, can be written as

$$Fixed\ leg = Cpn_T(t)E\left[\int_t^T e^{-\int_t^u rds} P[\tau > u] du | \mathcal{F}_t\right]$$

The floating payment is $CpnI_{\{t < \tau < T_N\}}$ at τ, so the floating leg of the climate default swap can be written as

$$Floating\ leg = E\left[\int_t^T (1 - R)e^{-\int_t^u rds} P[\tau \in du] du | \mathcal{F}_t\right]$$

It is linear in the recovery value R.

Equating the fixed leg and the floating one at time t the default climate rate $Cpn_T(t)$ at maturity T is obtained. Therefore, the par default climate rate is given by

$$Cpn_{T,par}(t) = \frac{\int_t^T (1-R)B(t,u)P[\tau \in du]du}{\int_t^T B(t,u)P[\tau > u]du}$$

The underlying probability of reaching the barrier level during the time increment dt is $P[\tau = dt] = \frac{dP[\tau \leq t]}{dt}$.

Given that no analytical survival probability[29] for an Ornstein-Uhlenbeck process is known by the authors, numerical tools should be used to estimate the first passage time of the sea level process X_t.

Climate Default Bond

A special case of the climate default swap is the climate default bond. Recalling the first passage time τ with barrier level b, denote the bond maturity as T and the protection maturity as T^* such that $T^* \leq T$. The protection maturity T^*, associated the first passage time τ of the barrier level b, is relevant for determining the bond payoff at bond maturity T.

Assuming a unity face value and following Longstaff and Schwartz (1995)[30], the payoff at maturity is

$$\phi = I_{\{\tau > T*\}} + I_{\{\tau \leq T*\}}(1-R)$$

The payoff would be 1 in the event that the first passage takes place when the protection is ended, while it would be $(1-R)$ in the event that the first passage takes place before the ending of the protection.

So, the climate default bond at time t_0 in the risk-neutral measure is:

$$CB(t_0, T^*, T) = E_{t_0}\left[e^{-\int_{t_0}^T r_s ds}\right] - E_{t_0}\left[e^{-\int_{t_0}^T r_s ds} RI_{\{\tau \leq T*\}}\right]$$

Since interest rates are independent of the climatic variable and thus deterministic, it is possible to simplify the notation of the price of the climate default bond as

$$CB(t_0, T^*, T) = B(t_0, T)\big(1 - RP(\tau \leq T^*)\big).$$

It consists in the estimation of a default event occurrence probability. In the limit, when $R \to 0$, the risk-free bond is recovered. Given that the yield at time t_0 is $Y(t_0, T) =$

---

[29] The proportion of units that survive beyond a specified time.

[30] In particular, the payoff structure for the valuation of floating-rate debt is recovered. Denote as $F(X, r, \tau, T)$ the value of one floating-rate coupon payment to be made at time T with the floating rate determined at time $\tau, \tau \leq T$. The payoff on this claim at time T is the value of r at time τ if default does not occur prior to T, and $(1 - \omega)r$ if it does. The payoff of this claim at time T can be expressed as $r(1 - \omega I_{\gamma \leq T})$, where I is the indicator function which takes value 1 if first-passage time γ is less than or equal than T and 0 otherwise.

$-\frac{1}{T-t_0} log CB(t_0, T^*, T)$, the spread with a risk-free bond is $Sp(t_0) = Y(t_0, T) +$ $\frac{1}{T-t_0} log B(t_0, T)$. The spread, recalling the simplified version of climate default bond price formula, can be written as $Sp(t_0) = -\frac{1}{T-t_0} log(1 - RP(\tau \leq T^*))$.

2.2.3 The estimation

Although the model is a continuous stochastic one, in order to infer the model parameters, the authors have chosen an alternative approach to the Linear Inverse Modelling (LIM) method described by Penland and Magorian (1993) to estimate mean reversion speed of the model. This alternative approach consists in exploiting the fact that the AR(1) model is the discrete equivalent of the Ornstein–Uhlenbeck process. Thus, the Ornstein–Uhlenbeck process is discretized and the AR(1) model is recovered.

To price climate derivatives, an appropriate time scale is needed. Sub-annual time scale does not matter for the long-term predictions required by these financial products. It is not just about the need; it is about the correctness. In fact, the longer-term climate variations are not correctly represented looking at the lag-1 autocorrelation of monthly data. Moreover, the annual cycle in mean temperature must be correctly removed. To avoid any of these problems, annual data are considered. The chosen unit of time (ut) is the sampling interval, presently 1 year. The SDEs are integrated using 50-time steps per sampling interval ($\Delta t = \frac{1}{50} ut$).

In order to simulate the model trajectories, parameters' estimates to some historical data are needed. Thus, artificial data are constructed using different climate models: these climate models are allowed to run freely under fixed boundary conditions, that is fixed greenhouse gas concentrations, and no changes in any of the other external factors (volcanic eruptions, changes in solar forcing and human factors are considered so). Excluding changes in the external factors and fixing GHG concentration, since factors influencing the balance of energy entering and leaving the Earth system, allows to work under constant forcing conditions. Indeed, climate forcing is, quoting Denning (2018), "*the difference between the rate of energy received by absorption of solar radiation and the rate of energy emitted by the top of the Earth's atmosphere*". Effects deriving from occasional and unpredictable events (e.g., volcanic eruptions) are thus excluded. In this way, the purely internal variability of the atmosphere–ocean system is estimated.

In the example presented in Bloch, Annan, and Bowles (2011), annual mean temperature data are generated by the UK Hadley Centre (HadCM3) and the Japanese MIROC climate models run for 2000 years.

Assuming $(X_t)_{t\geq 0}$ is an Ornstein–Uhlenbeck process with positive constant parameters ρ and σ, the dynamics of the model are

$$dX_t = \rho(\bar{X} - X_t)dt + \sigma dW_t$$

The authors assume that, letting $T = N\Delta t$, these dynamics can be discretized as

$$X_n = \rho\bar{X}\Delta t + (1 - \rho\Delta t)X_{n-1} + \sigma\sqrt{\Delta t}\,y \qquad n = 1, \ldots, N$$

where $y \sim N(0,1)$, which means that the distribution of y is time-independent. Given X_0, the parameters ρ and σ are unknown and must be estimated.

Setting $K_1 = e^{-\rho\Delta t} \approx (1 - \rho\Delta t)$ and $\bar{\sigma} = \sigma\sqrt{\Delta t}$, the process is rewritten as

$$X_n = C + K_1 X_{n-1} + \bar{\sigma}y_n$$

for $C = (1 - K_1)\bar{X}$. The sequence $X_0, \ldots, X_N$ is a first-order autoregressive sequence with lag-1 correlation coefficient K_1. Linearly interpolating the values $X_n = X(n\Delta t)$ for $n \in [1, N]$, the desired path is recovered. The equation for X_n is the recursive representation of the AR(1) process with conditional mean and variance

$$E[X_n|X_{n-1}] = C + K_1 X_{n-1}$$

$$Var[X_n|X_{n-1}] = \bar{\sigma}^2.$$

Lagging that equation by p period (where $p = 1$ is the original equation) and recursively substituting the result in the original equation, one obtains the following formula

$$X_n = C\sum_{j=0}^{p-1} K_1^j + K_1^p X_{n-p} + \bar{\sigma}\sum_{j=0}^{p-1} K_1^j y_{n-j}$$

where

$$C\sum_{j=0}^{p-1} K_1^j = (1 - K_1)\,\bar{X}\sum_{j=0}^{p-1} K_1^j = \bar{X}\sum_{j=0}^{p-1} K_1^j - K_1\bar{X}\sum_{j=0}^{p-1} K_1^j = \bar{X}\sum_{j=0}^{p-1} K_1^j - \bar{X}\sum_{j=0}^{p-1} K_1^{j+1}$$

Assuming stationarity, which occurs in the event that $|K_1| < 1$, and taking the limit $p \to \infty$, K_1^p will approach zero. From the infinite geometric series, one obtains the following formula

$$X_n = \bar{X} + \bar{\sigma}\sum_{j=0}^{\infty} K_1^j y_{n-j}$$

since $\frac{C}{1-K_1} = \bar{X}$, which is an infinite-order moving average.

Recalling Hamilton (1994), in fact, an infinite-order moving average process, which is denoted as MA(∞) process, is described as

$$Y_t = \mu + \sum_{j=0}^{\infty} \psi_j \varepsilon_{t-j} = \mu + \psi_0 \varepsilon_t + \psi_1 \varepsilon_{t-1} + \psi_2 \varepsilon_{t-2} + \cdots$$

When the coefficient $|\psi| < 1$, the condition $\sum_{j=0}^{\infty} |\psi_j| < \infty$ is satisfied: a sequence of numbers $\{\psi_j\}_{j=0}^{\infty}$ satisfying this condition is absolutely summable (and so also square summable). Therefore, the variable X_n can be written as an infinite sum of past shocks, whose most distant shocks have increasingly smaller weights. Since $|K_1| < 1$, the coefficients are geometrically declining . When $K_1 = 1$ the unit root case is obtained and X_n has infinite memory, which means that past shocks never die out. Thus, the closer K_1 is to unity, the more distant past matters.

According to Hamilton (1994), an MA(∞) process which satisfies the condition $\sum_{j=0}^{\infty} |\psi_j| < \infty$ is ergodic for the mean and if the ε are Gaussian the process is ergodic for all moments. Since in the model we are exploring each y_{n-j} is an i.i.d. standard normal and $|K_1| < 1$, the unconditional mean and variance can be computed as

$$E[X_n] = \bar{X}$$

$$Var(X_n) = \bar{\sigma}^2 \sum_{j=0}^{\infty} K_1^{2j} Var(y_{n-j}) = \frac{\bar{\sigma}^2}{1 - K_1^2}$$

It can be noted that the unconditional variance is larger than the conditional one when $K_1 \neq 0$. Going forward to the future the number of shocks increases so that the variance grows as a function of K_1.

The equations on the process X_t are simpler if the time series is first reduced to zero mean by subtracting the sample mean as

$$V_n = X_n - \bar{X} \text{ for } n = 1, \dots, N$$

where X_n is the original time series, $\bar{X}$ is the sample mean and V_n is the mean-adjusted series. The AR(1) model for the mean-adjusted series in year n becomes

$$V_n = K_1 V_{n-1} + \bar{\sigma} y_n$$

Then, a time series of random noise is generated by sampling from an appropriate distribution. Assuming some starting values for V_{n-1}, a time series of V_n is recursively generated. The usual assumption is that the noise is normally distributed with mean zero and variance equal to the variance of the residuals from fitting the AR(1) model to the data. Simulations can be used to

generate empirical confidence intervals of the relationship between the observed time series and the climate variable. A prediction form of the AR(1) model is $\hat{V}_n = \hat{K}_1 V_{n-1}$, where the hat indicates an estimate. The equation can be applied one step ahead to get the estimate $\hat{V}_n$ from the observed V_{n-1} while k-step-ahead prediction can be made by applying the above equation recursively. The resulting anomaly temperature from the zero mean time series representation is more easily measurable than the true global temperature because the former is homogeneous over large scales showing no predictable trends or seasonality, while the latter varies much more rapidly given the observing stations 'incomplete coverage. Given that the autoregressive parameter of global temperature is estimated by modelling the time series with an autoregressive process $AR(p)$ for $p > 1$, an autocorrelation analysis is performed to determine the order p: in particular, an autocorrelation function (acf) test called correlogram is performed, measuring the correlation ρ_k between observations at different times, for lags k ranging from 0 to 9 years. The acf of an AR(1) model declines geometrically as a function of lag: the chosen climate model should exhibit the same behaviour (in the example for the MIROC model the same behaviour is observed, for the HadCM3 model not completely). Thus, the Maximum Likelihood (ML) method is followed for estimating the parameters of the AR(1) model with data generated from the statistically more significant climate model (MIROC one in the example). From the estimated parameters it is possible to infer the parameters of the temperature process described above. From the estimated autoregressive parameter $\hat{K}_1$, the speed of mean reversion $\theta = \frac{1-\hat{K}_1}{\Delta t}$ for the temperature process is obtained. In the AR(1) model, the estimated first order autoregressive coefficient $\hat{K}_1$ is normally distributed with variance $Var(\hat{K}_1) = \frac{(1-\hat{K}_1^2)}{N}$. Therefore, the 95% confidence interval for $\hat{K}_1$ is $95\% \, CI = \hat{K}_1 \pm 2\sqrt{Var(\hat{K}_1)}$. Given that the noise in the change of temperature dY_t is assumed to be normally distributed with mean zero and variance equal to the variance of the residuals from fitting the AR(1) model to the data, hence, knowing the estimated volatility $\hat{\sigma}$ and that $\Delta t = 1$, the instantaneous volatility of the temperature process σ_Y is derived. Then, knowing the model parameters, a Monte Carlo simulation can be performed to simulate the trajectories dY_t, dX_t and dV_t of the model and so the climate default bond/swap can be computed.

2.3 Climate linkers from Chikhani and Renne (2021)

Climate linkers, which have been designed in Chikhani and Renne (2021), are defined as "*long-dated financial instruments (bonds, swaps, and options) with payoffs indexed to climate-related variables, e.g., temperatures, sea levels, or carbon concentrations*" by the authors themselves.

2.3.1 The rationale

In the authors' intentions these financial instruments would serve three main purposes:

1) They would facilitate the sharing of (physical) long-term climate risks. Indeed, they would be an additional source of reinsurance capacity for the insurance industry and would provide direct capacity to those seeking to transfer long-term climate-related exposure.

2) The existence of a novel market for climate risks may stimulate investors to better understand climate risks and take them into account in their analyses.

3) They would offer a public good by making market participants reveal their expectations regarding future climate. From this information, which would be captured in real-time at high frequency, it would be possible to extract expected trajectories of future temperatures from market quotes of temperature-indexed swaps or bonds[31] and so to judge the perceived credibility and effectiveness of international commitments to climate targets.

For what concerns the first point, it is important to remind that insurance-linked securities (ILS) are typically short-term instruments (most CAT bonds have three years maturity). Given that climate change is a slow-moving and long-term phenomenon, over such limited horizons it is essentially predictable. An ILS risk level does not change between inception and redemption. Although ILS enhance the insurance sector capacity to deal with natural catastrophes reducing the insurance gap[32], they are not helpful for transferring long-term climate risks. Reinsurance capacity would be enhanced by climate linkers because of their distinctive capacity of transferring these risks.

Moreover, climate linkers' availability would help the (re)insurance industry address worse-than-expected long term scenarios and provide new diversification opportunities for long-term investors.

For what concerns second and third points, it is worth noting that expectations and trajectories would be adjusted for risk: risk premiums are embedded in expectations extracted from market prices. These market-based expectations may not coincide with future climate physical expectations. Changes in climate linkers may be interpreted as changes in expectations in the event that risk premium components of their prices vary relatively slowly through time.

---

[31] In the same manner as inflation expectation measures are currently extracted from inflation linkers.

[32] The difference between insured and total losses.

Moreover, models could be used to try and extract risk premiums from observed market prices to recover the corrected physical expectations. Naturally, such market-based measures would not directly improve climate change understanding.

Market-based measures would however be valuable for the following reasons:

- Considering that market participants would need climate models for the pricing of these instruments, they would engage in their development contributing to research efforts on climate modelling. Assuming similarities in the launch phase between weather derivatives and climate linkers, it may be useful to refer to Purnanandam and Weagley (2016) which reports that the launch of a weather derivative on a city's temperature results in more precise temperature measurement by the dedicated weather station. Given that data collected by weather stations become reference points for many contracts, the increase in third parties 'interest and scrutiny creates even more pressure on weather stations to produce better measures. Following this reasoning, climate models would be refined after the launch of climate linkers on the market to better reflect climate dynamics.

- The observation of changes in these prices (available at high frequency) would allow measuring the influence of different types of news on agents' expectations. Typically, one could observe how markets evaluate the effectiveness of policies announced during international summits.

- The trajectories of climate-related variables extrapolated from observed prices may be used to construct "market-based" scenarios. These scenarios constructed from market data, in addition to model-based scenarios constructed from model output data, may be used to price long-term insurance premiums or assets exposed to climate risks. Importantly, if climate options were available, the definition of worst-/best-cased scenarios (corresponding to specific probabilities) could also be derived. The latter may for instance help design climate stress tests.

According to the authors, governments may be the initial issuers of climate-indexed debt instruments. The major benefits of the issuance of these novel types of bonds for governments are the potential widening of the investor basis which would support the demand for sovereign debt, the strengthening of their incentives to implement policies fighting climate risks given the increase in their long-term exposure to these risks and the expectation of earning climate-risk premiums when issuing such instruments.

For what concerns the latter reason, higher payoffs would be delivered in "bad states of nature". Although expected returns of these assets are lower than standard bonds' ones, investors should

be willing to buy these bonds. Moreover, these issuances should be expected to result in lower debt service for the government as of the date of issuance.

Anyway, this reasoning has two main drawbacks:

1. the premium would be reduced/cancelled in the early years because of the empirically observed negative "novelty premium". Investors in fact tend to ask for higher premiums to hold new issued type of assets.

   In Costa, Chamon, and Ricci (2008) the so called novelty premium is hypothesized to be due to *the novelty of the instrument, the complexity of the pricing valuation, its liquidity, market concerns about the accuracy of variables that affect the payment, co-movements of return with other assets, the difficulty of fitting this new financial product in the overall asset-liability management, and potentially risk aversion*. Novelty premium declines as the markets deepen. For example, novelty premium on Argentina's GDP-linked warrants recorded a decline of about 600bp during the first 18 months after issuance.

2. public debt managers ought not to only target the minimization of the average debts' costs. They ought to consider borrowing costs in relation to risk. As reported in Coe, Pesaran, and Vahey (2003), according to the World Bank-IMF Guidelines (2001) public debt management main objective is *to ensure that the government's financing needs and its payment obligations are met at the lowest possible cost over the medium to long run, consistent with a prudent degree of risk*.

However, the introduction of sovereign climate-indexed bonds would encourage the development of climate derivatives markets as it happened for the market of inflation indexed derivatives following the introduction of U.S. government inflation-linked bonds. Thus, governments could have an important role in reducing entry costs paving the way for private issuances. Issuers would be likely firms involved in climate-risk mitigation activities such as renewable-energy producers and electric vehicle makers.

2.3.2 The products

The range of financial instruments proposed encompasses swaps, bonds and options in order to satisfy different investors and hedgers needs.

Temperature Indexed Swap

A zero-coupon Temperature Indexed Swap (TIS) is a derivative product which represent the agreement between two counterparties to exchange, at predetermined dates, a fixed rate payment on the notional amount N, which is determined at the time the swap is negotiated, for a payment indexed to the reference index, the temperature measure T, which is observed after

the negotiation. Current negotiation date is denoted by t. The indexed payment is made by the protection seller to the protection buyer. Given that the maturity date is $t + h$, the temperature seller will pay $T_{t+h}N$ to the temperature buyer on date $t + h$ (this is the protection leg of the swap). The fixed rate payment is paid by the protection buyer to the protection seller. The protection buyer pays $T_{t,h}^S N$ to the protection seller (this is the premium leg of the swap). So, just to summarize, the protection buyer receives $(T_{t+h} - T_{t,h}^S)N$ on date $t + h$, while the protection seller receives $(T_{t,h}^S - T_{t+h})N$ on date $t + h$. The temperature swap rate $T_{t,h}^S$, which is negotiated by the two counterparties on date t, is such that the two legs' values are equal on date t.

Considering the baseline case with risk-neutral agents and risk-free interest rates independent from temperatures, it is possible to state that $T_{t,h}^S = \mathbb{E}_t[T_{t+h}]$ under the absence of arbitrage opportunities, where $\mathbb{E}_t$ denotes the expectation conditional on the information available on date t. Thus, rewriting previous formulas, the protection buyer receives $(T_{t+h} - \mathbb{E}_t(T_{t+h}))N$ at maturity. When temperature rises above its expected path, the temperature buyer receives more from the temperature seller than what he pays, and vice versa.

Relaxing the risk-neutral assumption and denoting by $\mathcal{M}_{t,t+h}$ the stochastic discount factor (s.d.f.) between dates t and $t + h$, the price of the protection leg is $\mathbb{E}_t[T_{t+h}, \mathcal{M}_{t,t+h}]$, while the price of the premium leg is $T_{t,h}^S \mathbb{E}_t[\mathcal{M}_{t,t+h}]$. Given that the two legs of the swap have the same value at date t, the following formula is obtained:

$$T_{t,h}^S = \mathbb{E}_t\left[\frac{\mathcal{M}_{t,t+h}}{\mathbb{E}_t[\mathcal{M}_{t,t+h}]}T_{t+h}\right].$$

Thus, the TIS rate can be seen as a risk-adjusted expectation of T_{t+h}, and that the risk-adjustment depends on $\frac{\mathcal{M}_{t,t+h}}{\mathbb{E}_t[\mathcal{M}_{t,t+h}]}$. Formally, $T_{t,h}^S$ is called h-forward risk-neutral expectation of T_{t+h}, and $\frac{\mathcal{M}_{t,t+h}}{\mathbb{E}_t[\mathcal{M}_{t,t+h}]}$ is the Radon-Nikodym derivative linking the physical and risk-neutral measures. The h-forward risk-neutral measure $\mathbb{Q}^h$ is equivalent (in the measure sense) to the physical one. So, $T_{t,h}^S$ can be rewritten as $T_{t,h}^S = \mathbb{E}_t[T_{t+h}] + prem_{t,h}$, with $prem_{t,h} = \frac{Cov_t[T_{t+h}, \mathcal{M}_{t,t+h}]}{\mathbb{E}_t[\mathcal{M}_{t,t+h}]}$. This formulation shows that $prem_{t,h}$, the difference between the swap-implied temperature ($T_{t,h}^S$) and the expected temperature ($\mathbb{E}_t[T_{t+h}]$), depends on the covariance between temperatures and the s.d.f.. So, if states of higher temperature are perceived as "bad states of the world" (states of high marginal utility, or high s.d.f.) then the swap-implied temperature is above its expectation because the covariance term is then positive. In that case, the protection buyer is willing to lose money, on average, to be hedged against temperature risk.

Temperature Indexed Bond

A zero-coupon Temperature Indexed Bond (TIB) is a debt instrument whose payoff is indexed to a given measure of temperature. Denoting the issuance date by t and the maturity at issuance by h, the payoff, settled on date $t + h$, is of the form:

$$1 + \chi(T_{t+h} - T_{t,h}^0)$$

where $T_{t,h}^0$ is a temperature defined by the issuer on the issuance date and parameter χ is a leverage factor. The temperature $T_{t,h}^0$ could for instance be set to the expected temperature on date $t + h$ (as of date t), that is $T_{t,h}^0 = \mathbb{E}_t[T_{t+h}]$. In that case, the expected payoff of the TIB would be equal to 1. While the expected payoff of the TIB is equal to that of a standard zero-coupon bond when $T_{t,h}^0 = \mathbb{E}_t[T_{t+h}]$, the price of the two types of bonds (with matching maturities) are not necessarily equal. Formally, the TIB price is then given by:

$$\mathbb{E}_t[\mathcal{M}_{t,t+h}\{1 + \chi(T_{t+h} - \mathbb{E}_t(T_{t+h}))\}] = \mathbb{E}_t[\mathcal{M}_{t,t+h}] + \chi prem_{t,h}$$

where $prem_{t,h}$ is defined, as before, $prem_{t,h} = \frac{Cov_t[T_{t+h}, \mathcal{M}_{t,t+h}]}{\mathbb{E}_t[\mathcal{M}_{t,t+h}]}$ and $\mathbb{E}_t[\mathcal{M}_{t,t+h}]$ is the price of a zero $-$ coupon bond with a deterministic payoff of 1 at maturity. Therefore, the difference between the TIB price and $\mathbb{E}_t[\mathcal{M}_{t,t+h}]$ is equal to $\chi prem_{t,h}$. It can be noted that the TIB payoff $1 + \chi(T_{t+h} - T_{t,h}^0)$ turns negative if $T_{t+h} < T_{t,h}^0 - \frac{1}{\chi}$. To prevent this, TIBs could embed options for the payoff to be equal to $max[1 + \chi(T_{t+h} - T_{t,h}^0), 0]$.

Temperature options

A temperature option is a derivative instrument whose payoff is nonlinearly indexed to a given temperature measure.

Three option types are considered as shown in *Table 6*.

Table 6: Temperature options

Option type	Price (notation)	Payoff (settled on maturity date $t + h$)
Digital	$Dig_{t,h}(T_K)$	$\mathbf{1}_{\{T_{t+h} > T_K\}}$
Call	$Call_{t,h}(T_K)$	$(T_{t+h} - T_K)^+ = \mathbf{1}_{\{T_{t+h} > T_K\}}(T_{t+h} - T_K)$
Put	$Put_{t,h}(T_K)$	$(T_{t+h} - T_K)^- = \mathbf{1}_{\{T_{t+h} < T_K\}}(T_K - T_{t+h})$

Source: Chikhani and Renne (2021)

T_K is the temperature option strike level determined during the negotiation phase at initial date t, while T_{t+h} is the temperature option underlying level at maturity date $t + h$. For example, a temperature call of strike 2°C allows, for instance, to get the payoff $(T_{t+h} - 2)$ on date $t +$

h if $T_{t+h} > 2$, while a temperature put of strike 2°C allows to get the payoff $(2 - T_{t+h})$ on date $t + h$ if $T_{t+h} < 2$.

2.3.3 The model

Chikhani and Renne (2021) designs climate linkers relying on DICE (Dynamic Integrated Climate-Economy) model as proposed in Nordhaus (2016). Since its initial development, the DICE model has been revised many times: the last available version is indeed DICE-2016R. The DICE model is one of three integrated assessment models used to estimate the Social Cost of Carbon (SCC) in the United States. Integrated assessment models (IAMs) are practical frameworks trying to combine multidisciplinary knowledge, which seek to achieve, as stated in Grobecker, Coronili, and Cannon (1974), three main objectives:

1) coordinated exploration of possible future paths of human and natural systems
2) knowledge development about key issues of policies formation
3) research needs' prioritization in order to enhance the ability to identify solid strategic options

The DICE model was proposed for the first time in Nordhaus (1992): it attempts to use economics tools in order to determine an efficient strategy for addressing the global warming issue. According to the author, societies should undertake environmental policies only when their benefits exceed their costs: the level of environmental control should be at that point where the incremental benefits of additional controls no longer exceed the incremental costs. For what concerns the global warming, this approach is easy to articulate, but difficult to execute. Given the need of an economic model of climate change capable of considering the long-time lags between actions or policies and responses, the basic approach is to use an adjusted Ramsey model of optimal economic growth and to calculate the optimal path for both capital accumulation and GHG-emission reductions. The Ramsey model is modified to include climate investments, which are analogous to capital investments in the standard model.

Indeed, in the neoclassical growth model, society invests in tangible capital goods cutting down on consumption today in order to increase consumption in the future. So far as the climate change issue is concerned, by analogy, society must take action today reducing consumption by devoting resources to GHG emissions reduction. In this way, economically harmful climate change effects would be prevented and, therefore, consumption possibilities would be increased in the future. The resulting trajectory could be interpreted as either the most efficient path for slowing climate change given initial endowments or as the competitive equilibrium among market economies where the externalities are internalized using the appropriate social shadow

prices for GHGs. This model allows for different policies in the transition path from those in the ultimate steady state. Thus, it allows a range of sensitivity analyses.

Returning to Chikhani and Renne (2021), in **Figure 15**, the authors' intentions as well as the awaited results are highlighted.

Figure 15: Approach
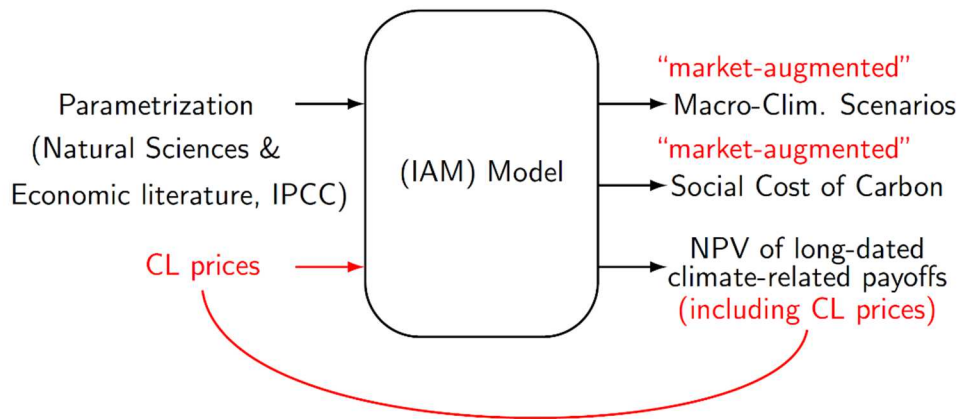
Source: Chikhani and Renne (2021), slides 24 March 2022

So, the model consists in the extension of the standard tools of modern economic growth theory with the addition of both a climate sector and a closed-loop interaction between the climate and the economy. In Nordhaus (1992) and in Nordhaus subsequent papers the specific list of DICE model's equations is provided. The equations are divided into three groups representing the main building blocks: the objective function, the economic relationships and the climate-emissions relationships. The parameters' empirical derivation is also provided. The same structure is maintained in Chikhani and Renne (2021).

In **Figure 16**, the model is schematically represented highlighting the main channels relating climatic and economic variables.

Figure 16: Model representation
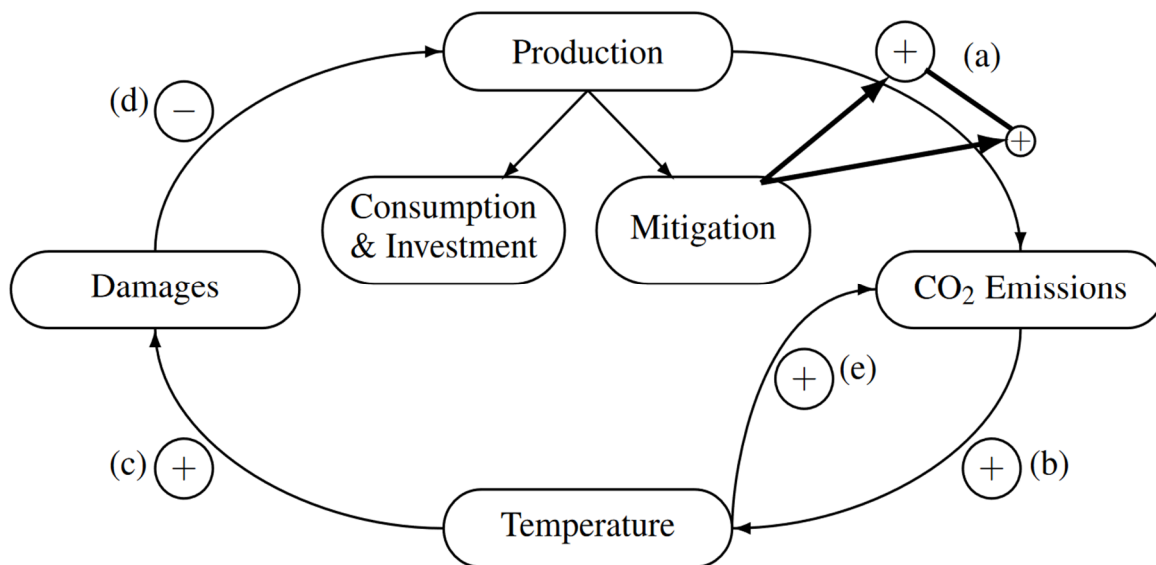
Source: Chikhani and Renne (2021)

The letters indicate the chronological order of the detrimental effects. At first, production involves CO_2 emissions, even though mitigation reduces the magnitude of the positive relation production - emissions (a). As a consequence of the increase in emissions, the temperature anomaly increases (b). Larger temperatures are linked to an increase in the probability of climate related damages (c), which have a negative impact on production because of the resultant reduction in the quality of capital (d). In the meanwhile, temperature increase raises emissions because it is associated to an increase in the probability of triggering a climate change positive feedback loop (e).

Positive feedback loops are processes that amplify the effects of climate forcings and thus cause a further increase in temperatures as compared to an initial warming.[33] Steffen et al. (2018) reports that most of the feedbacks can show both continuous responses and tipping point behaviours. In the latter behaviour, the feedback process becomes self-perpetuating after a critical threshold is crossed and so the change is abrupt. Subsystems exhibiting this behaviour are called "tipping elements". The type of behaviour (i.e., continuous response or tipping point) can depend on the magnitude or the rate of forcing, or a combination of the two. Just to give an idea, the forcing is the difference between incoming and outgoing radiation. Since Earth absorbs energy from the sun, it must eventually emit an equal amount of energy to space. Climate

---

[33] NASA, "The Study of Earth as an Integrated System", accessed 07 August 2022, https://climate.nasa.gov/nasa_science/science/

forcing factors change the climate system altering the energy balance: when incoming energy is greater than outgoing energy, the planet warms.[34]

Anyway, feedbacks may exhibit gradual changes before the tipping point is reached.

As *Figure 17* shows, the tipping elements are classified into three groups according to the estimated threshold temperature. Potential tipping cascades can be triggered by the global temperature rise up to the level of the low temperature cluster. The global average temperature could be pushed even higher if tipping in mid and high temperature clusters is induced by the low cluster tipping elements and non-tipping elements feedbacks (with no apparent thresholds) such as the change in the land and ocean physiological carbon sinks.

Figure 17: Global map of potential tipping cascades
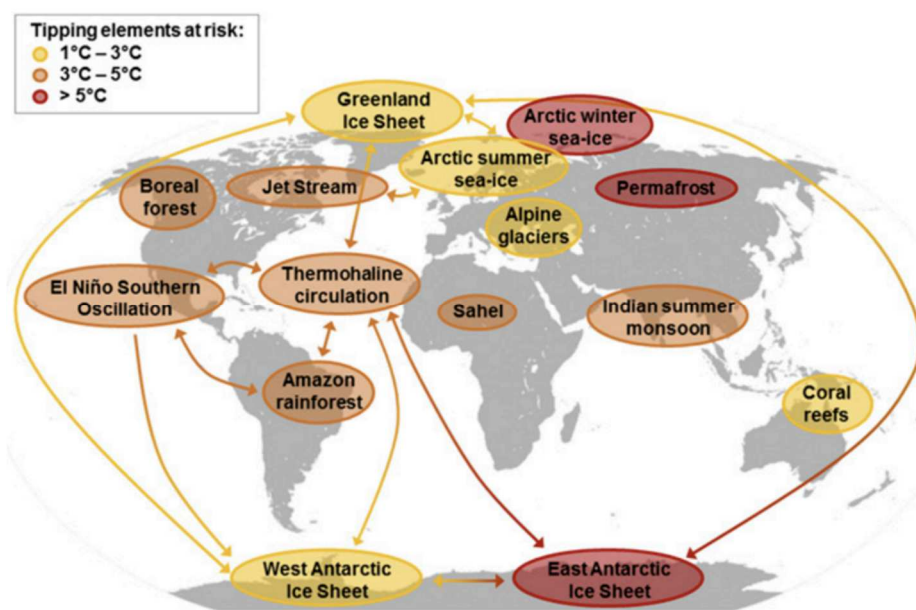
Source: Steffen et al. (2018)

After having triggered a feedback tipping point, as reported in Lemoine and Traeger (2016), even though the level of emissions is reduced, the climate sensitivity to CO_2 is increased. So, despite the emissions reduction, the temperature will increase more strongly than in the situation where no tipping point has been triggered. This additional warming due to, for example, the release of CO_2 and methane trapped in the permafrost illustrates the strong domino effect deriving from the feedback tipping point.

By going into the detail of the model, temperatures are taken into account as temperature anomalies from the 1850 – 1900 baseline period which can be considered as an approximation

---

34 NOAA, "Climate forcing", accessed 10 August 2022, https://www.climate.gov/maps-data/climate-data-primer/predicting-climate/climate-forcing

of the pre-industrial period. This choice is consistent with the Paris Agreement's objectives formulation.

Following the original DICE model, the focus is on two global temperatures lower ocean (T_{LO}) and atmosphere (T_{AT}), whose dynamics depend on radiative forcings due to greenhouse gases (F). The atmosphere temperature, which is the main driver of damages to the economy, can be determined as:

$$T_{AT,t} = T_{AT,t-1} + \xi_1 \left\{ F_t - \frac{\tau}{\nu} T_{AT,t-1} - \xi_2 \left[T_{AT,t-1} - T_{LO,t-1} \right] \right\}$$

where:

- ξ_1 is the climate equation coefficient for upper level
- ξ_2 is the transfer coefficient upper to lower stratum
- F_t represents the dynamics of radiative forcings
- τ represents the forcings of equilibrium CO_2 doubling
- ν is the equilibrium temperature impact

This equation is recalled from Nordhaus (1992) with some slight changes (mainly in the notation). In Nordhaus (1992), in fact, the atmosphere and upper ocean temperature is presented as follows

$$T(t) = T(t-1) + (1/R_1)\{ F(t) - \lambda T(t-1) - (R_2/\tau_{12})[T(t-1) - T^*(t-1)] \}$$

where:

- $T^*(t)$ is the deep oceans temperature
- R_1 is the thermal capacity of the upper stratum
- R_2 is the thermal capacity of the deep oceans
- τ_{12} is the transfer rate from the upper layer to the lower layer
- λ is a feedback parameter

The dynamics of radiative forcings F_t are considered in the linear approximation:

$$F_t = \tau log_2(m_0) + \frac{\tau}{\log(2)m_0} \left(\frac{M_{AT,t}}{M_{PI}} - m_0 \right) + F_{EX,t} + \sigma_F \eta_{F,t}$$

where:

- $F_{EX,t}$ is the (exogenous) part of radiative forcings that is due to non-CO_2 greenhouse gases
- $M_{AT,t}$ is the mass of carbon in the atmosphere, constituting one of the three reservoirs used to capture the carbon cycle
- M_{PI} is its preindustrial level

- m_0 is the value of $\frac{M_{AT,t}}{M_{PI}}$ at which the linearization is performed

- $\eta_{F,t}$ is the persistent Gaussian shock aimed at capturing the uncertainty associated with the climate sensitivity parameter characterising the relationship between atmospheric carbon concentrations and temperatures.

The abovementioned carbon cycle consists in a loop between atmosphere, land, and ocean describing the journey of carbon atoms (mainly in the form of carbon dioxide (CO_2) and methane (CH_4)) on the Earth. Thus, vector M_t components are the carbon masses in atmosphere (AT), upper ocean (UP), and lower ocean (LO).

The carbon cycle is described as

$$M_t = \begin{bmatrix} M_{AT,t} \\ M_{UP,t} \\ M_{LO,t} \end{bmatrix} = \varphi^{\Delta t} M_{t-1} + \frac{\Delta t}{3.666} \begin{bmatrix} \varepsilon_{t-1} \\ 0 \\ 0 \end{bmatrix}$$

where:

- φ is a square matrix, whose column components sum to one, describing yearly transfers of carbon between atmosphere and oceans.

- ε_{t-1} accounts for total carbon dioxide (CO_2) emitted into the atmosphere for each year of period t (one period lasts $\Delta t = 5$ years), converted into carbon masses by applying the conversion rate $\frac{1}{3.666}$.

Total emissions ε_t are defined as

$$\varepsilon_t = \varepsilon_{land,t} + \varepsilon_{ind,t} + N_t$$

where:

- $\varepsilon_{ind,t}$ is an endogenous component representing the industrial emissions due to human activity

- $\varepsilon_{land,t}$ is an exogenous component also representing emissions due to deforestation

- N_t is a persistent shock whose probability of occurring increases with temperature in the atmosphere. It is meant to account for feedback effects related to tipping points' literature.

  In order to do this, N_t is drawn from a gamma-zero distribution[35], which is a distribution featuring a Dirac mass at zero. The probability of having a non-zero N_t

---

[35] From Monfort et al. (2015), letting X be a non-negative random variable. X is said to follow a Gamma-zero distribution with parameters $\lambda > 0$ and $\mu > 0$, denoted $X \sim \gamma_0(\lambda, \mu)$, if its conditional distribution given $Z \sim P(\lambda)$ is $X \mid Z \sim \gamma_Z(\mu)$.

depends on T_{AT}. Although this probability is typically small, N_t still can jump: when it happens, a large and sudden increase in emissions takes place, which further increases temperature, and so on.

Formally, N_t can be written as

$$N_t = \gamma_0 \left(\frac{\rho_N}{\mu_N} N_{t-1} + l_0^{(N)} + l_1^N T_{AT,t-1}, \mu_N \right).$$

The model also encompasses the global mean sea level, which is denoted by H_t. Following the specification proposed by Vermeer and Rahmstorf (2009), it is

$$H_t = H_{t-1} + \Delta t \times a_{SAT} (T_{AT,t} - T_{0,S}) + b_{SAT} \Delta T_{AT,t} + \sigma_H \eta_{H,t}$$

where $T_{0,S}$ is the average atmospheric temperature for the period $1951 - 1980$.

It is a semi-empirical equation: it exploits the link between global sea level and global temperature in past observational data for projecting the future.

For what concerns the economic block underlying the model, a standard production economy where capital quality can be damaged by climatic disasters is considered. On each period, agents allocate production (Y_t) between consumption (C_t), investment in productive capital (Inv_t) and investment in low carbon emissions technologies (Ψ_t).

The production of date t is given by:

$$Y_t = A_t K_t \quad \text{with } A_t = \bar{A} + \sigma_A \eta_{A,t}$$

where:

- A_t is the productivity
- K_t is the quantity of productive capital
- $\bar{A}$ is the average productivity
- $\eta_{A,t} \sim N(0,1)$ is a productivity shock

The dynamics of productive capital are governed by:

$$K_t^* = (1 - dep)K_{t-1} + Inv_t$$
$$K_t = \exp(-D_t)K_t^*$$

The p.d.f. $f_X(x; \lambda, \mu)$ is given by $f_X(x; \lambda, \mu) = \sum_{z=1}^{+\infty} \left[\frac{exp(-x/\mu) \, x^{z-1}}{(z-1)! \, \mu^z} \times \frac{\exp(-\lambda)\lambda^z}{z!} \right] 1_{\{x>0\}} + \exp(-\lambda)1_{\{x=0\}}$, while the Laplace transform of X $\varphi_X(u; \lambda, \mu)$ is given by $\varphi_X(u; \lambda, \mu) = \exp \left[\lambda \frac{u\mu}{(1-u\mu)} \right] for \, u < \frac{1}{\mu}$. Even though the density function of the p.d.f. is complex, the Laplace transform of the Gamma-zero distribution is easy to manipulate. The Gamma-zero distribution, as can be noted from the p.d.f. formula, has a point-mass located at $x = 0$ and so $P(X = 0) = \exp(-\lambda)$.

where:

- *dep* is the depreciation rate
- D_t (≥ 0) represents climatic disasters.
- K_t^* represents planned capital

The productive capital K_t is smaller than K_t^* when $D_t > 0$, that is to say when a climatic disaster occurs. So, the production is persistently affected by climatic disasters. Even variable D_t is drawn from a gamma-zero distribution (which features a Dirac mass at zero). The probability of having $D_t = 0$ is equal to $\exp(-l_0^{(D)} - l_1^{(D)} T_{AT,t-1})$. The probability of $D_t > 0$ positively depends on the atmospheric temperature. Knowing that the increase in industrial emissions pushes temperatures upwards increasing the likelihood of disasters which are harmful for the production, agents are prompted to invest in low-carbon technologies. For a given production level, these technologies allow reducing carbon emissions. Specifically, investing in these technologies allows to reduce the emissions arising out of the production of one unit of goods by the mitigation rate factor μ_t (with $0 \leq \mu_t \leq 1$), whose enhancement is costly. Associated abatement costs are given by:

$$\Psi_t = \Lambda_t Y_t, \quad \text{with } \Lambda_t = \mu_t^{\theta_2} BC_t$$

where:

- BC_t decreases through time in a deterministic way reflecting the fact that the technological progress will reduce the backstop price.
- $\mu_t^{\theta_2}$ captures the fact that the marginal cost of mitigation is increasing on a certain date (with $\theta_2 > 1$).

The agents' output allocation decision between mitigation (Ψ_t), investment in productive capital (Inv_t), and consumption (C_t) depends on their preferences. In order to facilitate resolution, it is assumed that agents have Epstein-Zin preferences with a unit elasticity of intertemporal substitution (EIS).

The agents' optimization problem is simplified: on the initial date $t = 0$, agents decide on a parametric path for the mitigation rate μ_t. So, the parametric path, based on the shapes of emission control rates obtained in standard IAMs, is

$$\mu_t = \min\left[\exp\left(-|\theta_{a,opt}| + |\theta_{b,opt}| \times t\right); 1\right].$$

where $|\theta_{a,opt}| > |\theta_{b,opt}| T^*$, with $T^* = 12$ in order to ensure that complete mitigation is not obtained before 2080 ($T^* = 12$). $\theta_{a,opt}$ and $\theta_{b,opt}$ are chosen by agents on $t = 0$ with the aim

of maximizing their utility. Agents commit to the parametric path and dynamically adjust C_t and Inv_t over time.

However, the equations presented above do not cover the entire model, which is composed of many other endogenous and exogenous (e.g., carbon intensity σ_t, backstop price BP_t, exogenous land emissions $\varepsilon_{land,t}$, exogenous radiative forcings $F_{EX,t}$, abatement costs Λ_t) equations describing the behaviour of all the variables contained in the formulas above reported. For viewing all formulas, please refer to Chikhani and Renne (2021), namely Section 4 and Appendix A.

Solving the model essentially amounts to determining the law of motion of consumption. The consumption growth can be expressed as

$$\Delta c_t = \mu_{c,t} + \sigma_{c,t}\eta_{A,t} - D_t$$

where $\mu_{c,t}$ and $\sigma_{c,t}$ are deterministic functions of the model parameters.

The authors made the model conditionally affine: in this way, closed-form solutions are obtained for conditional moments and distributions. This approach is similar to that one followed in Traeger (2021) for the Analytic Climate Economy (ACE) model (an IAM really close to Nordhaus DICE) which combines a general production system with cutting-edge climate dynamics and solves in closed form thanks to an affine value function.

Affine models are mainly used for what concerns interest rates and in particular term structure models. Recalling Piazzesi (2010), in the context of factor models of the yield curve, the dynamics of the short rate r are replaced by the assumption that the short rate r is a function $R(x)$ of x and $x \in \mathbb{R}^N$ is a time-homogeneous Markov process all under the risk neutral measure. So, x is the state vector. The assumption implies that the conditional expectation in the formula of the price of a zero-coupon bond (whose pay-off is 1 at maturity) $P_t^{(\tau)} = E_t^*\left[exp\left(-\int_t^{t+\tau} r_u du\right)\right]$ is some function F of time-to-maturity τ and the state x_t at time t, or $P_t^{(\tau)} = F(x_t, \tau)$. Functional-form assumptions are made in affine term structure models. The functional-form assumptions are on the short-rate function $R(x)$ and the process x for the state vector under the risk-neutral measure. The short rate is given by $r = R(x) = \delta_0 + \delta_1^T x$ for $\delta_0 \in \mathbb{R}$ and $\delta_1 \in \mathbb{R}^N$, where the choice of short-rate parameters δ_0 and δ_1 depends on the number of factors in the model. The main advantage of making functional-form assumptions lies in the fact that it leads to tractable pricing formulas.

Given that the law of motion of the state vector X_t (gathering all economic and climatic variables) is of the affine class and that the underlying stochastic discount factor $\mathcal{M}_{t,t+h}$ is

exponential affine in X_t, Chikhani and Renne (2021) framework is tractable: it is possible to calibrate this theoretical model and find a solution to it without using the computationally costly Monte Carlo method.

In particular, the state vector X_t is affine conditional on some deterministic processes (e.g., the backstop price). The affine property of the state vector does not preclude disasters such as falls in consumption due to climate events and adverse feedback loops.

The conditional Laplace transform of X_t characterizing the state vector dynamics is of the form

$$\mathbb{E}_t[\exp(u'X_{t+1})] = \exp\left(\alpha_t(u) + \beta_t(u)'X_t\right)$$

where functions α_t and β_t deterministically depend on the model parameters. It is affine in its past values in a time dependent but deterministic fashion. Knowing these functions, the multi-horizon Laplace transform can be easily deduced as

$$\mathbb{E}_t[\exp(u'X_{t+h})] = \exp\left(a_{t,h}(u) + b_{t,h}(u)'X_t\right)$$

where functions $a_{t,h}$ and $b_{t,h}$ are recursively defined. Knowing the multi-horizon Laplace transform is equivalent to knowing the distribution of X_{t+h} conditional on X_t. Thus, through the inverse Fourier transform, as shown in Duffie, Pan, and Singleton (2000), the conditional distribution of any of the state variable (also including any variables' linear combination) at any horizon can be recovered.

2.3.4 The pricing

As already mentioned, the existence of recursive formulas to price long-term assets results from:

  a) the affine property of X_t
  b) the fact that the underlying stochastic discount factor $\mathcal{M}_{t,t+1}$ is exponential affine in X_t.

Exploiting these framework characteristics, pricing methodology is provided for each type of climate linkers illustrated in section 2.3.2. Pricing formulas are directly recalled from section III of Chikhani and Renne (2021) online appendix.

Temperature Indexed Swaps

Thanks to Corollary 1 the computation of the two conditional expectations in $T_{t,h}^S = \mathbb{E}_t\left[\frac{\mathcal{M}_{t,t+h}}{\mathbb{E}_t[\mathcal{M}_{t,t+h}]}T_{t+h}\right]$ is possible. In the model, the s.d.f. $\mathcal{M}_{t,t+h}$ is available in closed form.

  Corollary 1

  Considering an asset whose payoff, settled on date $t+h$, is $\omega'X_{t+h}$, the date-t price of this asset is:

$$\tilde{\varphi}_t^{(h)}(\omega) = \lim_{\varepsilon \to 0} \frac{\varphi_t^{(h)}(\varepsilon\omega) - \varphi_t^{(h)}(0)}{\varepsilon},$$

where the computation of $\tilde{\varphi}_t^{(h)}(\omega)$ is given by Proposition 2.

Temperature Indexed Bonds

Temperature Indexed Bonds pricing relies on Corollary 2, which is reported below.

Corollary 2

Denoting by ω_T the vector that is such that $T_t = \omega_T' X_t$, the date-t price of the TIB considered is:

$$\left(1 - \chi T_{t,h}^0\right)\varphi_t^{(h)}(0) + \chi\varphi_t^{(h)}(\omega_T)$$

where the computation of $\varphi_t^{(h)}(0)$ and $\varphi_t^{(h)}(\omega)$ is explained by Corollary 1 and Proposition 2.

Temperature options

Temperature options pricing relies on Proposition 1, which is reported below.

Proposition 1

Consider an asset whose payoff, settled on date $t + h$, is

$$exp(\omega' X_{t+h})\, 1_{\{a' X_{t+h} < b\}}$$

The date-t price of this asset is given by:

$$\hat{\varphi}_t^{(h)}(\omega, a, b) = \frac{\hat{\varphi}_t^{(h)}(\omega)}{2} - \frac{1}{\pi}\int_0^\infty \frac{Im\left[\hat{\varphi}_t^{(h)}(\omega + iax)exp\,(-ibx)\right]}{x}\, dx,$$

where $Im(x)$ denotes the imaginary part of x and where $\varphi^{(h)}$ is defined as in Proposition 2.

The common pricing part of all the instruments, mainly consistent in Proposition 2 and Proposition 3, provides the computation procedure of the variables contained in the formulas above and illustrates the assumptions made by the authors. Thus, they are reported afterward.

Proposition 2 is referred for what concerns the computation of $\varphi_t^{(h)}$ which is recurrent in all pricing formulas.

Proposition 2

Considering an asset whose payoff, settled on date $t + h$, is $exp(\omega' X_{t+h})$, the date-t price of this asset is given by:

$$\varphi_t^{(h)}(\omega) := exp\left(\varphi_{0,t}^{(h)}(\omega) + \varphi_{1,t}^{(h)}(\omega)' X_t\right),$$

The functions $\varphi_{0,t}^{(h)}(\omega)$ and $\varphi_{1,t}^{(h)}(\omega)$ are defined as

$$\begin{cases} \varphi_{0,t}^{(h)}(\omega) = -\eta_{0,t} - \alpha_t(\pi_t) - \cdots - -\eta_{0,t+h-1} - \alpha_{t+h-1}(\pi_{t+h-1}) + \psi_{0,t}^{(h)}(u_1, \dots, u_h) \\ \varphi_{1,t}^{(h)}(\omega) = -\eta_{1,t} - \beta_t(\pi_t) + \psi_{1,t}^{(h)}(u_1, \dots, u_h), \end{cases}$$

where:

- the $\eta_{0,t}$s, the $\eta_{1,t}$s and the π_t, which is the vector of prices of risk, are defined as

$$\begin{cases} \pi_t = (1-\gamma)\mu_{u,1,t+1} - \gamma\mu_{c,1,t+1} \\ \eta_{0,t} = -log\delta + \mu_{c,0,t+1} + \alpha_t\{(1-\gamma)(\mu_{u,1,t+1} + \mu_{c,1,t+1})\} - \alpha_t(\pi_t) \\ \eta_{1,t} = \beta_t\{(1-\gamma)(\mu_{u,1,t+1} + \mu_{c,1,t+1})\} - \beta_t(\pi_t) \end{cases}$$

  The (recursive) computation of $\mu_{u,1,t+1}$ results from Proposition 3.

  δ denotes the rate of preference for present.

- the functions $\psi_{0,t}^{(h)}$ and $\psi_{1,t}^{(h)}$ are defined, for all t and for $h > 1$, as

$$\begin{cases} \psi_{0,t}^{(h)}(u_1, \dots, u_h) = \psi_{0,t+1}^{(h-1)}(u_2, \dots, u_h) + \alpha_t\left(u_1 + \psi_{1,t+1}^{(h-1)}(u_2, \dots, u_h)\right) \\ \psi_{1,t}^{(h)}(u_1, \dots, u_h) = \beta_t\left(u_1 + \psi_{1,t+1}^{(h-1)}(u_2, \dots, u_h)\right), \end{cases}$$

- u_k is defined as

$$\begin{cases} -\eta_{1,t+k} - \beta_{t+k}(\pi_{t+k}) + \pi_{t+k-1} & for\ k = 1, \dots, h-1 \\ \pi_{t+k-1} + \omega & for\ k = h \end{cases}$$

Proposition 3 is reported in order to provide all the elements for a clear and complete understanding of Proposition 2 since the (recursive) computation of $\mu_{u,1,t+1}$ is needed.

Proposition 3

As already stated, an agent featuring Epstein and Zin (1989) preferences, with a unit elasticity of intertemporal substitution (EIS), is considered.

The time-t utility u_t of a consumption stream (C_t) is recursively defined by:

$$u_t = (1-\delta)c_t + \frac{\delta}{1-\gamma}\log(\mathbb{E}_t exp[(1-\gamma)u_{t+1}]),$$

where:

- c_t denotes the logarithm of the agent's consumption level C_t
- δ denotes the time discount factor
- γ denotes the risk aversion parameter

Knowing that Δc_t is affine in X_t, it can be written as

$$\Delta c_t = c_t - c_{t-1} = \mu_{c,0,t} + \mu'_{c,1,t}X_t$$

where:

- X_t is the state vector, which admits an exponential affine log-Laplace transform

  $\psi_t(u, X_t) := log\mathbb{E}_t(\exp(u'X_{t+1})) = \alpha_t(u) + \beta_t(u)'X_t$ with functions α_t and β_t deterministic.

- $\mu_{c,0,t}$ and $\mu_{c,1,t}$ are deterministic processes

In this context and for $t \geq t_0$,

$$\mu_{u,0,t} \equiv \mu_{u,0}, \mu_{u,1,t} \equiv \mu_{u,1},$$

$$\mu_{c,0,t} \equiv \mu_{c,0}, \ \mu_{c,1,t} \equiv \mu_{c,1}, \alpha_t(\cdot) \equiv \alpha(\cdot) \ and \ \beta_t(\cdot) \equiv \beta(\cdot),$$

we have:

$$u_t = c_t + \mu_{u,0,t} + \mu'_{u,1,t} X_t,$$

where the computation of $\mu_{u,0,t}$ and $\mu_{u,1,t}$ is described as

$$\begin{cases} \mu_{u,0,t} = \delta(\mu_{u,0,t+1} + \mu_{c,0,t+1}) + \dfrac{\delta}{1-\gamma} \alpha_t\{(1-\gamma)(\mu_{u,1,t+1} + \mu_{c,1,t+1})\} \\ \mu_{u,1,t} = \dfrac{\delta}{1-\gamma} \beta_t\{(1-\gamma)(\mu_{u,1,t+1} + \mu_{c,1,t+1})\} \end{cases}$$

and where, for $t \geq t_0$, $\mu_{u,1,t}$ solves:

$$\mu_{u,1} = \frac{\delta}{1-\gamma} \beta_t\{(1-\gamma)(\mu_{u,1} + \mu_{c,1})\}$$

and $\mu_{u,0,t}$ satisfies:

$$\mu_{u,0} = \frac{\delta}{1-\delta}\mu_{c,0} + \frac{\delta}{1-\delta}\frac{1}{1-\gamma}\alpha\{(1-\gamma)(\mu_{u,1} + \mu_{c,1})\}.$$

Many parameters (which can be found in Chikhani and Renne (2021), Table 4 of Appendix A) in these formulas are directly taken from existing literature and in particular from DICE16. Meanwhile, some parameters, which are specific to the model and thus have no equivalent in other studies (e.g., D_t and N_t, the parameters representing, respectively, economic damages and feedback loops) are determined through a moment-fitting approach (the results can be found in Chikhani and Renne (2021) Table 2 of Appendix B) by minimizing a loss function reflecting the distance between targeted moments found in the literature and their model-implied equivalents. This calibration approach is not feasible in standard IAMs which require simulations to compute long-term moments since they are not available in closed-form. Solving the following optimization problem, the calibrated parameters $\hat{\theta}$ are obtained as

$$\hat{\theta} = argmin_\theta (\gamma - \psi(\theta))' \Omega (\gamma - \psi(\theta)),$$

where:

- γ is the vector of targeted moments
- θ is the vector of free parameters
- $\psi(\theta)$ are the model-implied moments.

- Ω is a diagonal matrix whose diagonal entries are the moments' weights

The loss function $\left(\gamma - \psi(\theta)\right)'\Omega\left(\gamma - \psi(\theta)\right)$ is minimized for $\hat{\theta} = \theta$.

As already mentioned above, Chikhani and Renne (2021) has the merit of offering quasi-closed-form valuation formulas relying on Fourier analysis. Indeed, it provides the possibility of recovering the probability density function (p.d.f.) of any state variables' linear combination, at any horizon.
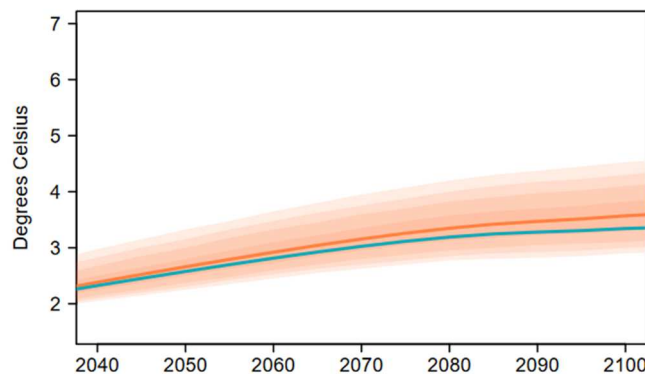
Figure 18: Physical p.d.f of atmospheric temperatures
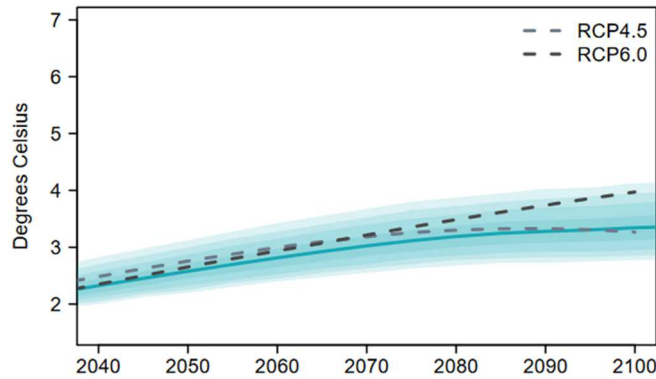
Source: Chikhani and Renne (2021)

Figure 18 represents the physical p.d.f. of atmospheric temperatures in comparison with two RCP (Representative Concentration Pathways) scenarios. These emissions scenarios define trajectories representing greenhouse gas and aerosol concentrations for particular radiative forcing values in the years 2100. In particular, RCP4.5 and RCP6.0 are two intermediate stabilisation pathways. Radiative forcing is respectively stabilised at approximately 4.5 W/m^2 and 6.0 W/m^2 after 2100.[36] The 50%, 80%, 90% and 95% confidence intervals are represented as shaded areas.

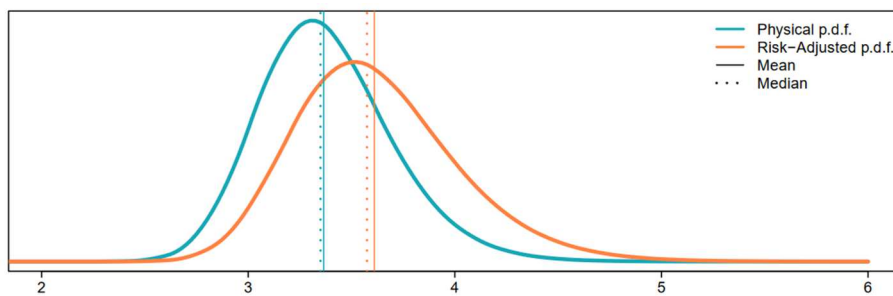*Figure 19: Risk-adjusted p.d.f. of atmospheric temperatures*

Source: Chikhani and Renne (2021)

---

[36] 'Glossary', IPCC Data Distribution Centre, accessed 21 May 2022, https://www.ipcc-data.org/guidelines/pages/glossary

Figure 19 represents the risk-adjusted p.d.f. of atmospheric temperatures (in orange) in comparison with the physical one seen in *Figure 18* (in cyan), up to 2100. The risk-adjusted distribution represented consists in the term structure of temperature swap prices $\left(T_{0,h}^{S}\right)$.

The 50%, 80%, 90% and 95% confidence intervals using risk-adjusted probabilities are represented as shaded areas. Risk-adjusted p.d.f. is shifted up with respect to the physical one. This means that in the process of pricing temperature-indexed instruments the states of the world characterised by higher temperature are overweighted by risk-adjusted probabilities. The model is able to recognize that high temperatures are associated to states of high marginal utility and so lower consumption: this tends to result in an increase in the risk-adjusted probabilities.

Figure 20: Conditional distribution of atmospheric temperature in 2100

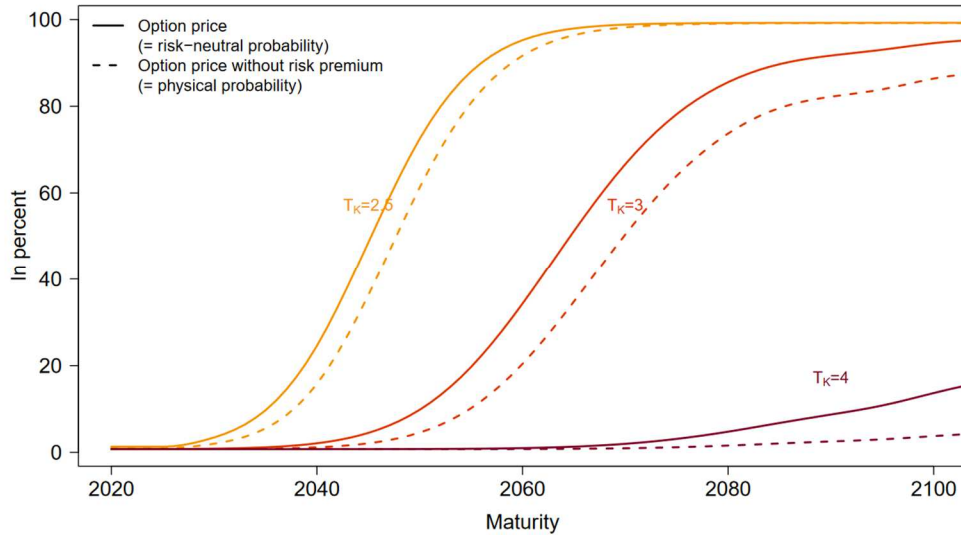*Source: Chikhani and Renne (2021)*

Figure 20 plots the conditional distributions of atmospheric temperatures in 2100 under physical and risk-adjusted p.d.f.. As seen before, risk-adjusted p.d.f. is shifted to the right w.r.t. the physical one. Moreover, the risk-adjusted p.d.f. is flatter than the physical one, indicating that the overall quantity of risk is higher in the risk-adjusted world. In the risk-neutral measure, the p.d.f has a heavier right tail, which means that high temperatures extreme scenarios are particularly risk-sensitive.

Getting to the valuation issue, digital options are considered for expository purposes.

Recalling *Table 6*, the payoff of this option type (settled on maturity date $t + h$) is expressed as $\mathbf{1}_{\{T_{t+h} > T_K\}}$. The price is denoted as $Dig_{t,h}(T_K)$.

Digital options prices can be interpreted as risk-adjusted probabilities of exceedance of a predetermined threshold, the strike T_K, by future temperatures. It is important to note that the option strike is defined as the increase in temperatures with respect to the starting period. This clarification is necessary because in the following chapter the notation will be changed for easier readability of the results.

Figure 21: Price of digital options

Source: Chikhani and Renne (2021)

Figure 21 plots digital options prices for different strikes, notably $T_K = 2.5$, $T_K = 3$, $T_K = 4$, and maturities up to 2100. More precisely, the solid lines display $Dig_{t,h}(T_K)\,/B_{t,h}$ for different maturities h: the option prices $Dig_{t,h}(T_K)$ are divided by the prices of zero-coupon bond of the same maturities $B_{t,h} = \mathbb{E}_t(\mathcal{M}_{t,t+h})$ in order to make these prices comparable to probabilities. The probabilities obtained through this computation are the risk-adjusted ones. Risk-adjusted probabilities are once again higher than the physical ones (represented by the dashed lines). Moreover, ratios between risk-adjusted and physical probabilities increase with the temperature strike, reaching substantial levels for high temperature. The deviations between solid and dashed lines indeed represent climate risk premiums.

2.4 Climate derivatives from Little et al. (2015)

Although Little et al. (2015) was published in the time that elapses the publication of the two papers presented in the previous sections, it is presented last because of the slightly different concept behind the model employed.

2.4.1 The rationale

The issue addressed in Little et al. (2015) is related to susceptibility of the Tasmanian salmon aquaculture industry to warming ocean temperatures: salmon were in fact grown in coastal waters occasionally exceeding a thermal limit of about 18 °C. Anyway, there was little doubt about the further coastal warming which was going to come. The authors propose a solution to sustain the efforts already underway to reduce the risk of warming coastal waters by aquaculture companies suggesting the sale of climate derivatives which could provide additional capital for these efforts. Clearly, this model can be modified and adapted to other indexes and other

63

locations maintaining the same setup. Climate derivatives include Call and Put options, which are both considered in American and European type. It is necessary to highlight that, even though it may seem pretty similar to a weather derivative in the functioning, this financial instrument generically called climate derivative stands out for its long maturity (10 – 20 years) which let it satisfy totally different investors' needs with respect to weather derivatives (which have 1 – 3 years maturities, as discussed in section 1.5) being able to account for climate change effects.

The up-front payment would be used by aquaculture companies to invest in adaption measures to climate change such as the relocation of production facilities to cooler open-ocean areas or the selective breeding of thermally tolerant fish. Considering a European Put option, if the underlying temperature measure at maturity did not exceed the strike threshold, a pay-out would be made by the contracted aquaculture company to the contract owners or investors. The total pay-out would be computed as

$$total\ payout = (C * \#\ degrees\ below\ the\ strike) * option\ price * \#\ options\ issued.$$

Despite the due payment, the aquaculture company would not incur the risks and costs associated with a higher temperature benefitting from this fact. On the contrary, if underlying temperature measure exceeded the strike threshold, the contracted aquaculture company would benefit from the investment made for adaption to higher water temperatures and no pay-out would be required. The counterparties/investors would benefit from climate derivatives: these instruments, quoting authors 'words *offer the opportunity to hedge against potential economic losses, or take advantage of different climate outlooks or risk tolerances, and align incentives to provide a mutual benefit"*. In this specific case, possible counterparties for a European put option contract offered by the aquaculture industry would be those who would suffer economically if warming did not occur and so may wish to offset this risk (e.g., agricultural businesses making investments in warm climate crops).

2.4.2 The pricing

The derivative trade price relies on the underlying index/asset price forecast, the pay-out and exercise conditions, the strike and the maturity.

The strike temperature is set to 18°C. The underlying index is defined as the average annual summer (January, February, March) sea surface temperature (SST) in the D'Entrecasteaux Channel of south east Tasmania (43.05°S, 147.18°E). It is necessary to specify that, in order to better reflect the risk of a general temperature trend crossing the threshold, a 4-year average summer SST is used as the underlying index. Using summer SST of each year may overemphasize the influence of interannual variability.

Model forecasts for SST are obtained from the Climate Futures for Tasmania based on an ensemble of 12 GCM forecasts consisting of two IPCC Emission scenarios (A2, B1) and six different GCMs (CSIRO-Mk3.5, GFDL-CM2.0, GFDL-CM2.1, ECHAM5/MPI-OM, MIROC3.2, UKMO-HadCM3). As specified in Grose et al. (2010), the A2 emissions scenario results in higher emissions and a stronger climate response, while the B1 emissions scenario results in lower emissions and a weaker climate response. These two emissions scenarios are chosen because they are the highest and lowest emissions scenarios where GCM simulations are available, thus gives a range of possible future climate responses. It is reported that, quoting Le Quéré et al. (2009), in the period 2000 – 2010 human emissions mimicked the A2 emissions scenario.

A single modelling simulation gives a single projection of an emissions scenario, analogous to a single replication of an experiment. More simulations give further replicates of that experiment and help to give an estimate of the range of possible outcomes for a given emissions scenario. For this reason, the project has undertaken the maximum number of modelling simulations that computation time allows, with the downscaling of six GCMs (CSIRO-Mk3.5, GFDL-CM2.0, GFDL-CM2.1, ECHAM5/ MPI-OM, UKMO-HadCM3 and MIROC3.2) for both the A2 and B1 emissions scenarios. The good performance over the Australian region is the reason for which these six models have been chosen. Multi-model ensemble simulations are reported to generally provide more robust information than simulations from any single model. Given the focus on the change with respect to the mean state of the general climate, the results of the ensemble of all the models (rather than any one particular simulation) are considered.

The data from these models are dynamically downscaled to the region using the CSIRO stretched-grid global atmospheric CCAM (Conformal Cubic Atmospheric Model) for the period from 2010 to 2050.

Generally speaking, the dynamical downscaling is a method which uses a limited-area high-resolution model, which is called regional climate model (RCM), driven by boundary conditions from a GCM and using physical principles to obtain smaller-scale climate information.

The above mentioned CCAM is a three-dimensional atmospheric model which is able to simulate climate and weather at fine spatial resolutions (down to/beyond kilometre scales) also accounting for the differences in the predictions of global climate models characterised by lower resolution. This detail is achieved by employing a variable resolution and global cubic grid design. The Conformal Cubic grid is realised by projecting a cube onto the surface of a sphere.

As reported in Thatcher and McGregor (2009), the relationship between conformal cubic coordinates (A, B, C) on the surface of a unit cube and Cartesian coordinates (X', Y', Z') on the surface of a sphere is described by

$$(X', Y', Z') = \frac{(A, B, C)}{(A^2 + B^2 + C^2)^{1/2}} R$$

where A, B, and C values lie between -1 and 1 and R is the radius of the sphere (the Earth). In CCAM, the degree of grid stretching is controlled by the Schmidt (1977) transformation, which allows the global grid to be focused over a particular region. Anyway, improving the resolution for the region requires reducing the resolution for the opposite side of the globe. The stretched (X, Y, Z) Cartesian grid coordinates are related to the unstretched ones (X', Y', Z') through the Schmidt factor. In addition to the use of highly stretched grids (e.g., Schmidt factor > 3), CCAM also uses a multiply nested grid approach, which consists in placing finer grids (sub-grids) inside a given grid, where each sub-grid can contain several nested grids. As stated in Yorke and Kaisig (1995), this hierarchy of nested grids makes the spatial resolution increase. This approach is particularly effective for simulating the regional climate. Using it, the CCAM in fact can better represent topography including mountainous regions and can also account for local atmospheric processes and their associated climate impacts, such as reduced rainfall in some elevated areas. In addition, thanks to this approach, CCAM can also better simulate extreme weather features, such as tropical cyclones or bushfire weather.[37]

Coming back to the pricing framework, three autoregressive moving average (ARMA) models of order $0 - 2$ are fitted to each GMC forecast generating the probabilities associated with SST projections for the period $2010 - 2050$. GCM trajectories can be visualized in *Figure 22*: each panel represents one of the twelve downscaled GCM trajectories (in blue), its mean (in black) ± 1 SD (in grey) forecast for the period $2010 - 2050$ and the 18 °C strike (in red).

---

[37] 'Conformal Cubic Grid', CSIRO Confluence, accessed 27 May 2022, https://confluence.csiro.au/display/CCAM/Conformal+Cubic+Grid

Figure 22: Summer SST forecasts
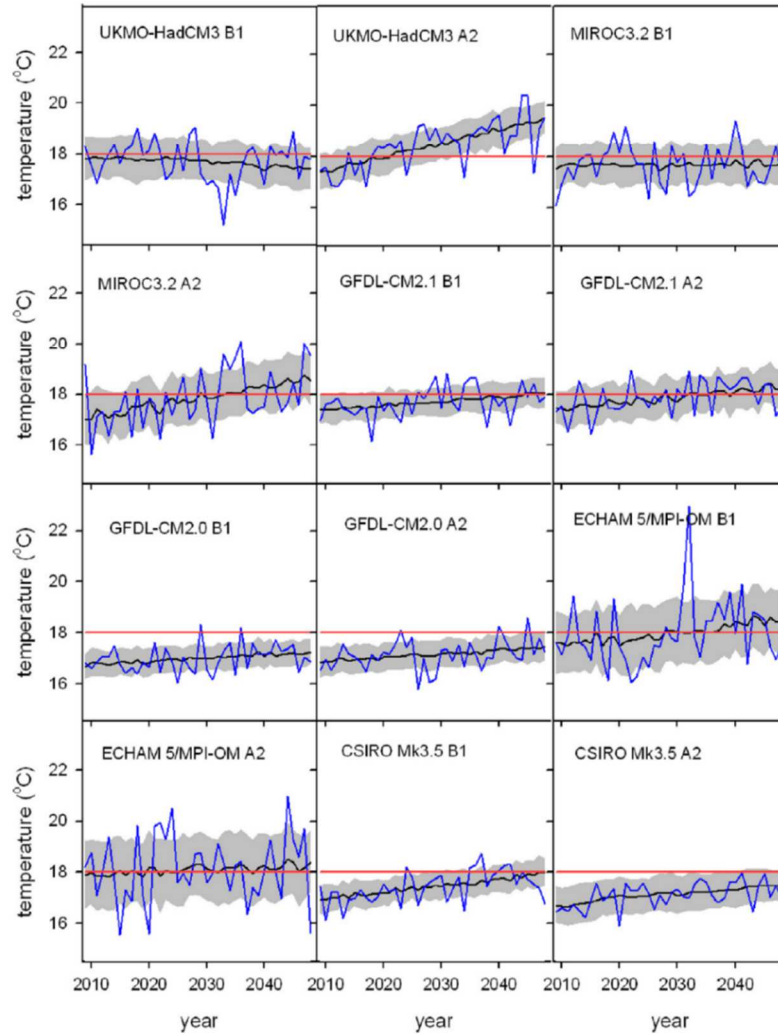
Then, from the three fitted ARMA models, for each GCM forecast, one model is selected. The choice was based on the lowest Akaike Information Criterion (AIC) value[38].

Parameters' estimates can be found in Little et al. (2015), p.11, Table 1. Afterwards, 100 multivariate normal samples of the estimated parameter coefficients (intercept, trend, autoregressive, and moving average) for each selected ARMA model are taken. They are used to obtain an ARMA simulation of SST from 2010 to 2050. So, on the whole, a set of 1200 downscaled time series of SST is produced.

Prices are calculated by discretizing the real-valued underlying index $x_{k,t}$ from simulation k of the set in year t. The discretization is done into 1000 discrete bins, so $s = 1 \ldots 1000$, as $a_{k,t,s} =$

---

[38] AIC values are computed as $AIC = -2\ln(L) + 2k$, where $L = likelihood$ and $k = number\ of\ parameters$. The lowest possible AIC indicates the best balance of model fit with generalizability. This serves the eventual goal of maximizing fit on out-of-sample data.

1, such that $\tilde{x}_{s_t} \leq x_{k,t} < \tilde{x}_{(s+1)_t}$, with $\tilde{x}_{s_t}$ and $\tilde{x}_{(s+1)_t}$ representing the underlying index at time t, of two discrete contiguous bins s, and $s + 1$. For clarity, $a_{k,t,s}$ takes value 1 when the underlying index of the simulation k at time t occurs in bin s.

The derivative price is the payment the writer of the contract requires as compensation for incurring the risk of a pay-out. This risk depends both on the probability of the pay-out occurring and the size of the potential pay-out.

The probability of pay-out is computed from the set of 1200 time series trajectories and it is, as well as all probabilities considered, the statistical physical probability. Although this choice is questionable, it is not new to some of the authors as Little et al. (2014) demonstrate. The choice of using this probability is viable only when it is implicitly assumed a zero risk premium. Anyway, assuming a null risk premium is a simplistic approach, which surely would not reflect reality.

The pay-out size for a Put option is defined as a function based on the underlying index relative to the strike,

$$
I_{t,s_t} = \begin{cases} C \left| \tilde{x}_{s_p} - \tilde{x}_{s_t} \right| & \text{if } \tilde{x}_{s_t} < \tilde{x}_{s_p} \\ 0 & \text{if } \tilde{x}_{s_t} \geq \tilde{x}_{s_p} \end{cases}
$$

where:

- C is a scaled pay-out parameter
- $\tilde{x}_{s_p}$ is the discretized value for the bin representing the strike
- $\tilde{x}_{s_t}$ is the discretized value of the underlying index for bin s at time t.

This pay-out function implies that pay-out increases with the deviation of the underlying index from the strike.

Conversely, the pay-out size for a Call option is defined as

$$
I_{t,s_t} = \begin{cases} C \left| \tilde{x}_{s_p} - \tilde{x}_{s_t} \right| & \text{if } \tilde{x}_{s_t} > \tilde{x}_{s_p} \\ 0 & \text{if } \tilde{x}_{s_t} \leq \tilde{x}_{s_p} \end{cases}
$$

where the inequality conditions in the pay-out function are reversed.

In order to calculate prices, the probability of the discretized underlying index occurring in bin s at time t $p(\tilde{x}_{s_t})$ is determined as:

$$
p(\tilde{x}_{s_t}) = \frac{1}{n_k} \sum_k a_{k,t,s}
$$

where n_k is the number of simulations in the set. In simple terms, probability $p(\tilde{x}_{s_t})$ is computed counting how many times, checking all the k simulations, the discretized underlying index occurs in bin s at time t and dividing the count number by the number of simulations. Then, the present value of the expected pay-out at maturity date $t = T$ is calculated and discounted using a backward induction process to time $t = 0$ recurrently.

The first backward induction process step can be written as

$$E[I_{T-1,s_{T-1}}] = e^{-\delta} \sum_{s_T} I_{T,s_T} p(s_T|s_{T-1})$$

where:

- $E[I_{T-1,s_{T-1}}]$ denotes the expected pay-off for discrete bin s_{T-1} at time $T-1$
- $p(s_T|s_{T-1})$ is the conditional probability that the index value will be in bin s at time T, knowing that it was in bin s at time $T-1$. It is calculated as $p(s_T|s_{T-1}) = p(s_T, s_{T-1})/p(s_{T-1})$ denoting as $p(s_T, s_{T-1})$ the probability of the index being in bin s_{T-1} at time $T-1$, and bin s_T at time T.
- δ is the discount rate.

A European option contract can be exclusively exercised at maturity since not allowing the exercise time choice: its price is independent of the underlying index state prior to maturity and can be easily computed as the expected pay-off at time T.

It is not necessary to compute the expected pay-off at time T as $E[I_{t,s_t}] = \max(0, e^{-\delta} E[I_{t+1,s_{t+1}}])$ at each t (relying on the backward induction) because the pay-off obtained at each time step t in the backward induction process to $t = 0$ is non-negative since $I_{t,s_t} \geq 0$ by construction.

An American option contract can be exercised prior to the maturity date T: it is path dependent and the decision on whether to exercise the contract taking the pay-out or wait is required at each time t. This decision is embedded in the expected pay-off of each time t $E[I_{t,s_t}]$ which consists in the maximum between the pay-out expected exercising the contract I_{t,s_t} or that one expected waiting $e^{-\delta} E[I_{t+1,s_{t+1}}]$. To clarify, each time t expected pay-off for an American option can be expressed as

$$E[I_{t,s_t}] = \max(I_{t,s_t}, e^{-\delta} E[I_{t+1,s_{t+1}}]).$$

Formally, the price is defined as $E[I_{t=0,s_{t=0}}]$.

In the event of initial state uncertainty at time $t = 0$, the price can be determined as the expected outcome across all possible initial states,

$$E[I_{t=0}] = \sum_{s_{t=0}} p(s_{t=0})E[I_{t=0,s_{t=0}}]$$

The example provided in the paper considers a European put option which can be exercised at maturity to give a C = \$100 pay-out for each degree deviation of the summer SST from the strike level of 18 °C. Prices are calculated over the maturity periods T of 10 and 20 years, discounted to present value at a rate of 7%.

Figure 23: Little et al. (2015) European Put option prices
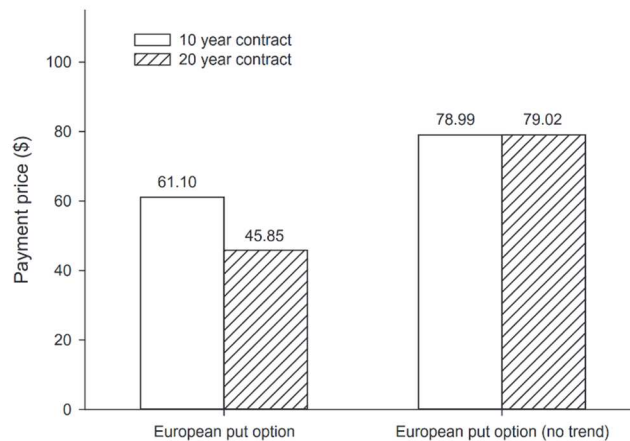
Source: Little et al. (2015)

In *Figure 23,* the computed derivative prices are shown. The forecasts upon which the prices are computed have been obtained from ARMA simulations performed with and without the temperature long-term trend for 10 and 20-year to maturity options. Without the warming trend (the trend is set to 0), the prices are higher and so lower SSTs and a higher likelihood of a pay-out are expected.

2.5. A short discussion

After having illustrated the different financial instruments and the models which can be used for their valuation, the strength points and the criticalities of each climate derivative prototype are shortly discussed.

Bloch, Annan, and Bowles (2010) and Bloch, Annan, and Bowles (2011)

Bloch model is to be praised because it offers one of the earliest examples of climate derivatives designing different instruments in order to cover different investors 'needs.

In these papers the existence of a rightly understood climate risk is recognised: it is defined as the risk of loss when a climate variable (e.g., temperature or sea level) rises above a defined level.

Applying the logic of pricing credit derivative products to climate derivatives allows for an efficient solution to be reached across multiple projects (already built and newly planned

projects) redistributing risks to parties in a position to shoulder them at minimum cost: a market between natural hedgers on both sides of the trade would arise. As a result, new-build projects may defend against a higher sea-level-rise outcome through relatively modest expenditures at inception. In fact, they could monetize their guaranteed future cash flows by underwriting the risks of previously built projects which may be subject to large retrofitting expenditures in the event that the high sea-level outcome occurs.

Anyway, one of the criticalities of this model consists in the fact that the estimation of the parameters relies on only one global climate model (GCM). As shown in Little et al. (2015) and in particular in *Figure 22*, GCM forecasts trajectories can exhibit quite different behaviours: the differences in that case do not matter given that prices are computed on a set of 1200 time series trajectories, but in this case they can lead to very different results.

Chikhani and Renne (2021)

This paper has the great merit of offering a new category of financial instruments able to encompass climate variables and their economic effects. This model of climate derivative does not cover any specific climate change effect since it is said it incorporates equations describing all climate dynamics. Given the generality of the risks covered, a wide range of investors may be interested. Even though it is mainly a theoretical proposal, it may open the way to similar financial instruments relying on more advanced climate models in the future able to avoid the bias identified in IAM assumptions. It is to say that this model relies upon a huge number of assumptions and data recovered from other studies and papers.

The choice of relying on IAMs is debatable as also admitted by Jean Paul Renne during the seminar about its paper on 24th March 2022, part of the Virtual Seminar on Climate economics series hosted by the Federal Reserve Bank of San Francisco. The author did not deny the possibility of improvement and revision of the model in the future. On that occasion, Richard Tol, Professor of Economics at the University of Sussex and of Economics of Climate Change at the Vrije Universiteit Amsterdam, expressed his concern about the model. One of the main issues he raised was the mismatch between what the authors had said they wanted to do and what they actually did. He casted doubts on the whole underlying idea of the model. Given that the authors, directly quoting R. Tol speech, *"have tried to link things it is possible to observe in the financial markets to what goes on in integrated assessment models (IAM), this attempt clearly presumes that there is a link in the first place. In reality, climate policy is not even close to IAM. Governments set a target, which is surely not a cost-benefit analysis: at best they do cost effectiveness analysis."* Although these two techniques look similar, the difference between cost effectiveness analysis and cost benefit analysis is that the former compares the

relative costs and outcomes (effects) of a project checking how much it costs to get a certain amount of output from a policy whereas the latter assigns a monetary value to the measure of the effect of a project checking whether the economic benefits outweigh the economic costs of a given policy. Keeping on quoting the speech "*the approach is naïve because what goes on in the real world in terms of markets has nothing to do with what is done in IAM that is computing first best climate policy*". This speech should be considered as part of the already established criticism literature of the integrated assessment models.

Ackerman et al. (2009) points out that the costs of environmental protection and mitigation consist of well-defined monetary expenditures, while its benefits are difficult to quantify since intrinsically unpredictable and unpriceable. The adoption of energy-efficient industrial machineries, household appliances and vehicles as well as the higher and more widespread exploitation of renewable sources of energy require purchases of marketed goods and services: the resulting cash flows can be easily accounted. But, either way, the evolution of these technologies is uncertain over the long term, which is the time span mainly involved in climate modelling. Mitigation costs' forecasts depend on assumptions about the pace of development of new (and existing) technologies and their costs. Given that AIMs typically adopt conservative assumptions about the pace of technical change, IAMs overestimate the costs of achieving stabilization targets.

Another relevant IAMs' issue concerns the significant degree of subjective judgment involved in estimating the value of climate damages. Indeed, IAMs are completely dependent on the shape of their assumed damage functions. The damage function shape issue is also addressed in Pindyck (2013). Greatest uncertainties in IAMs are related to the economic impact of higher temperatures. Quoting Nordhaus (2008), the damage functions continue to be a major source of modelling uncertainty in the DICE model. Many different damage functions have been proposed in IAMs. For example, Nordhaus (2008) DICE model uses an inverse-quadratic loss function which can be written as

$$L = \frac{1}{[1 + \pi_1 T + \pi_2 (T)^2]}$$

Moreover, Weitzman (2009) proposed an exponential-quadratic loss function, which can be written as

$$L(T) = \exp\left[-\beta(T)^2\right]$$

and which records greater losses with large Ts.

Anyway, these loss functions and those ones proposed in other IAMs are not based on any economic theory. The damage functions used in most IAMs are just arbitrary functions with

low theoretical or empirical foundation describing how the level of GDP goes down when T goes up (even though it would be more correct make T affect the growth rate of GDP). The criticality emerges not so much when temperature increases of 2 or 3°C, but when it largely increases (5°C or more) because the damage functions do not provide meaningful results about the damages that should be expected. IAM damage functions are in fact calibrated to give small damages for small temperature increases. The models ignore the possibility of a catastrophic climate outcome for what concerns the size of the economic effect in terms of human welfare decline deriving from climate change effects (so, not in terms of the size of the temperature increase).

The difficulties in the new market creation may be uniquely solved by the initial government initiative. Governments will need to commit themselves to the respect of climate targets. Anyway, climate targets are surely not the main matter for governments' policy and, in case of geopolitical issues, they can be set aside. The proposals to limit the energetic consequences of the sanctions on Russia after the outbreak of the Ukrainian War such as the re-commissioning of some decommissioned coal power plants are illustrative. Theoretically, given that prices would be available at high frequency, the observation of their changes would allow measuring the influence of different types of news on agents' expectations. But how would such a news be reflected in climate linkers' prices?

Little et al. (2015)

As recognised by the authors, climate derivatives, after the appropriate changes, could be used to manage climate risk in situations other than coastal aquaculture (e.g., coastal defences referring to Bloch, Annan, and Bowles (2011)). However, for the sake of consistent treatment, the coastal aquaculture case continues to be considered.

Regardless of the occasion of use, climate derivatives presence on the market would benefit both issuers and investors. For what concerns issuers' benefit, two main risk management strategies can be distinguished: the proactive risk management strategy and the reactive one.

The proactive risk management strategy would consist in raising money selling European put option type climate derivative contracts.

The alternative reactive risk management strategy would consist in selling American call option type climate derivative contracts. If the average summer SST during the lifetime of the contract rose above the strike level, the issuing company would pay-out to the contract owners. The

issuing company would purchase a contract (e.g., insurance policy) with the aim of having a compensation if the average summer SST rose above the strike level.

For what concerns investors' benefit, as already stated, climate derivatives would provide the opportunity of:

- hedging against potential economic losses
- taking advantage of different climate outlooks/risk tolerances
- aligning incentives to provide a mutual benefit.

Quoting the words of the authors, this type of climate derivatives can be applied "wherever there is a well-defined index, threshold, and a basis for predicting future probabilistic outcomes". The Tasmanian example is surely remarkable, but it is not easily replicable. For the correct functioning of the pricing methodology employed, which encompasses process-based climate models, great accuracy of local climate data is clearly required.

As reported in Tabor and Williams (2010), regional climate model used in the dynamical downscaling are computationally expensive because they must numerically solve many thermodynamic equations e.g., those describing the passage of radiation through the atmospheric and cloud formation) at a short time step, at a high spatial resolution and across multiple layers of the atmosphere. Consequently, for many regions only a limited number of RCM simulations currently are available. Dynamical downscaling cost is deemed by UNFCCC to be high and impractical except for academic or government institutions.[39]

And, even if it were possible to obtain the same data for any location, the great geographical specificity of this instrument would cast doubts on the liquidity of the market associated. This issue cannot be underestimated, especially considering the area with low population and/or economic activity density.

Moreover, the authors outlined the risk market in climate derivatives for supporting climate adaptation strategies, but they left open questions about the merits, risks and institutional design of the market. For managing the risk associated with counterparty capability of settling their obligations, the establishment of institutions such as clearinghouses would also be required.

The main problem of the pricing framework the authors proposed is that there is no consideration of any risk premium and so the reference probability remains the real-world one. Estimating the risk premium, which is realistically non-null, and changing probability measure to risk-neutral one would give strength to the methodology employed, which otherwise is weak.

---

[39] "Dynamical Downscaling", UNFCCC, accessed 2 August 2022,

https://unfccc.int/files/adaptation/methodologies_for/vulnerability_and_adaptation/application/pdf/dynamical_downscaling.pdf

These changes are surely not easy, but they are necessary to allow the model to go beyond the current status of first approximation by providing solidity.

CHAPTER 3: Models for pricing temperature options

After having seen the different prototypes of climate derivatives, temperature options designed in Chikhani and Renne (2021) have been chosen as the instrument of reference for this chapter. Exploiting the fact that a market for this type of derivatives still does not exist, there are many possibilities to explore for what concerns the models which can be applied for the valuation. In fact, although climate derivatives have been jointly presented with specific models for temperature or, more broadly, climate forecasts, they do not depend on those models. As it will be possible to see simplifying the pricing method comes at the cost of richness of information retrievable. Nonetheless too expensive and complex, albeit accurate, techniques may be disadvantaged in favour of simpler and quicker techniques. Chikhani and Renne (2021) model for pricing indeed requires not only financial and mathematical knowledge, but also physical and climatological understanding. Moreover, it should be recalled that Chikhani and Renne (2021) original pricing method is not devoid of criticalities: the high number of assumptions concerning the climate and economic blocks, the chosen calibration parameters and the use of IAMs outside the scope of first best policy estimation are a cause for concern. Thus, it is even further worth exploring another possibility for pricing temperature options.

Thus, temperature options designed in Chikhani and Renne (2021) will be priced in a manner as close as possible to the traditional options' pricing technique. Clearly, the stochastic model which is behind the underlying needs to be chosen in order to reflect the temperature behaviour. After having defined the stochastic models leading the temperature path, Call and Put temperature options are priced starting from the payoffs already presented in *Table 6*. For practicality, the payoffs are recalled hereafter in *Table 7*.

Table 7: Payoffs of the options to be priced

Option type	Payoff (settled on maturity date $t + h$)
Call	$(T_{t+h} - T_K)^+ = \mathbf{1}_{\{T_{t+h} > T_K\}}(T_{t+h} - T_K)$
Put	$(T_{t+h} - T_K)^- = \mathbf{1}_{\{T_{t+h} < T_K\}}(T_K - T_{t+h})$

3.1 The Vasicek model

3.1.1 The model

Temperature is assumed to be driven by an Orstein-Uhlenbeck process. Although this choice is based on the literature of stochastic modelling of temperature, appropriate modifications have been made.

In Tong et al. (2020), letting (Ω, F, P) be a probability space with an information filtration $(\mathcal{F}_t)_{t \geq 0}$, the temperature process S is modelled as

$$S(t) = \Lambda(t) + Y(t)$$

where $\Lambda(t)$ is the seasonal trend term and $Y(t)$ is the de-seasonalized temperature process specified as a time-changed OU process, that is

$$Y(t) = X(T(t)),$$

where T is a time change process and X is an OU process

$$dX(t) = \kappa(\theta - X(t))dt + \sigma dW(t).$$

In Zahrnhofer (2009), temperature is the solution of the following stochastic differential equation (SDE):

$$dS(t) = \theta(M - S(t))dt + \sigma(t)dW(t),$$

According to this SDE, the temperature process reverts to the constant M. For modelling the trend and seasonality of the temperature, the author replaced the constant M with the deterministic function $M(t)$. To obtain a stochastic process reverting to $M(t)$, the term $\frac{dM(t)}{dt}$ is added.

So, the model for the evolution of temperature as an Ornstein Uhlenbeck process

$$dS(t) = \left[(\theta(M(t) - S(t)) + \frac{dM(t)}{dt} \right] dt + \sigma(t)dW(t)$$

The author has chosen $M(t)$ as follows

$$M(t) = a + bt + c\sin(\omega t + \varphi)$$

with $\omega = \frac{2\pi}{365}$. After appropriate modifications of the previous equation, the parameters are estimated through OLS. Using the parameters estimated in this way is said to give a good fit of periodic temperature data.

In Chikhani and Renne (2021) the authors envisioned an instrument which ought to take into account the global mean temperature avoiding geographical specificities. Temperature models are often created to price short-term maturity instruments such as weather derivatives for which seasons have a great importance. In our case, given that global mean temperature is considered and that maturities number decades of years, the parameters used to model seasonality are not necessary and so, recovering the original specification of Ornstein-Uhlenbeck processes, a constant is used for the moment.

The Ornstein-Uhlenbeck stochastic differential equation for the global average temperature (so, de-seasonalized) $X(t)$ has the following form:

$$dX(t) = \theta\big(\mu - X(t)\big)dt + \sigma dW(t)$$

where:

- θ is a non-negative decay rate which represent the speed of response of the process
- μ is a mean value for X towards which it tends to move (long-term mean);
- σ measures the strength of the stochastic perturbation
- $W(t)$ is a standard Brownian motion.

The choice of using a constant parameter μ is not without critics: even though it is possible to set the long-term mean in a way that is deemed to reflect the increase in the mean global temperature, this would require the knowledge of the long-term mean at maturity with certainty. A question remains as to the calibration of the mean-reversion rate parameter θ to provide a realistic increase in the average global temperature.

The above model specification is also known as Vasicek model. The Vasicek model is mainly used for modelling the evolution of interest rates. It is a single-factor model, which means that the movement of the interest rates is modelled based on a single stochastic factor which is the so-called market risk factor, represented by the Wiener process. This is surely a limitation when it comes to interest rates because in the real-world interest rates may be affected by multiple factors. The major drawback of the Vasicek model consists in the fact that the short rate r_t, for each time t, can be negative with positive probability (since negative interest rates have been observed in reality in recent years, it is no longer a real issue). Anyway, given the difficulty of predicting the interest rates evolution, the Vasicek interest rate model is still a useful model available to investors and analysts.

Going back to the temperature path, following the Euler method as in Higham (2001), the SDE can be discretized and approximated as

$$X_{n+1} = X_n + \theta(\mu - X_n)\Delta t + \sigma\Delta W_n.$$

The interval is discretized in order to apply a numerical method to the SDE over $[0, t]$ as $\Delta t = t/n$, where t denotes the maturity of the option and n denotes the number of the chosen discretization points. So, the discretized Brownian path uses a constant step-size: ΔW_n should be interpreted as $(W_{n+1} - W_n)$.

In order to assess the plausibility of the choice of using this model in order to describe the temperature evolution, at first, the calibration of the model is performed using the global average temperature time series data[40] for the last 20 years (yellow line in *Figure 24*). The data source is the NASA's Goddard Institute for Space Studies (GISS). As anticipated, temperature measures are no longer denoted as anomaly with respect to a base level: they are expressed as the effective temperature summing the anomaly value to the temperature base level one for better readability.

Figure 24: Global average temperature time series (1880 - 2021)
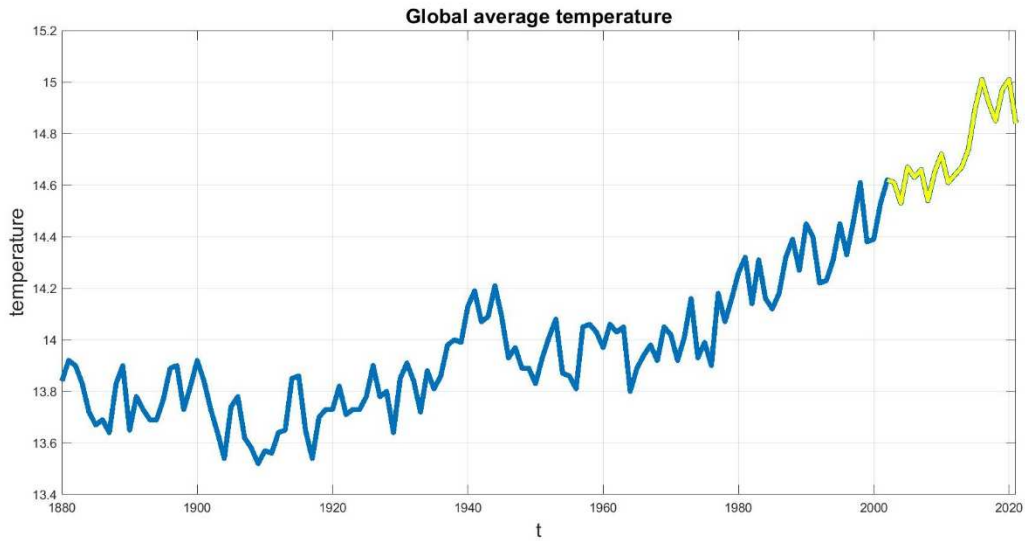
Looking at *Figure 24*, there is clearly the presence of a growing trend since the 1970s, which supports the doubts concerning the use of mean-reverting process at a constant level.

Anyway, before arriving to conclusions, it appears appropriate to calibrate the parameters and check the results of the simulations. The parameters θ, μ and σ have been calibrated through the maximum likelihood estimation (MLE). Hereafter the final formulas are provided. Denote X_i as an observation. Based on Bernal (2016) and van den Berg (2011) in order to calibrate the parameters, the following preliminary computations are required:

$$X_x = \sum_{i=1}^{n} X_{i-1}$$

$$X_y = \sum_{i=1}^{n} X_i$$

$$X_{xx} = \sum_{i=1}^{n} X_{i-1}^2$$

[40] NASA, "Global Temperature", accessed 15 July 2022, https://climate.nasa.gov/vital-signs/global-temperature/

$$X_{xy} = \sum_{i=1}^{n} X_{i-1} X_i$$

$$X_{yy} = \sum_{i=1}^{n} X_i^2$$

The long-term mean is computed as

$$\mu = \frac{X_y X_{xx} - X_x X_{xy}}{n(X_{xx} - X_{xy}) - (X_x^2 - X_x X_y)}.$$

The mean reversion rate is computed as

$$\theta = \frac{1}{\Delta t} * \frac{X_{xy} - \mu X_x - \mu X_y + n\mu^2}{X_{xx} - 2\mu X_x + n\mu^2}.$$

The variance is computed as

$$\hat{\sigma}^2 = \frac{1}{n} * \left[X_{yy} - 2\alpha X_{xy} + \alpha^2 X_{xx} - 2\mu(1-\alpha)(X_y - \alpha X_x) + n\mu^2(1-\alpha)^2 \right]$$

$$\sigma^2 = \hat{\sigma}^2 * \frac{2\theta}{1-\alpha^2}$$

with $\alpha = 1 - \theta * \Delta t$.

After having performed the calibration, whose results are reported in **Table 8,** it is possible to obtain the temperature paths through a Monte Carlo simulation.

Table 8: Parameters obtained through MLE

parameter	value
θ	0.8030
μ	14.7930
σ	0.1736

The time horizon of this simulation is 20 years, from 2002 to 2021. Given that global average temperature time series is constituted of annual data, it has been decided to use 20 discretization points in the simulation for $[0, t]$, where $t = 20$, in order to maintain the same Δt of the real time series. Anyway, generating daily ($n = 7300$, neglecting leap years) or weekly data ($n = 1040$) and then considering only those corresponding to yearly data leads to pretty much the same results. In order to start the simulation of the temperature paths, a starting point is needed:

x_0 denotes the value of x in the first of the 20 discretization points constituting the temperature path. The starting point x_0 is set to the 2002 global average temperature, which is 14.62°C[41]. After having determined and computed the time step given by the ratio between the maturity of the options and the number of discretization points, the discretized M trajectories of the Brownian motion over $[0, t]$ are simulated. To sum up, these furher required parameters are summarized in *Table 9*.

Table 9: Other required Monte Carlo simulation inputs

parameter	value
x_0	14.62
t	20
n	20
M	10000

θ, μ and σ in the code are respectively denoted as `theta`, `mu` and `sigma`.

The Matlab code lines directly concerning the temperature paths simulation are the following:

```
for j = 1 : n-1
    for s = 1 : M
        x(s,1)=x0;
        x(s,j+1) = x(s,j) + dt * theta * ( mu - x(s,j)) +
        sigma * dw(s,j);
    end
end
```

At this point, we may be tempted to directly compare real time series and simulated paths. Well, comparisons between real time series and simulated paths are difficult because there is no telling whether the real time series represents an outlier.

Constructing a confidence interval based on our simulations gives us a glimpse of the capability of the model to produce data similar to real ones. The objective is to demonstrate that the real time series is a plausible output of the model: it is pursued by gradually reducing the interval

---

[41] The global mean surface air temperature for the base period 1951-1980 was 14°C with an uncertainty of several tenths of a degree. In 2002, the annual average anomaly was about 0.62°C. (Earth Observatory Nasa, accessed 16 July 2022, https://earthobservatory.nasa.gov/world-of-change/global-temperatures)

Although the uncertainty about the precise global mean temperature for the period 1951-1980, the value of 14.62°C has been chosen as starting point for temperature path simulations.

of the simulations' values considered, while checking whether real time series is still in the range.

After having calculated different confidence intervals, it is proved that the minimum percentage of simulations' values to be considered in order to observe that the real time series is still contained in the interval is 85%.

Figure 25: Confidence interval
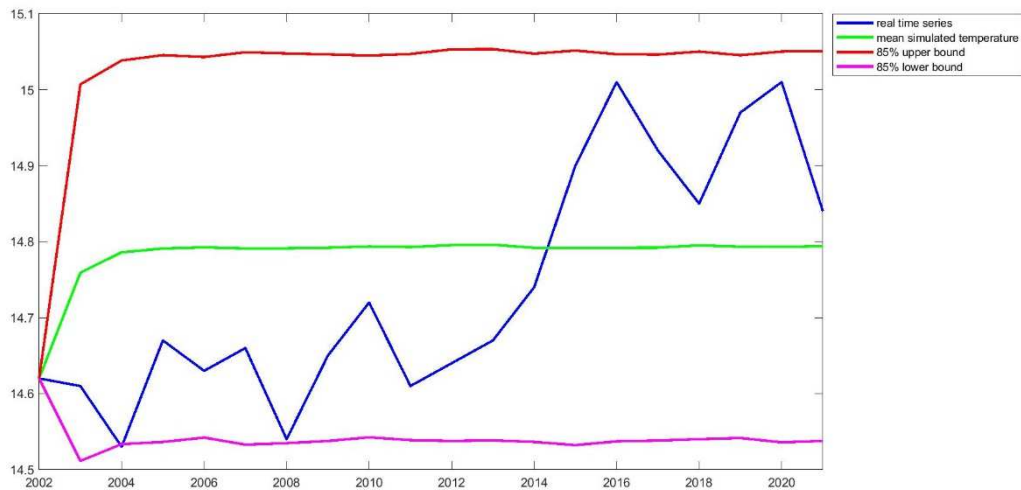
Indeed, *Figure 25* shows that, even though the upper 7,5% and the lower 7,5% of the values of x in each date are not considered, real time series is contained in the interval. Since the temperature evolution is contained in this narrow interval, we may say that what it is observed in reality represents a typical trajectory generated by the model.

It is necessary to consider that using the same parameters calibrated from the real time series for performing simulations in the risk-neutral probability amounts to implicitly assuming the coincidence of the risk-neutral probability with the physical-statistical one. As discussed in section 2.4, this coincidence would imply a null risk premium. As it will be possible to see in the following simulations, we observed that for low levels of θ prices are much higher than for levels close to that one computed from MLE. A slightly higher level of θ than the real one may respond to our need of representing prices computed in the risk neutral measure. This choice would be highlighted in defining the parameters for the base scenario simulation.

As already mentioned, the chosen technique for pricing these options is the Monte Carlo method. A Monte Carlo simulation is performed in Matlab using the inputs presented in *Table 10.*

Table 10: Monte Carlo simulation inputs, Vasicek model

parameters	value
θ	0.9
μ	15
σ	0.18
x_0 [42]	14.84
T_K	15
r	0.01
t	20
n	1000
M	10000

where:

- T_K is the temperature strike
- r is the discount rate
- t is the maturity of the option

For the supposed adjustment to risk-neutral measure, θ is 0.1 higher than the calibrated value. This slightly higher level of θ than the real one is assumed to respond to the need of representing prices computed in the risk neutral measure which thus consider the risk premium.

After having computed the paths, given that European options are being priced, final temperature values are taken to compute Call and Put options' payoffs. Thus, the option exercise is not allowed before maturity.

Considering the paths 'final values x_T , for each single path, Call option payoff is computed as the maximum between $x_T - T_K$ and 0, while Put option payoff is computed as the maximum between $T_K - x_T$ and 0.

Computing Monte Carlo prices consists in discounting to the present the mean of all Call or Put payoffs. The resulting prices of this first simulation are respectively 0.0446 for Call option and 0.0439 for Put option. These results in themselves means little: that is why the discussion about

---

[42] In 2021, the annual average anomaly was about 0.84°C. (Earth Observatory Nasa, accessed 16 July 2022, https://earthobservatory.nasa.gov/world-of-change/global-temperatures)

Although the abovementioned uncertainty about the precise global mean temperature for the period 1951-1980, the value of 14.84°C has been chosen as starting point for temperature path simulations.

Call and Put prices is postponed to the following subsection after having gained further information.

3.1.2 Changing inputs

Once having defined the base scenario, it is possible to test the response of prices changing one input at a time.

In particular, inputs changed in the following simulations are respectively θ, μ and σ.

The first input considered is θ, the nonnegative decay rate representing the speed of response of the temperature process. The values of θ employed in the simulation ranges from slower (0.5) to quicker (1.3) mean-reversion, represented as

`theta=[0.5:0.1:1.3]'`.

In order to compute the prices for each value of theta, it would be necessary to make some small adjustments to the code: in particular, another `for loop` is added.

The resulting process is

```
for k=1:size(theta,1)
    for j = 1 : n-1
        for s=1:M
            x(s,1) = x0;
            x(s,j+1) = x(s,j) +  theta(k) * ( mu - x(s,j) ) * dt +
            sigma * dw(s,j);
        end
    end
    x_T(:,k)= x(:,end);
    payoff_Call(:,k)= max(x_T(:,k)-T_K,0);
    payoff_Put(:,k)= max(T_K-x_T(:,k),0);
    MC_price_Call(k,1)=mean(payoff_Call(:,k))*exp(-r*t);
    MC_price_Put(k,1)=mean(payoff_Put(:,k))*exp(-r*t);
end
```

So, the procedure is exactly equal to that one seen for the base scenario except the fact that, given the need to compute payoffs and prices for each value of theta, even the code lines referred to them have been included into the additional `for loop`.

For the overall view of the code lines describing this model, section A.1 of the Appendix should be referred.

From *Figure 26* it is possible to note that Call and Put prices exhibit the same behaviour to changes in theta. As the steepness of the curve proves, changes in theta when its value is low (e.g., $\theta = 0.5$ and $\theta = 0.6$) have a greater impact on prices than changes when its value is high. It should be noted that the similarity between Call and Put prices and thus the corresponding lines just comes from the initial choice of the parameters μ and T_K.

Figure 26: Call and Put prices sensitivity to θ
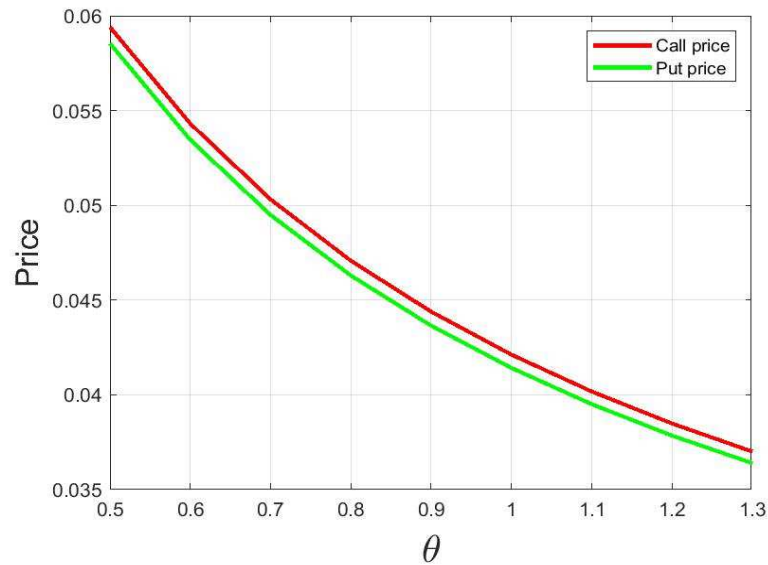
After having set each of the other input parameters to its base scenario value, the second input considered is μ, the mean value towards which temperature tends to move in the long run. The values of μ employed in the simulation are ranging from 15 to 16, represented as `mu=[15:0.1:16]'`.

Although an increase of just over 1°C may not seem so high, it should be remembered that the considered time horizon is 20 years. Thus, an increase of just over 1°C would represent an extreme scenario.

After having assigned the `for loop` variable to the correct parameter, the temperature paths are computed as usual. The results are shown in *Figure 27*.
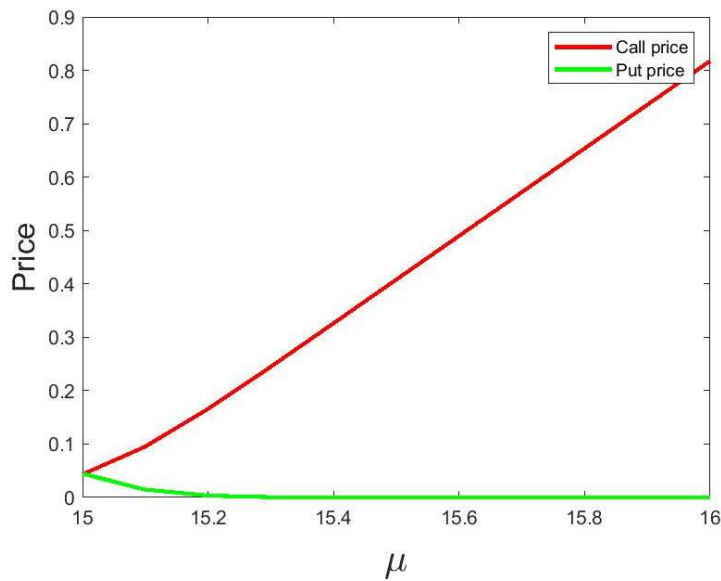
It is possible to see that the parameter μ greatly influences the Call price. This is pretty obvious due to the fact that the temperature strike is fixed to 15: the more the mean towards which the path will move increase the more payoff enlarges and so does the price. Using the same temperature strike for Put options would make little sense. The temperature strike value is almost equal to the starting value: buying such an option would be little profitable in a world affected by climate change because future temperature level would hardly remain pegged to the current temperature level. Only for $\mu <$ 15.2 Put prices appear visually more than 0, even if close. Moreover, the decrease in prices is evident as soon as μ leaves the temperature strike value.

In order to produce meaningful results for Put options, the temperature strike must be changed. The chosen temperature strike is the largest value of the set of values of μ employed in the simulation. So, T_K is set to 16.

Figure 28: Call and Put prices sensitivity to μ ($T_K = 16$)
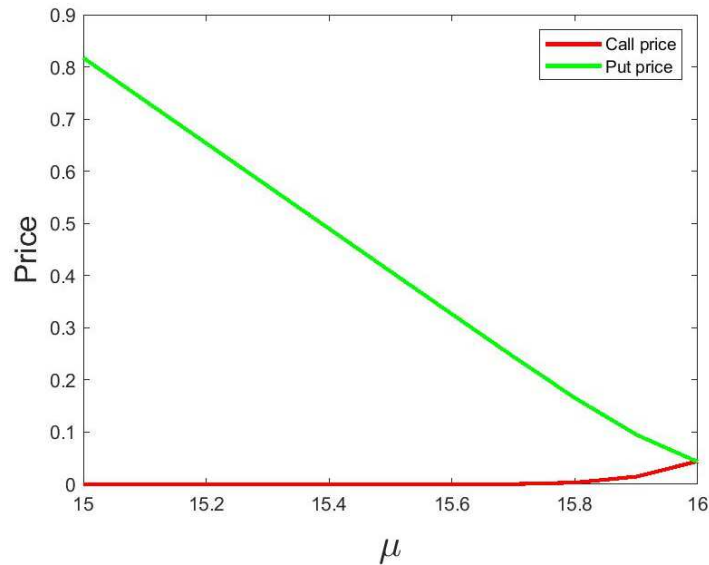
As showed in *Figure 28,* we now obtain meaningful results for Put options. This situation corresponds to the reverse of the previous one: only for values of μ close to the temperature strike Call prices are different from 0 even if very close. Put option payoff is clearly maximized when the mean is at the farthest point from the temperature strike and so does the price.

Then, after having seen the extreme cases with $T_K = 15$ and $T_K = 16$, T_K is set to the intermediate level of 15.5 for completeness. The results are plotted in *Figure 29*.

Figure 29: Call and Put prices sensitivity to μ ($T_K = 15.5$)
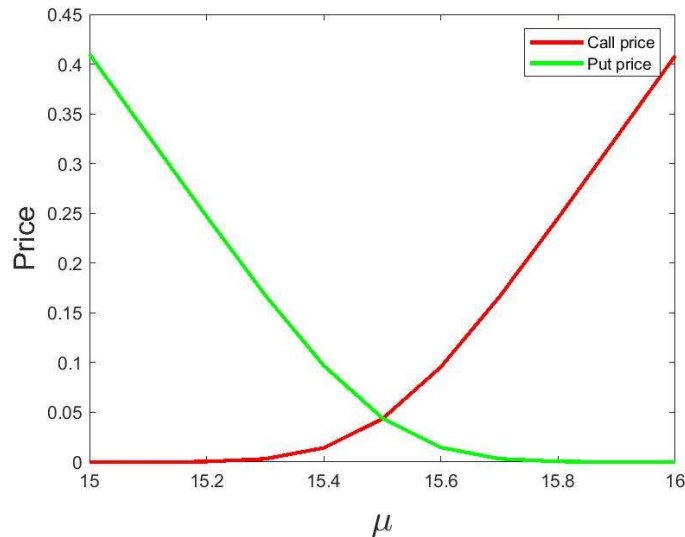
Entering such a strike value makes both types of option valuable. By the way, their respective maximum prices are halved with respect to the previous cases. For a Call option, the price is maximized when $T_K = 15$ and $\mu = 16$, while for a Put option the price is maximized when $T_K = 16$ and $\mu = 15$. In both cases the gap between T_K and μ is the widest: this means that the pay-offs are likely to be high given that temperature paths move towards μ. In the set of this

simulation, the pay-offs are as high as possible and so are the prices. Hence, reducing the gaps between T_K and μ entails reducing the maximum possible pay-offs. As a consequence, the highest prices' level is lower than before.

The third input considered is σ, the strength of the stochastic perturbation.

Before starting, the temperature strike has been set again to $T_K = 15$ as well as other parameters are set to their base scenario values.

The values of σ employed in the simulation ranges from weaker (0.1) to stronger (0.5) stochastic perturbations. They are set as follows

```
sigma = [0.1:0.05:0.5]'.
```

In *Figure 30*, it can be noted that the increase in σ is associated to a positive and linear increase in both Call and Put prices. This is due to the fact that the oscillations of the simulated paths are wider: as a consequence, for both type of options, the payoffs are wider and so are the prices.

Figure 30: Call and Put prices sensitivity to σ
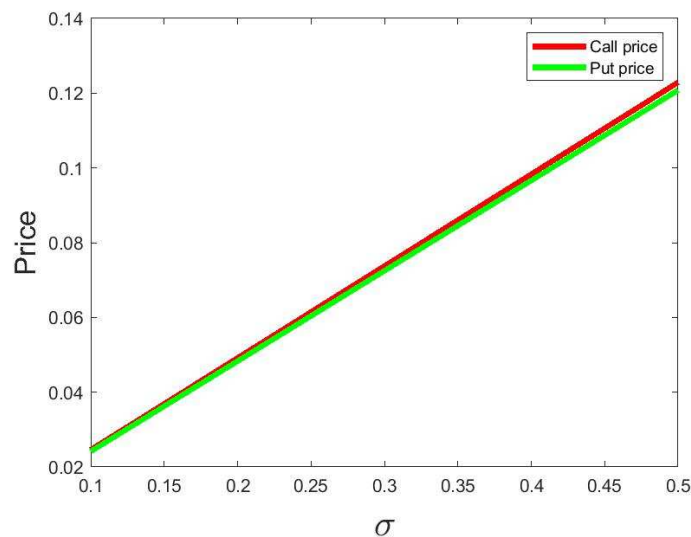
To sum up, the parameters which have greater impact on prices are μ and σ. Naturally, the change of parameter μ has a different impact on Call and Put prices, while the change of the parameters θ and σ seems to have the same impact on Call and Put prices.

3.2 The Hull-White model

3.2.1 The model

The use of Hull-White model for modelling the temperature path already exists in the literature (e.g., Dischel (1998), McIntyre and Doherty (1999)).

Anyway, this model is mainly used for modelling the evolution of interest rates. It has been designed in Hull and White (1990) to overcome the limitation of the Vasicek model consisting in the poor fit of the initial term structure. As Hull and White (1994) reports, although negative

interest rates can occur in this model, it is both capable of fitting an arbitrary initial term structure and analytically tractable. As the Vasicek model, it a single-factor Markov model. It is also called extended Vasicek model because it is a version of that model which let parameters vary through time. Moreover, many specifications of the Hull-White model can be found. In Hull and White (1996), the stochastic differential equation is represented as

$$dr = a[\theta(t) - r]dt + \sigma dz$$

where $\theta(t)$ denotes the time-varying long-term mean towards r reverts, a denotes the reversion rate and σ denotes the volatility factor.

In this specification, the parameters a and σ are not time-varying because, when they are, volatility term structure could be non-stationary: the model implied future volatility structure can somewhat differ from the current volatility structure. Thus, when they are constant, the volatility structure stays stationary (although the model consistency with market prices is weakened).

The Hull-White model which is used in the following simulations for modelling the global average temperature is the following

$$dX(t) = \theta(\mu(t) - X(t))dt + \sigma dW(t)$$

In simple terms, the only difference between the Hull-White model and the Vasicek model used in the simulations performed in section 3.1 consists in the fact that the long-term mean μ becomes a time-dependent variable. Although the introduction of this time-dependence may seem a minor change, it let us consider further scenarios in which worse-than-expected climate conditions occur. The now time-dependent variable μ is assumed to follow a linear evolution through time for simplicity. In addition to the base scenario with constant μ, four additional scenarios have been conceived: each of them is characterised by an increase of +0.25°C at maturity with respect to the previous one. So, starting from a long-term mean of 15°C and considering its increase of, respectively, +0.25°C, +0.5°C, +0.75°C and +1°C, the long-term mean values are 15.25°C, 15.5°C, 15.75°C and 16°C.

In the code, these increases in temperature are stored in the variable wrs, which is defined as wrs=[0:0.25:1]'.

Hereafter the code lines are partially reported in order to highlight the changes.

```
for z=1:size(wrs,1);
    for j = 1 : n-1
        mu(z,1) = stmu;
        mu(z,j+1) = mu(z,j) + wrs(z)/(n-1);
        for s=1:M
```

```
        ⋮
    x(s,j+1) = x(s,j) + dt * theta * ( mu(z,j) - x(s,j) ) +
               sigma * dw(s,j);
      end
    end
    ⋮
end
```

So, each value of μ is computed as its previous value, to which is added the $^1/_{n-1}$ part of the conceived increase. Small changes have been made to the rest of the code: they mainly concern the necessary changes for including the time-dependent μ in the simulation of temperature paths. For the overall view of the code lines describing this model, section A.2 of the Appendix should be referred.

In **Table 11** the inputs employed for the first Monte Carlo simulation are listed.

Table 11: Monte Carlo simulation inputs, Hull-White model

parameters	value
θ	0.9
starting μ	15
σ	0.18
x_0	14.84
T_K	15
r	0.01
t	20
n	1000
M	10000

where the *starting* μ is the value from which the long-term mean evolution starts and it corresponds to `stmu` in the code. The results of this first simulation are shown in **Figure 31.**

*Figure 31: Call and Put prices with evolving μ ($T_K = 15$)*
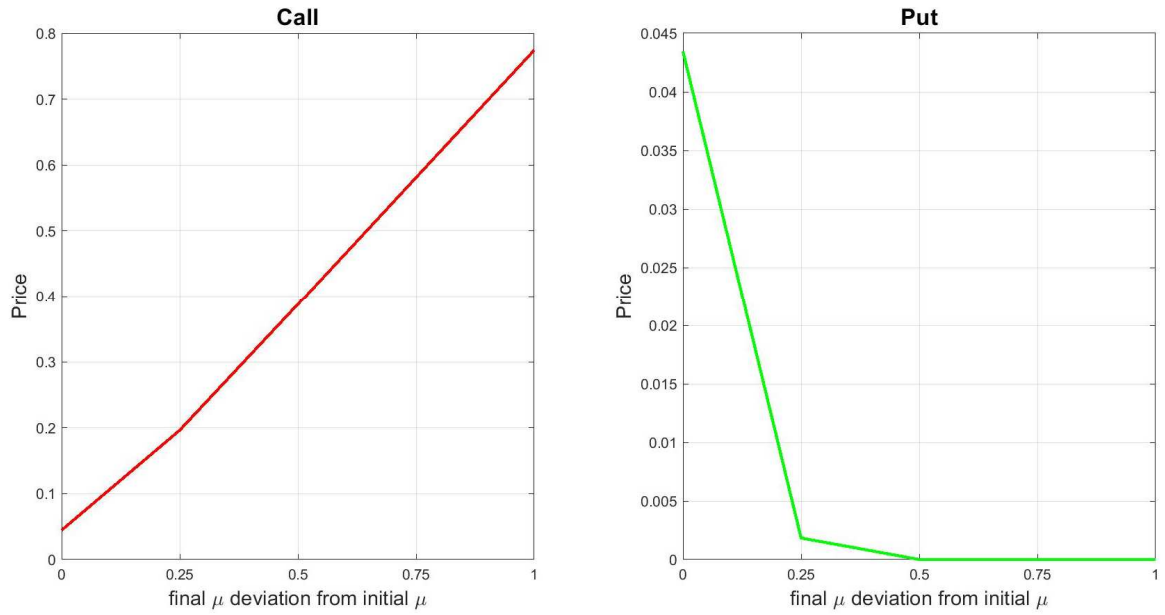
It is clear that, since $T_K = 15$, Call prices increase with the increasing deviation from the initial μ. Indeed, the more the gap between the strike and the long-term mean widens during the time to maturity the more pay-offs are higher near maturity.

Entering $T_K = 15$ for a Put option when μ has a constant value of 15 is a questionable, but legitimate choice given the oscillations of the temperature path. The price is indeed slightly higher than zero. Entering $T_K = 15$ for Put options when μ deviates from this starting level in a more or less wide fashion would lead Put prices to zero right away.

Setting $T_K = 16$, the situation would be at the opposite extreme as shown in ***Figure 32***.

Figure 32: Call and Put prices with evolving μ ($T_K = 16$)

91
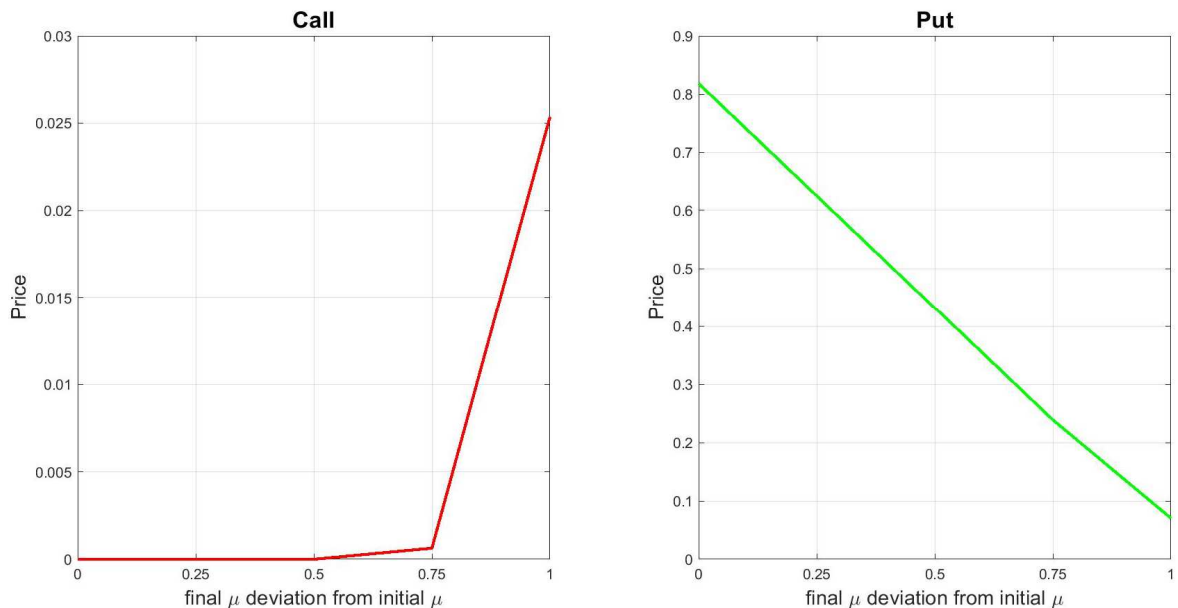
Call prices would remain equal/close to zero for all scenarios except on the +1°C scenario with $\mu = 16$ at maturity. In this case, the price is in fact slightly higher than zero due to the oscillations of the temperature path. Put prices would decrease with the increasing deviation from the initial μ. The more the gap between the strike and the long-term mean narrows during the time to maturity the more pay-offs are lower near maturity and so are the prices.

Setting $T_K = 15.5$, as shown in **Figure 33**, Call and Put prices are comparable, even though the Call and Put maximum prices are lower than Call option maximum price with $T_K = 15$ and Put option maximum price with $T_K = 16$.

Figure 33: Call and Put prices with evolving μ ($T_K = 15.5$)
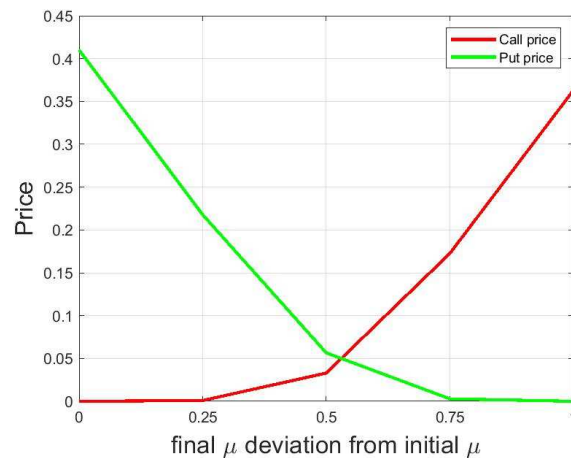

3.2.2 Changing inputs

Given the results of the above simulations and the discussion about the fair strike level to be used in simulations with the parameter μ evolving through time, we have decided to additionally perform the simulations for $T_K = 15.5$. Simulations for $T_K = 15$ cannot be ruled out for purposes of comparability with the results obtained for the Vasicek model.

Other parameters are initially set to their base scenario level (see **Table 11**). Indeed, the response of prices is tested changing one input at a time.

The first input considered is the speed of reversion rate θ. The values of θ employed in the simulation ranges from 0.5 to 1.3, as in the Vasicek model analysis. They are represented as theta=[0.5:0.1:1.3]'.

Figure 35: Call prices with evolving μ changing θ ($T_K = 15$)
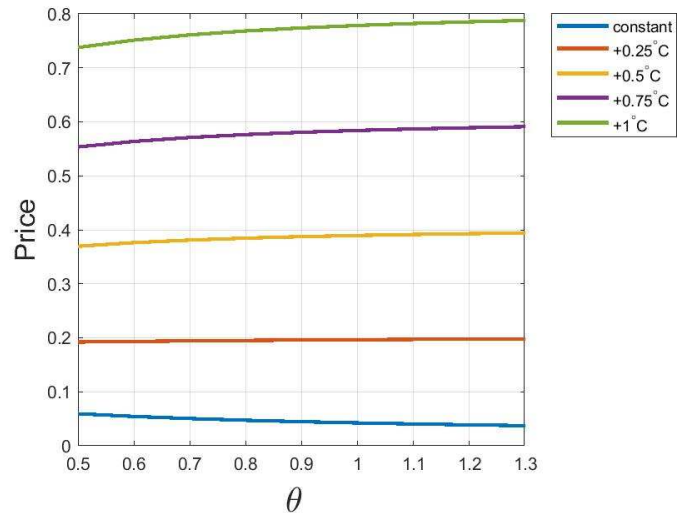
As shown in *Figure 34*, an increase in θ is associated to a slightly decrease in Call prices when μ is constant and so the model corresponds to the Vasicek-type one. Anyway, when μ increases during the time to maturity of the option, an increase in θ is associated to a slightly increase in Call prices. This behaviour is more pronounced for scenarios with higher μ at maturity.

Figure 34: Put prices with evolving μ changing θ ($T_K = 15$)
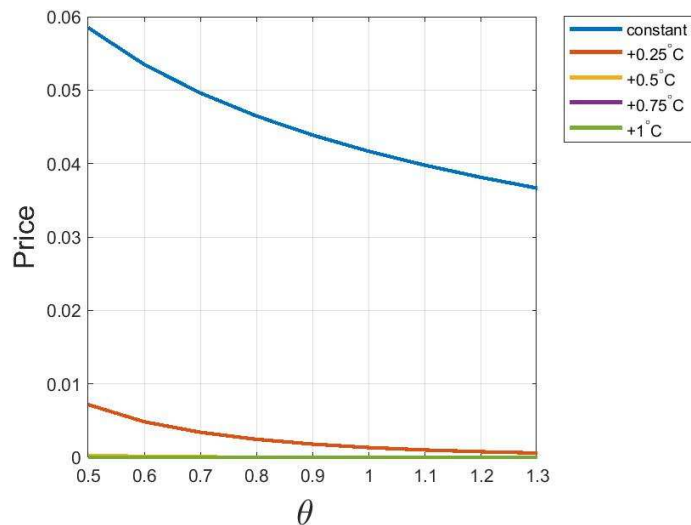
Looking at *Figure 35*, an increase in θ is associated to a decrease in Put prices. This behaviour is observed both in the case μ is constant and so the model corresponds to the Vasicek-type model and in the case μ increases during the time to maturity of the option. Only the price +0.25°C scenario, among the evolving μ scenarios, is visible.

Now, the simulation is performed again setting the temperature strike to $T_K = 15.5$

Figure 36: Call prices with evolving μ changing θ ($T_K = 15.5$)

As shown in **Figure 36**, an increase in θ is associated to a slight decrease in Call prices in +0.25°C and +0.5°C scenarios. Anyway, when μ increases more (i.e., +0.75°C and +1°C) during the time to maturity of the option, the increase in θ is associated to a slight increase in Call prices. This behaviour is more pronounced in the +1°C scenario.
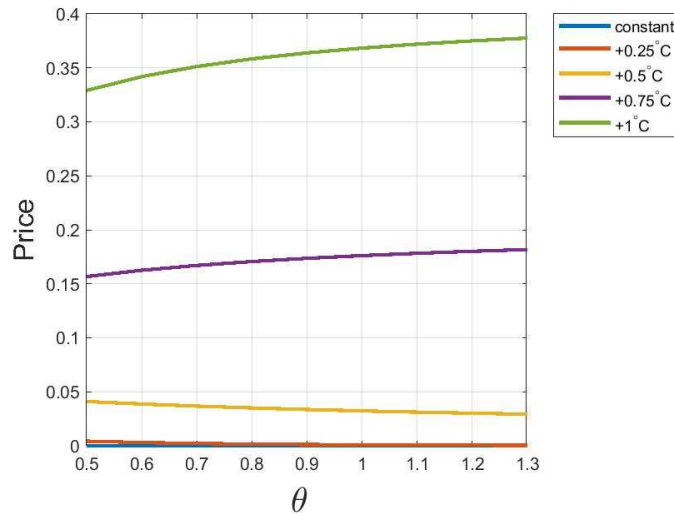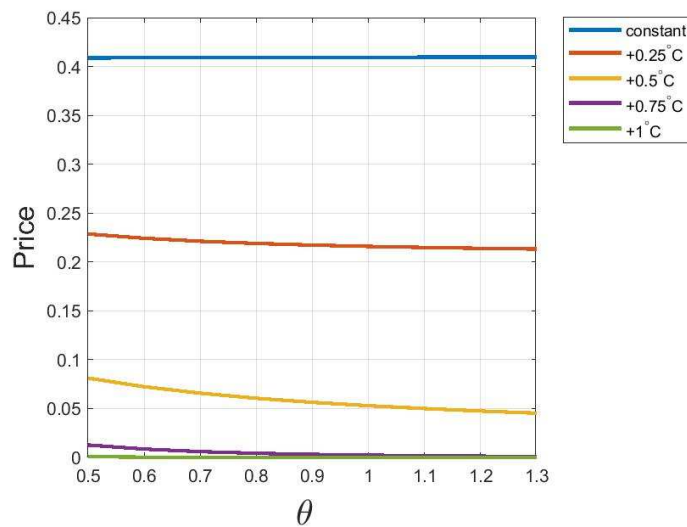
Figure 37: Put prices with evolving μ changing θ ($T_K = 15.5$)

Looking at **Figure 37**, an increase in θ is associated to a slight decrease in Put prices. This behaviour is mainly observed in the case μ increases during the time to maturity of the option. In the case μ is constant and so the model corresponds to the Vasicek-type model, despite the increase in θ, the price line is almost flat.

Some scenarios lines in **Figure 35**, **Figure 36** and **Figure 37** are not visible: this is not due to the effect of the change of θ value on prices, but rather to the effect of the evolution of μ through

time. Even in the base scenario simulations with $T_K = 15$ and with $T_K = 15.5$ in fact the prices associated to these scenarios were close/equal to zero.

Considering prices for different values of *starting* μ is hardly compatible with the current model. Surely there is no problem in simulating temperature paths with different values of *starting* μ and maintaining the linear evolution of μ during the time to maturity of the option. The problem is that it would make little sense because of the huge and highly unrealistic increases in the long-term mean implied.

The second input considered is thus the parameter σ, which represents the strength of the stochastic perturbation. Before starting, the speed of reversion rate θ has been set again to $\theta = 0.9$.

The values of σ employed in the simulation are ranging from 0.1 to 0.5, as in the Vasicek model analysis. They are set as follows

```
sigma = [0.1:0.05:0.5]'.
```

Figure 38: Call prices with evolving μ changing σ ($T_K = 15$)
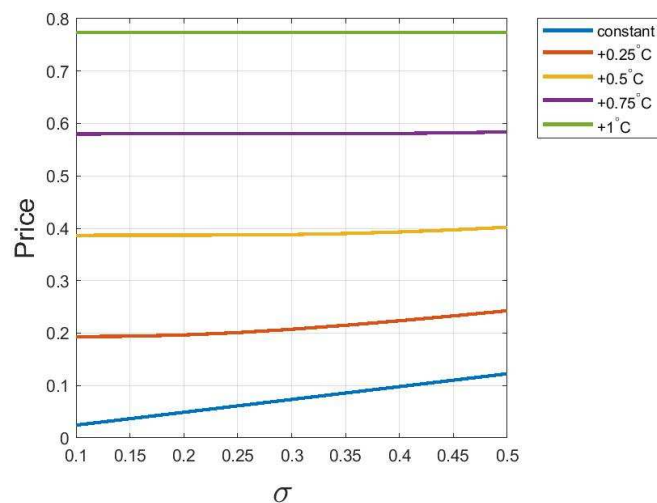
Looking at **Figure 38**, the constant μ scenario exhibits a linear increase in Call prices for increasing values of σ as seen in the Vasicek model analysis. This behaviour is not observed in the other scenarios: actually, the increase in μ through time seems to dampen the effect on prices deriving from the increase in σ. Indeed, the lines for the +1°C and +0.75°C scenarios are only slightly increasing.

95

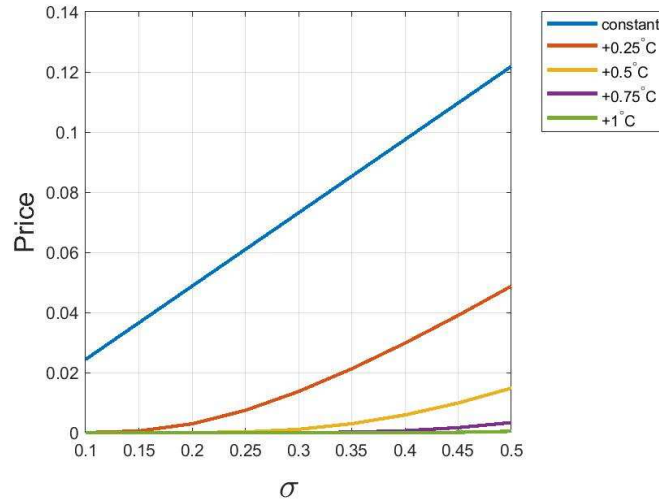**Figure 39: Put prices with evolving μ changing σ ($T_K = 15$)**

Figure 39 shows that, again, the constant μ scenario exhibits a linear increase in Put prices for increasing values of σ as seen in the Vasicek model analysis. In other scenarios the effect of the increase in σ on prices is damped by the decrease in prices associated to the increase in μ through time.

Now, the simulation is performed again setting the temperature strike to $T_K = 15.5$.

Figure 40: Call and Put prices with evolving μ changing σ ($T_K = 15.5$)
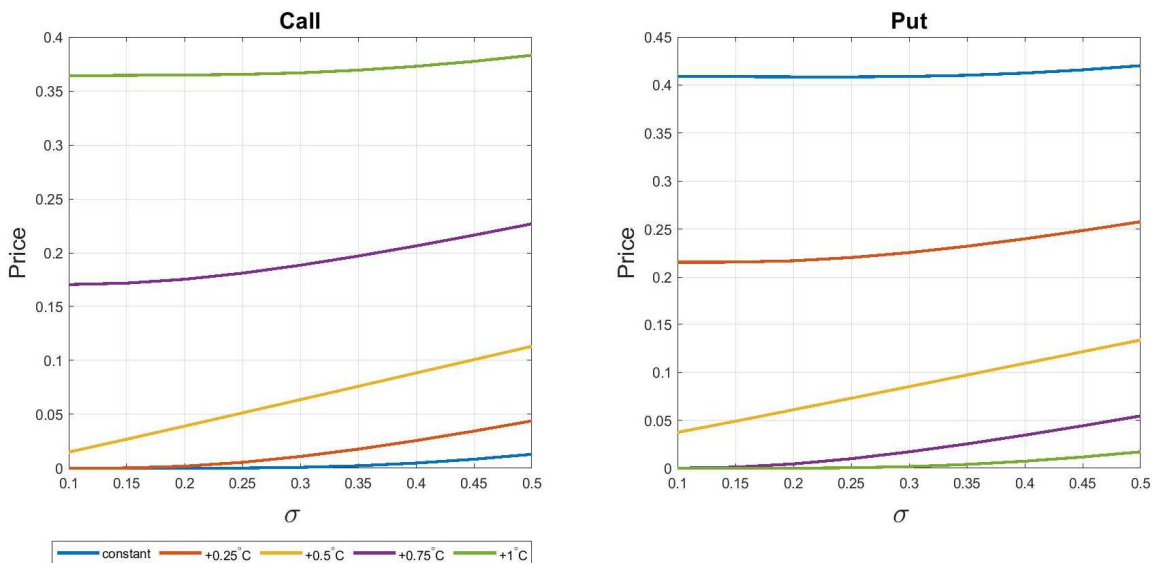
In **Figure 40**, the +0.5°C scenario line in both graphs exhibits a linear increase for increasing values of σ. This behaviour is not observed in the other scenarios.

Concerning Call prices, for scenarios with an increase in μ above 0.5°C, the more μ increases during the time to maturity, the more σ seems required to be high to begin affecting the Call price. For scenarios with an increase in μ below 0.5°C, the more μ increases during the time to maturity, the less σ seems required to be high to begin affecting the Call price.

Concerning Put prices, for scenarios with an increase in μ below 0.5°C the less μ increases during the time to maturity, the more σ seems required to be high to begin affecting the Call price. For scenarios with an increase in μ above 0.5°C the more μ increases during the time to maturity, the more σ seems required to be high to begin affecting the Call price.

The results obtained for all simulations with $T_K = 15.5$ can be better understood looking at *Figure 33*: Call and Put prices' lines are just about vertically symmetrical. This characteristic is represented in the graphs for simulations with different values of θ and, more visibly, σ.

3.3 A short discussion

From the Appendix it is apparent that this pricing method which employs a stochastic model to describe the temperature process and simulates it using a Monte Carlo simulation is both conceptually and algorithmically simple. It can adjust well to the need of reviewing the future temperature estimates: changes to the temperature process' dynamics are easily implementable. Anyway, side by side with the conceptual and algorithmic simplicity of Monte Carlo technique stands the high (and potentially extreme) computational costs associated to it, as also stated in Shonkwiler and Mendivil (2009). In general, requiring many samples for good approximation purposes is in fact translated into the possibility of a large total runtime in the event that each single sample runtime is high. In our context this is not an issue: the computational speed is extremely high due to the fact that the model and the payoffs are pretty simple. It can be an issue in the case that stochastic models more complicated than Hull-White model are employed. For our purposes, the possibility of verifying the response to single input changes and the conceptual and algorithmic simplicity of the method (thus also the transparency of the results) are elements in favour of the temperature paths' modelling using the Vasicek and the Hull-White stochastic models and the simulation of these paths using the Monte Carlo method for pricing temperature options.

Now, we need to distinguish between the Vasicek model and the Hull-White one.

The Vasicek model could be useful in a situation in which the long-term mean is already known at $t = 0$. This is surely not the case in a climate-worsening situation, when the long-term mean can vary after $t = 0$. So, although the results of the comparison between the real time series and the paths simulated entering the calibrated parameters from it are quite encouraging, the limits of the model are apparent for what concerns the simulation of evolving scenarios.

The Hull-White model employed is able to overcome the limit imposed by the constant long-term mean parameter μ encompassing different intensity levels of increase through time in that parameter. Imposing a linear increase in that parameter is surely a great simplification of reality, but it still succeeds in conveying the idea of the effect of the climate worsening on the prices of

these derivatives. Anyway, it would be possible to adapt the simulations for the Hull-White model assuming different non-linear functional forms for the evolution of the long-term mean parameter in order to represent the dynamics of the temperature path in a more realistic way.

The capacity to represent the climate change effect is essential for the stochastic model describing the underlying process: temperature options are purposely designed for hedging the climate risk in the long term. So, using a stochastic model unable to represent such a factor would completely invalidate the pricing of these instruments. Between the two models presented in chapter 3, thus, Hull-White model is to be preferred considering also that non-linear functional forms for the evolution of μ through time can be implemented.

Conclusion

Although climate change effects are not only related to economic activities, the birth of the market of climate derivatives is highly desiderable: they can be useful to raise money to be invested in climate adaption and mitigation projects, whose aim go beyond the mere economic objective. For example, hyphotetical derivatives which take into account the sea water rise can surely be helpful at raising money for the construction of coastal defences. These defences, apart from protecting crops near the sea and fish farms, can also prevent the abandonement of houses, health issues due to new marshy areas and so on.

There are still no news about the potential issue of these instruments. It is clear that many chances are being lost given that climate change effects are already significantly affecting certain sectors of the economy with no relief apart from traditional insurances or short term instruments such as the weather derivatives. The upward trend in global temperature has started decades ago: if climate derivatives market had been operational, it would have had a relevant impact in the economy letting economic activities to cover the long term risk or invest in mitigation projects.

As discussed in Chapter 1, indeed, the already-existing financial instruments are not able to take into account the climate change and its effects. Furthermore, their validity may be jeopardised.

Difficulties have been encountered in gathering material in order to offer a comprehensive view of this potentially new financial instruments because there are few examples of climate derivatives in the literature and none in the reality. The reason may lie in the awareness of the difficulties in starting a new market and, after the initial phase, of the possible low liquidity of this market.

In the last chapter, a different methodology for pricing temperature options is proposed. Two stochastic models are used to represent the dynamics of the underlying process, the Vasicek model and the extended Vasicek model, i.e. the Hull-White model. The Hull-White model is in fact the extended version of the Vasicek model since it encompasses a time-varying long term mean. This characteristic is proved to improve the capacity of the model to represent climate dynamics and thus the Hull-White model should be preferred for pricing climate derivatives.

For the models considered, it would be possible to obtain explicit option valuation formulas and thus analytically compute option prices without resorting to Monte Carlo method. Anyway, the great advantage of using Monte Carlo method is that it can be used even when much more complicated models which do not admit explicit formulas are considered.

It is worth highlighting that the major limitation of the analysis performed surely lies in the modelling of the risk premium, which is just based on hypotheses given that the market for these derivatives still does not exist.

Even though the results obtained can not be evaluated with regard to their correctness, intended in absolute terms, it is possible to see that there are viable opportunities to price temperature options, and by extension climate derivatives, even outside the frameworks conceived by their authors. The complexity of the pricing method and of the model describing the underlying's dynamics as originally proposed by the authors may have played a role in the cooling of interest for the introduction of these financial instruments on the market. Their chances of being introduced on the market may increase in the future as a result of the occurrence of some conditions such as the achievement of a credibile intrument, the occurrence of several damages undeniably related to climate change in sectors most exposed to climate change and so the increase in pressure for a fair solution that allows the sharing of the risks.

Appendix – Matlab code

A. Computations

A.1 Vasicek Model

```matlab
%% Uploading and organising data
readtable('globalaveragetimeseries.xlsx'); % read the Excel sheet where
the data copied from NASA website are stored

dates=table2array(ans(1:end,1));
LAST20Y_AN = table2array(ans(123:end,2));
last20y_an = str2double(LAST20Y_AN);
for i=1:size(last20y_an,1)
    last20y(i,1) = last20y_an(i,1)+14;
end

ALL_AN = table2array(ans(:,2));
all_an = str2double(ALL_AN);
for i=1:size(all_an,1)
    all(i,1)=all_an(i,1)+14;
end

%% Calibration using Maximum Likelihood Estimators
n=size(last20y,1)-1;
X_x=sum(last20y(1:end-1));
X_y=sum(last20y(2:end));
X_xx=sum(last20y(1:end-1).^2);
X_xy=sum(last20y(1:end-1).*last20y(2:end));
X_yy=sum(last20y(2:end).^2);

mu=(X_y*X_xx - X_x*X_xy)/(n*(X_xx - X_xy)-(X_x^2-X_x*X_y));
dt=1;
theta = (( X_xy - mu*X_x - mu*X_y + n*mu^2) / ( X_xx - 2*mu*X_x + n*mu^2)
) / dt ;
a = 1 - theta* dt ;
sigmahat2 = (X_yy - 2*a*X_xy + a^2*X_xx - 2*mu*(1-a)*(X_y-a*X_x) +
n*mu^2*(1-a)^2)/n ;
sigma = sqrt (sigmahat2*2*theta/(1-a^2));

%% SIMULATION OF CALIBRATED PARAMETERS
% set time horizon
t = 20;
% set number of discretization points of the interval [0,t]
n = 20;
dt = t / n;
% set number of simulations
M= 10000;
% simulate M discretized trajectories of Brownian motion over [0,t]
dw = sqrt ( dt ) * randn ( M, n );
```

```matlab
% set parameters and strike price
theta = 0.8030; % nonnegative decay rate which determines how fast x(t)
will move towards mu.
mu = 14.793; % mean value towards which the process tends
sigma = 0.1736; % relative magnitude of stochastic perturbations.
x0 = 14.62; % starting value
T_K=15;
r=0.01;

% Euler approximate integration process for temperature path
x = zeros ( M , n );
for j = 1 : n-1
    for s=1:M
        x(s,1)=x0;
        x(s,j+1) = x(s,j) + dt * theta * ( mu - x(s,j) )+ sigma * dw(s,j);
    end
end

% confidence interval real time series
for i=1:size(x,2)
    meansim(i)=mean(x(:,i));
    SEM(i) = std(x(:,i));
    ts(i,:) = tinv([0.075  0.925],length(x(:,i))-1);
    CI(i,:) = meansim(i) + ts(i,:)*SEM(i);
end

%% FIRST SIMULATION
% set time horizon
t = 20;
% set number of discretization points of the interval [0,t]
n = 1000;
dt = t / n;
% set number of simulations
M= 10000;
% simulate M discretized trajectories of Brownian motion over [0,t]
dw = sqrt ( dt ) * randn ( M, n );
% set parameters and strike price
r=0.01;
theta = 0.9; % nonnegative decay rate which determines how fast x(t) will
move towards mu.
mu = 15; % mean value towards which the process tends
sigma = 0.18; % relative magnitude of stochastic perturbations.
x0 = 14.84; % starting value
T_K=15;

%  Euler approximate integration process
x = zeros ( M , n + 1 );
for j = 1 : n
    for s=1:M
```

```matlab
            x(s,1)=x0;
            x(s,j+1) = x(s,j) + dt * theta * ( mu - x(s,j)) + ...
            sigma * dw(s,j);
        end
end


% compute M realizations of the payoffs (Call and Put)
x_T= x(:,end);
payoff_Call= max(x_T-T_K,0);
payoff_Put= max(T_K-x_T,0);

% compute Monte Carlo price
MC_price_Call=mean(payoff_Call)*exp(-r*t);
MC_price_Put=mean(payoff_Put)*exp(-r*t);

%% SIMULATION FOR DIFFERENT VALUES OF THETA
t = 20;
n = 1000;
dt = t / n;
M= 10000;
dw = sqrt ( dt ) * randn ( M, n );
theta=[0.5:0.1:1.3]';
mu = 15;
sigma = 0.18;
x0 = 14.84;
T_K=15;
r=0.01;

% Euler approximate integration process for temperature path
x = zeros ( M , n );
for k=1:size(theta)
    for j = 1 : n-1
        for s=1:M
            x(s,1)=x0;
            x(s,j+1) = x(s,j) + theta(k) * ( mu - x(s,j) ) * dt ...
            + sigma * dw(s,j);
        end
    end
    % take realizations of x at maturity
    x_T(:,k)= x(:,end);
    % compute they payoffs
    payoff_Call(:,k)= max(x_T(:,k)-T_K,0);
    payoff_Put(:,k)= max(T_K-x_T(:,k),0);
    % compute Monte Carlo price
    MC_price_Call(k,1)=mean(payoff_Call(:,k))*exp(-r*t);
    MC_price_Put(k,1)=mean(payoff_Put(:,k))*exp(-r*t);
end
```

```matlab
%% SIMULATION FOR DIFFERENT VALUES OF MU
t = 20;
n = 1000;
dt = t / n;
M= 10000;
dw = sqrt ( dt ) * randn ( M, n );
theta = 0.9; % will move towards mu.
mu=[15:0.1:16]'; % mean value towards which the process tends
sigma = 0.18; % relative magnitude of stochastic perturbations.
x0 = 14.84; % starting value
T_K=15;
r=0.01;

% Euler approximate integration process for temperature path
x = zeros ( M , n );
for k=1:size(mu,1)
    for j = 1 : n-1
        for s=1:M
            x(s,1)=x0;
            x(s,j+1) = x(s,j) +  theta * ( mu(k) - x(s,j) ) * dt ...
            + sigma * dw(s,j);
        end
    end
    % take the realizations of x at maturity
    x_T(:,k)= x(:,end);
    % compute the payoffs
    payoff_Call(:,k)= max(x_T(:,k)-T_K,0);
    payoff_Put(:,k)= max(T_K-x_T(:,k),0);
    % compute Monte Carlo price
    MC_price_Call(k,1)=mean(payoff_Call(:,k))*exp(-r*t);
    MC_price_Put(k,1)=mean(payoff_Put(:,k))*exp(-r*t);
end

%% SIMULATION FOR DIFFERENT VALUES OF SIGMA
t = 20;
n = 10000;
dt = t / n;
M= 10000;
dw = sqrt(dt) * randn(M,n);
theta = 0.9;
mu = 15;
sigma = [0.1:0.05:0.5]';
x0 = 14.84;
T_K=15;
r=0.01;

% Euler approximate integration process for temperature path
x = zeros(M,n);
```

```matlab
for k=1:size(sigma,1)
    for j = 1 : n-1
        for s=1:M
            x(s,1)=x0;
            x(s,j+1) = x(s,j) +  theta * ( mu - x(s,j) ) * dt ...
            + sigma(k) * dw(s,j);
        end
    end
    % take the realizations of x at maturity
    x_T(:,k)= x(:,end);
    % compute they payoffs
    payoff_Call(:,k)= max(x_T(:,k)-T_K,0);
    payoff_Put(:,k)= max(T_K-x_T(:,k),0);
    % compute Monte Carlo price
    MC_price_Call(k,1)=mean(payoff_Call(:,k))*exp(-r*t);
    MC_price_Put(k,1)=mean(payoff_Put(:,k))*exp(-r*t);
end
```

A.2 Hull-White model

```matlab
%% FIRST SIMULATION with mu evolving through time
% set time horizon
t = 20;
% set number of discretization points of the interval [0,t]
n = 1000;
dt = t / n;
% set number of simulations
M= 10000;
% simulate M discretized trajectories of Brownian motion over [0,t]
dw = sqrt ( dt ) * randn ( M, n-1 );
% set parameters and strike price
theta = 0.9; % nonnegative decay rate which determines how fast x(t) will
move towards mu.
sigma = 0.18; % relative magnitude of stochastic perturbations.
r=0.01;
x0 = 14.84; % starting value
T_K=15; %or T_K=16 or T_K=15.5
stmu=15; % mu starting value

% Euler approximate integration process for temperature path
x = zeros ( M , n );
wrs=[0:0.25:1]'; % different final levels of increase in mu

for z=1:size(wrs,1);
    for j = 1 : n-1
        mu(z,1) = stmu;
        mu(z,j+1)=mu(z,j)+wrs(z)/(n-1);
        for s=1:M
```

```matlab
            x(s,1)=x0;
            x(s,j+1) = x(s,j) + dt * theta * ( mu(z,j) - x(s,j) ) + sigma
             * dw(s,j);
        end
    end
    % compute M realizations of the payoffs (Call and Put)
    x_T(:,z)= x(:,end);
    payoff_Call(:,z)= max(x_T(:,z)-T_K,0);
    payoff_Put(:,z)= max(T_K-x_T(:,z),0);
    % compute Monte Carlo price
    MC_price_Call(z,1)=mean(payoff_Call(:,z))*exp(-r*t);
    MC_price_Put(z,1)=mean(payoff_Put(:,z))*exp(-r*t);
end

%% SENSITIVITY THETA
t = 20;
n = 1000;
dt = t / n;
M= 10000;
% simulate M discretized trajectories of Brownian motion over [0,t]
dw = sqrt ( dt ) * randn ( M, n );
% set parameters and strike price
theta=[0.5:0.1:1.3]';
stmu = 15;
sigma = 0.18;
x0 = 14.84;
T_K=15; %or T_K=15.5
r=0.01;

% Euler approximate integration process for temperature path
x = zeros ( M , n );
wrs=[0:0.25:1]';
% constant scenario
for k=1:size(theta,1)
    for j = 1 : n-1
        z=1;
        mu(z,1) = stmu;
        mu(z,j+1)=mu(z,j)+wrs(z)/(n-1);
        for s=1:M
            x(s,1)=x0;
            x(s,j+1) = x(s,j) +  theta(k) * ( mu(z,j) - x(s,j) ) * dt +
            sigma * dw(s,j);
        end
    end
    x_T(:,k)= x(:,end);
    payoff_Call(:,k)= max(x_T(:,k)-T_K,0);
    payoff_Put(:,k)= max(T_K-x_T(:,k),0);
    % compute Monte Carlo price
```

```matlab
        MC_price_Call1(k,1)=mean(payoff_Call(:,k))*exp(-r*t);
        MC_price_Put1(k,1)=mean(payoff_Put(:,k))*exp(-r*t);
end

% +0.25 scenario
for k=1:size(theta,1)
    for j = 1 : n-1
        z=2;
        mu(z,1) = stmu;
        mu(z,j+1)=mu(z,j)+wrs(z)/(n-1);
        for s=1:M
            x(s,1)=x0;
            x(s,j+1) = x(s,j) +  theta(k) * ( mu(z,j) - x(s,j) ) * dt +
            sigma * dw(s,j);
        end
    end
    x_T(:,k)= x(:,end);
    payoff_Call(:,k)= max(x_T(:,k)-T_K,0);
    payoff_Put(:,k)= max(T_K-x_T(:,k),0);
    % compute Monte Carlo price
    MC_price_Call2(k,1)=mean(payoff_Call(:,k))*exp(-r*t);
    MC_price_Put2(k,1)=mean(payoff_Put(:,k))*exp(-r*t);
end

% +0.5 scenario
for k=1:size(theta,1)
    for j = 1 : n-1
        z=3;
        mu(z,1) = stmu;
        mu(z,j+1)=mu(z,j)+wrs(z)/(n-1);
        for s=1:M
            x(s,1)=x0;
            x(s,j+1) = x(s,j) +  theta(k) * ( mu(z,j) - x(s,j) ) * dt +
            sigma * dw(s,j);
        end
    end
    x_T(:,k)= x(:,end);
    payoff_Call(:,k)= max(x_T(:,k)-T_K,0);
    payoff_Put(:,k)= max(T_K-x_T(:,k),0);
    % compute Monte Carlo price
    MC_price_Call3(k,1)=mean(payoff_Call(:,k))*exp(-r*t);
    MC_price_Put3(k,1)=mean(payoff_Put(:,k))*exp(-r*t);
end

% +0.75 scenario
for k=1:size(theta,1)
    for j = 1 : n-1
        z=4;
```

```matlab
            mu(z,1) = stmu;
            mu(z,j+1)=mu(z,j)+wrs(z)/(n-1);
            for s=1:M
                x(s,1)=x0;
                x(s,j+1) = x(s,j) +  theta(k) * ( mu(z,j) - x(s,j) ) * dt +
                sigma * dw(s,j);
            end
        end
        x_T(:,k)= x(:,end);
        payoff_Call(:,k)= max(x_T(:,k)-T_K,0);
        payoff_Put(:,k)= max(T_K-x_T(:,k),0);
        % compute Monte Carlo price
        MC_price_Call4(k,1)=mean(payoff_Call(:,k))*exp(-r*t);
        MC_price_Put4(k,1)=mean(payoff_Put(:,k))*exp(-r*t);
end


% +1 scenario
for k=1:size(theta,1)
    for j = 1 : n-1
        z=5;
        mu(z,1) = stmu;
        mu(z,j+1)=mu(z,j)+wrs(z)/(n-1);
        for s=1:M
            x(s,1)=x0;
            x(s,j+1) = x(s,j) +  theta(k) * ( mu(z,j) - x(s,j) ) * dt +
            sigma * dw(s,j);
        end
    end
    x_T(:,k)= x(:,end);
    payoff_Call(:,k)= max(x_T(:,k)-T_K,0);
    payoff_Put(:,k)= max(T_K-x_T(:,k),0);
    % compute Monte Carlo price
    MC_price_Call5(k,1)=mean(payoff_Call(:,k))*exp(-r*t);
    MC_price_Put5(k,1)=mean(payoff_Put(:,k))*exp(-r*t);
end

%% SENSITIVITY SIGMA
t = 20;
n = 1000;
dt = t / n;
M= 10000;
% simulate M discretized trajectories of Brownian motion over [0,t]
dw = sqrt ( dt ) * randn ( M, n );
% set parameters and strike price
theta = 0.9;
stmu = 15;
sigma = [0.1:0.05:0.5]';
x0 = 14.84;
```

```matlab
T_K=15; %or T_K=15.5
r=0.01;

% Euler approximate integration process for temperature path
x = zeros ( M , n );
wrs=[0:0.25:1]';

% constant scenario
for k=1:size(sigma,1)
    for j = 1 : n-1
        z=1;
        mu(z,1) = stmu;
        mu(z,j+1)=mu(z,j)+wrs(z)/(n-1);
        for s=1:M
            x(s,1)=x0;
            x(s,j+1) = x(s,j) +  theta * ( mu(z,j) - x(s,j) ) * dt +
            sigma(k) * dw(s,j);
        end
    end
    x_T(:,k)= x(:,end);
    payoff_Call(:,k)= max(x_T(:,k)-T_K,0);
    payoff_Put(:,k)= max(T_K-x_T(:,k),0);
    % compute Monte Carlo price
    MC_price_Call1(k,1)=mean(payoff_Call(:,k))*exp(-r*t);
    MC_price_Put1(k,1)=mean(payoff_Put(:,k))*exp(-r*t);
end

% +0.25 scenario
for k=1:size(sigma,1)
    for j = 1 : n-1
        z=2;
        mu(z,1) = stmu;
        mu(z,j+1)=mu(z,j)+wrs(z)/(n-1);
        for s=1:M
            x(s,1)=x0;
            x(s,j+1) = x(s,j) +  theta * ( mu(z,j) - x(s,j) ) * dt +
            sigma(k) * dw(s,j);
        end
    end
    x_T(:,k)= x(:,end);
    payoff_Call(:,k)= max(x_T(:,k)-T_K,0);
    payoff_Put(:,k)= max(T_K-x_T(:,k),0);
    % compute Monte Carlo price
    MC_price_Call2(k,1)=mean(payoff_Call(:,k))*exp(-r*t);
    MC_price_Put2(k,1)=mean(payoff_Put(:,k))*exp(-r*t);
end

% +0.5 scenario
```

```matlab
for k=1:size(sigma,1)
    for j = 1 : n-1
        z=3;
        mu(z,1) = stmu;
        mu(z,j+1)=mu(z,j)+wrs(z)/(n-1);
        for s=1:M
            x(s,1)=x0;
            x(s,j+1) = x(s,j) +  theta * ( mu(z,j) - x(s,j) ) * dt +
            sigma(k) * dw(s,j);
        end
    end
    x_T(:,k)= x(:,end);
    payoff_Call(:,k)= max(x_T(:,k)-T_K,0);
    payoff_Put(:,k)= max(T_K-x_T(:,k),0);
    % compute Monte Carlo price
    MC_price_Call3(k,1)=mean(payoff_Call(:,k))*exp(-r*t);
    MC_price_Put3(k,1)=mean(payoff_Put(:,k))*exp(-r*t);
end

% +0.75 scenario
for k=1:size(sigma,1)
    for j = 1 : n-1
        z=4;
        mu(z,1) = stmu;
        mu(z,j+1)=mu(z,j)+wrs(z)/(n-1);
        for s=1:M
            x(s,1)=x0;
            x(s,j+1) = x(s,j) +  theta * ( mu(z,j) - x(s,j) ) * dt +
            sigma(k) * dw(s,j);
        end
    end
    x_T(:,k)= x(:,end);
    payoff_Call(:,k)= max(x_T(:,k)-T_K,0);
    payoff_Put(:,k)= max(T_K-x_T(:,k),0);
    MC_price_Call4(k,1)=mean(payoff_Call(:,k))*exp(-r*t);
    MC_price_Put4(k,1)=mean(payoff_Put(:,k))*exp(-r*t);
end

% +1 scenario
for k=1:size(sigma,1)
    for j = 1 : n-1
        z=5;
        mu(z,1) = stmu;
        mu(z,j+1)=mu(z,j)+wrs(z)/(n-1);
        for s=1:M
            x(s,1)=x0;
            x(s,j+1) = x(s,j) +  theta * ( mu(z,j) - x(s,j) ) * dt +
            sigma(k) * dw(s,j);
```

```
            end
        end
        x_T(:,k)= x(:,end);
        payoff_Call(:,k)= max(x_T(:,k)-T_K,0);
        payoff_Put(:,k)= max(T_K-x_T(:,k),0);
        MC_price_Call5(k,1)=mean(payoff_Call(:,k))*exp(-r*t);
        MC_price_Put5(k,1)=mean(payoff_Put(:,k))*exp(-r*t);
    end
```

B. Figures

B.1 Vasicek model

```
% plotting the real time series
figure
set(gcf,'Position',[100,100,1300,600])
plot(dates,all,'LineWidth',4)
hold on
plot(dates(123:end),last20y,'LineWidth',1,'Color','y')
xlim([1880 2021])
xlabel ( 't', 'FontSize', 16 )
ylabel ( 'temperature', 'FontSize', 16 )
title ( 'Global average temperature', 'FontSize', 16 )
grid ( 'on' );


% confidence interval real time series
figure
set(gcf,'Position',[100,100,1300,600])
plot(dates(123:end),last20y,'LineWidth',2,'Color','b');
hold on
plot(dates(123:end),meansim,'LineWidth',2,'Color','g');
hold on
plot(dates(123:end),CI(:,2),'LineWidth',2,'Color','r');
hold on
plot(dates(123:end),CI(:,1),'LineWidth',2,'Color','m');
legend('real time series','mean simulated temperature',...
    '85% upper bound','85% lower bound','Location','northeastoutside')
xlim([2002 2021]);


% plotting the first simulation approximate solution.
tplot = linspace ( 0, t, n + 1 );
plot ( tplot, x, 'LineWidth', 1)
xlabel ( 't', 'FontSize', 16 )
ylabel ( 'X(t)', 'FontSize', 16, 'Rotation', 0, 'HorizontalAlignment',
'right' )
title ( 'Ornstein-Uhlenbeck temperature paths', 'FontSize', 16 )
grid ( 'on' );


% plot the prices for different theta values
figure
plot(theta,MC_price_Put,'LineWidth',2,'Color','g');
```

```matlab
hold on
plot(theta,MC_price_Call,'LineWidth',2,'Color','r');
legend('Put price','Call price');
xlabel('theta')
ylabel('Price')

% plot the prices for different mu values
figure
plot(mu,MC_price_Put,'LineWidth',2,'Color','g');
hold on
plot(mu,MC_price_Call,'LineWidth',2,'Color','r');
legend('Put price','Call price');
xlabel('mu')
ylabel('Price')

% plot the prices for different sigma values
figure
plot(sigma,MC_price_Put,'LineWidth',2,'Color','g');
hold on
plot(sigma,MC_price_Call,'LineWidth',2,'Color','r');
legend('Put price','Call price');
xlabel('mu')
ylabel('Price')
```

B.2 Hull-White model

```matlab
% plot the prices for first simulation with evolving mu
figure
plot(wrs,MC_price_Call,'LineWidth',2,'Color','r');
hold on
plot(wrs,MC_price_Put,'LineWidth',2,'Color','g');
legend('Call price','Put price');
xlabel('final \mu deviation from initial \mu','FontSize', 16)
xticks([0 0.25 0.5 0.75 1])
ylabel('Price','FontSize', 16)
grid on

% plot the prices with evolving mu through time and changing theta
figure
plot(theta,[MC_price_Call1 MC_price_Call2 MC_price_Call3 MC_price_Call4
MC_price_Call5],...
    'LineWidth',2);
legend('constant','+0.25^{\circ}C','+0.5^{\circ}C','+0.75^{\circ}C','+1^{\
circ}C','Location','bestoutside')
xlabel('\theta', 'FontSize', 20, 'Rotation', 0, 'HorizontalAlignment',
'right')
ylabel('Price', 'FontSize', 16)
xlim([0.5 1.3])
```

```matlab
grid on
figure
plot(theta,[MC_price_Put1 MC_price_Put2 MC_price_Put3 MC_price_Put4
MC_price_Put5],...
    'LineWidth',2);
legend('constant','+0.25^{\circ}C','+0.5^{\circ}C','+0.75^{\circ}C','+1^{\
circ}C','Location','bestoutside')
xlabel('\theta', 'FontSize', 20, 'Rotation', 0, 'HorizontalAlignment',
'right')
ylabel('Price', 'FontSize', 16)
xlim([0.5 1.4])
grid on

% plot the prices with evolving mu through time and changing sigma
figure
set(gcf,'Position',[100,100,1300,600])
subplot(1,2,1)
plot(sigma,[MC_price_Call1 MC_price_Call2 MC_price_Call3 MC_price_Call4
MC_price_Call5],...
    'LineWidth',2);
xticks([0.1:0.05:0.5])
xlim([0.1 0.5])
xlabel('\sigma', 'FontSize', 20, 'Rotation', 0, 'HorizontalAlignment',
'right')
ylabel('Price', 'FontSize', 16)
grid on
title('Call','FontSize', 16)
lgnd1=legend('constant','+0.25^{\circ}C','+0.5^{\circ}C','+0.75^{\circ}C',
'+1^{\circ}C','Location','southoutside','Orientation','horizontal')
subplot(1,2,2)
plot(sigma,[MC_price_Put1 MC_price_Put2 MC_price_Put3 MC_price_Put4
MC_price_Put5],...
    'LineWidth',2);
xlabel('\sigma', 'FontSize', 20, 'Rotation', 0, 'HorizontalAlignment',
'right')
ylabel('Price', 'FontSize', 16)
xlim([0.1 0.5])
xticks([0.1:0.05:0.5])
grid on
title('Put','FontSize', 16)
lgnd2=legend('constant','+0.25^{\circ}C','+0.5^{\circ}C','+0.75^{\circ}C',
'+1^{\circ}C','Location','southoutside','Orientation','horizontal')
lgnd2=legend('hide')
```

Bibliography

ACKERMAN, F., S. J. DECANIO, R. B. HOWARTH, AND K. SHEERAN. (2009): "Limitations of integrated assessment models of climate change" *Climatic Change*, 95, 297–315.

ALATON, P., B. DJEHICHE, AND D. STILLBERGER. (2002): "On modelling and pricing weather derivatives", *Applied Mathematical Finance*, 9, 1–20.

AMADEI, L., S. DI ROCCO, M. GENTILE, R. GRASSO, AND G. SICILIANO. (2011): "Credit Default Swaps: Contract Characteristics and Interrelations with the Bond Market", *Discussion Papers*, .

BERG, T. VAN DEN. (2011): "Calibrating the Ornstein-Uhlenbeck (Vasicek) model"

BERNAL, V. (2016): Calibration of the Vasicek Model: An Step by Step Guide

BERZ, G. A. (1992): "Greenhouse effects on natural catastrophes and insurance", *The Geneva Papers on Risk and Insurance*, 17, 386-392.

BIENER, C., AND M. ELING. (2012): "Insurability in Microinsurance Markets: An Analysis of Problems and Potential Solutions", *The Geneva Papers on Risk and Insurance - Issues and Practice*, 37, 77–107.

BLOCH, D., J. ANNAN, AND J. BOWLES. (2010): "Cracking the Climate Change Conundrum with Derivatives", *Wilmott Journal*, 2, 271–87.

---. (2011): "Applying Climate Derivatives to Flood Risk Management", *Wilmott (London, England)*, 2011, 88–103.

BRESSAN, G. M., AND S. ROMAGNOLI. (2021): "Climate risks and weather derivatives: A copula-based pricing model", *Journal of Financial Stability*, 54, 100877.

CERES. (2013): Insurer Climate Risk Disclosure Survey: 2012 Findings & Recommendations,.

CHAIYAPO, N., AND N. PHEWCHEAN. (2017): "An application of Ornstein-Uhlenbeck process to commodity pricing in Thailand", *Advances in Difference Equations*, 2017, 179.

CHARPENTIER, A., AND B. LE MAUX. (2014): "Natural catastrophe insurance: How should the government intervene?", *Journal of Public Economics*, 115, 1–17.

CHIKHANI, P., AND J.-P. RENNE. (2021): "Climate Linkers: Rationale and Pricing", *SSRN Electronic Journal.*

COE, P. J., M. H. PESARAN, AND S. P. VAHEY. (2003): "Scope for Cost Minimization in Public Debt Management: the Case of the UK", 29.

COLLIER, S. J., R. ELLIOTT, AND T.-K. LEHTONEN. (2021): "Climate change and insurance", *Economy and Society*, 50, 158–72.

COSTA, A., M. D CHAMON, AND L. A. RICCI. (2008): "Is There a Novelty Premium on New Financial Instruments? The Argentine Experience with GDP-Indexed Warrants", *IMF Working Papers*, 2008.

DELL, J., S. TIERNEY, G. FRANCO, R. G. NEWELL, R. RICHELS, J. WEYANT, T. J. WILBANKS, J. M. MELILLO, T. (T. C.) RICHMOND, AND G. W. YOHE. (2014): "Ch. 4: Energy Supply and Use. Climate Change Impacts in the United States: The Third National Climate Assessment", *U.S. Global Change Research Program*, , 113–29.

DELOITTE UNITED STATES. (2019): "Climate Risk: Regulators Sharpen Their Focus".

DENNING, A. S. (2018): "Combustion to Concentration to Warming: What Do Climate Targets Mean for Emissions? Climate Change and the Global Carbon Cycle", *Encyclopedia of the Anthropocene*, , p.443-452.

DUFFIE, D., J. PAN, AND K. SINGLETON. (2000): "Transform Analysis and Asset Pricing for Affine Jump-diffusions", *Econometrica*, 68, 1343–76.

GROBECKER, A. J., S. C. CORONILI, AND R. H. CANNON. (1974): *The Report of Findings: The Effects of Stratospheric Pollution by Aircraft,* Springfield, VA.: U.S. Department of Transportation. Climatic Impact Assessment Program. National Technical Information Service.

GROSE, M. R., I. BARNES-KEOGHAN, S. P. CORNEY, C. J. WHITE, G. K. HOLZ, J. BENNETT, S. M. GAYNOR, AND N. L. BINDOFF. (2010): "Climate Futures for Tasmania: general climate impacts technical report".

HAMILTON, J. D. (1994): *Time Series Analysis*, 1st ed., Princeton, New Jersey: Princeton University Press.

HIGHAM, D. J. (2001): "An Algorithmic Introduction to Numerical Simulation of Stochastic Differential Equations", *SIAM Review*, 43, 525–46.

HULL, J. (2015): *Options, Futures, and Other Derivatives*, Ninth edition, Boston: Pearson.

HULL, J., AND A. WHITE. (1990): "Pricing Interest-Rate-Derivative Securities", *The Review of Financial Studies*, 3, 573–92.

---. (1994): "Numerical Procedures for Implementing Term Structure Models I:Single-Factor Models", *The Journal of Derivatives*, , 7–16.

---. (1996): "Using Hull-White interest-rate trees", *Journal of Derivatives*, 3, 26–36.

IPCC. (2012): Managing the Risks of Extreme Events and Disasters to Advance Climate Change Adaptation: Special Report of the Intergovernmental Panel on Climate Change, Cambridge: Cambridge University Press.

JARZABKOWSKI, P., D. K. CHALKIAS, D. D. CLARKE, E. IYAHEN, D. STADTMUELLER, AND D. A. ZWICK. (2019): "Insurance for climate adaptation: opportunities and limitations", Global Commission on Adaptation, UN, Rotterdam, the Netherlands and Washington, DC, U.S., 43.

KURNIAWAN, H., E. R. PUTRI, C. IMRON, AND D. D. PRASTYO. (2021): "Monte Carlo method to valuate CAT bonds of flood in Surabaya under Jump Diffusion Process", *Journal of Physics: Conference Series*, 1821, 012026.

LE QUÉRÉ, C., M. R. RAUPACH, J. G. CANADELL, G. MARLAND, L. BOPP, P. CIAIS, T. J. CONWAY, ET AL. (2009): "Trends in the sources and sinks of carbon dioxide", *Nature Geoscience*, 2, 831–36.

LEMOINE, D., AND C. P. TRAEGER. (2016): "Economics of tipping the climate dominoes", *Nature Climate Change*, 6, 514–19.

LITTLE, L. R., A. J. HOBDAY, J. PARSLOW, C. R. DAVIES, AND R. Q. GRAFTON. (2015): "Funding climate adaptation strategies with climate derivatives", *Climate risk management*, 8, 9–15.

LITTLE, L. R., J. PARSLOW, G. FAY, R. Q. GRAFTON, A. D. M. SMITH, A. E. PUNT, AND G. N. TUCK. (2014): "Environmental Derivatives, Risk Analysis, and Conservation Management", *Conservation Letters*, 7, 196–207.

MONASTEROLO, I., AND L. DE ANGELIS. (2018): "Blind to Carbon Risk? An Analysis of Stock Market's Reaction to the Paris Agreement", *Ecological Economics*, 170.

MONFORT, A., F. PEGORARO, J.-P. RENNE, AND G. ROUSSELLET. (2015): "Staying at Zero with Affine Processes: An Application to Term Structure Modelling", *SSRN Electronic Journal*, .

MORANA, C., AND G. SBRANA. (2019): "Climate change implications for the catastrophe bonds market: An empirical analysis", *Economic Modelling*, 81, 274–94.

NEUMANN, WILLWERTH, MARTINICH, MCFARLAND, SAROFIM, AND YOHE. (2020): "Climate Damage Functions for Estimating the Economic Impacts of Climate Change in the United States", *Review of Environmental Economics and Policy*, 14, 25–43.

NORDHAUS, W. D. (1992): "The 'DICE' Model: Background and Structure of a Dynamic Integrated Climate-Economy Model of the Economics of Global Warming", *Cowles Foundation Discussion Papers*, 1009.

---. (2016): "Revisiting the social cost of carbon", *PNAS*, 114, 1518–23.

PENLAND, C., AND T. MAGORIAN. (1993): "Prediction of Niño 3 Sea Surface Temperatures Using Linear Inverse Modeling", *Journal of Climate*, 6, 1067–76.

PIAZZESI, M. (2010): "CHAPTER 12 - Affine Term Structure Models" in *Handbook of Financial Econometrics* (2010).

PINDYCK, R. S. (2013): "Climate Change Policy: What Do the Models Tell Us?", *NBER Working Paper Series*, 19244, 23.

PURNANANDAM, A., AND D. WEAGLEY. (2016): "Can Markets Discipline Government Agencies? Evidence from the Weather Derivatives Market", *The Journal of Finance*, 71, 303–34.

RILEY, W. J. (2008): "Algorithms for frequency jump detection", *Metrologia*, 45, 154–61.

SHONKWILER, R. W., AND F. MENDIVIL. (2009): *Explorations in Monte Carlo Methods,* Undergraduate Texts in Mathematics (UTM), Springer.

STEFFEN, W., J. ROCKSTRÖM, K. RICHARDSON, T. M. LENTON, C. FOLKE, D. LIVERMAN, C. P. SUMMERHAYES, ET AL. (2018): "Trajectories of the Earth System in the Anthropocene", *Proceedings of the National Academy of Sciences of the United States of America*, 115, 8252–59.

SWISS RE. (2021): Insurance-Linked Securities Market Insights, Swiss Re.

TABOR, K., AND J. W. WILLIAMS. (2010): "Globally downscaled climate projections for assessing the conservation impacts of climate change", *Ecological Applications: A Publication of the Ecological Society of America*, 20, 554–65.

TAVANAIE MARVI, M., AND D. LINDERS. (2021): "Decomposition of Natural Catastrophe Risks: Insurability Using Parametric CAT Bonds", *Risks*, 9, 215.

THATCHER, M., AND J. L. MCGREGOR. (2009): "Using a Scale-Selective Filter for Dynamical Downscaling with the Conformal Cubic Atmospheric Model", *Monthly Weather Review*, 137, 1742–52.

THORNES, J. E. (2003): "An introduction to weather and climate derivatives", *Weather*, 58, 193–96.

TONG, K. Z., A. LIU, K. Z. TONG, AND A. LIU. (2020): "Modeling temperature and pricing weather derivatives based on subordinate Ornstein-Uhlenbeck processes", *Green Finance*, 2, 1–19.

TRAEGER, C. P. (2021): "ACE – Analytic Climate Economy", *SSRN Electronic Journal*, .

WADE, K., AND JENNINGS. (2016): The Impact of Climate Change on the Global Economy,. TalkingPoint, Schroders, 1–11.

WARNER, K., N. RANGER, S. SURMINSKI, M. ARNOLD, J. LINNNEROOTH-BAYER, E. MICHEL-KERJAN, P. KOVACS, ET AL. (2009): "Adaptation to Climate Change: Linking Disaster Risk Reduction and Insurance", *Adaptation to Climate Change*, United Nations International Strategy for Disaster Reduction Secretariat (UNISDR), 30.

WILBANKS, T. J., V. BHATT, D. E. BILELLO, S. R. BULL, J. EKMANN, W. C. HORAK, Y. J. HUANG, ET AL. (2007): "Effects of Climate Change on Energy Production and Use in the United States", *Climate Change*, 96.

YORKE, H. W., AND M. KAISIG. (1995): "Use of multiply nested grids for the solution of flux-limited radiation diffusion and hydrodynamics", *Computer Physics Communications*, 89, Numerical Methods in Astrophysical Hydrodynamics, 29–44.

ZAHRNHOFER, M. (2009): "STOCHASTIC MODELING OF TEMPERATURE: AN EMPIRICAL STUDY WITH AUSTRIAN DATA", *Working Paper No. 3/2009,* The Economics of Weather and Climate Risks Working Paper Series.